Chem Soc Rev

RSCPublishing

THEMATIC ISSUE: LIQUID CRYSTALS
Guest editor: John Goodby

Thermotropic liquid crystalline glycolipids

J. W. Goodby,*[a] V. Görtz,[a] S. J. Cowling,[a] G. Mackenzie,[b] P. Martin,[c] D. Plusquellec,[d] T. Benvegnu,[d] P. Boullanger,[e] D. Lafont,[e] Y. Queneau,[e] S. Chambert[e] and J. Fitremann[f]

Are the liquid crystalline properties of the materials of living systems important in biological structures, functions, diseases and treatments? There is a growing consciousness that the observed lyotropic, and often thermotropic liquid crystallinity, of many biological materials that possess key biological functionality might be more than curious coincidence. Rather, as the survival of living systems depends on the flexibility and reformability of structures, it seems more likely that it is the combination of softness and structure of the liquid-crystalline state that determines the functionality of biological materials. The richest sources of liquid crystals derived from living systems are found in cell membranes, of these glycolipids are a particularly important class of components. In this *critical review*, we will examine the relationship between chemical structure and the self-assembling and self-organising properties of glycolipids that ultimately lead to mesophase formation.

1. Introduction

Solanin[1] (**1**), which is the poisonous material found in green potatoes, exhibits a thermotropic smectic A* phase. Cord Factor, the 6,6′-dimycolic ester of α,α-trehalose **2**, is associated

[a]*Department of Chemistry, The University of York, York, UK YO10 5DD*
[b]*Department of Chemistry, University of Hull, Hull, UK HU6 7RX*
[c]*Laboratoire de Physico-Chimie des Interfaces et Applications (LPCIA), FRE CNRS 2485, Fédération Chevreul FR CNRS 2638, IUT de Béthune, Université d'Artois, 62408 Béthune, France*
[d]*UMR CNRS 6226 "Sciences Chimiques de Rennes" Equipe Chimie Organique et Supramoléculaire, Ecole Nationale Supérieure de Chimie de Rennes, Avenue du Général Leclerc, 35700 Rennes, France*
[e]*Institut de Chimie et de Biochimie Moléculaires et Supramoléculaires, UMR 5246; CNRS; Université de Lyon; Université Lyon 1; INSA-Lyon; CPE-Lyon, Bât. Curien, 43 Bd du 11 Novembre 1918, F 69622 Villeurbanne, France*
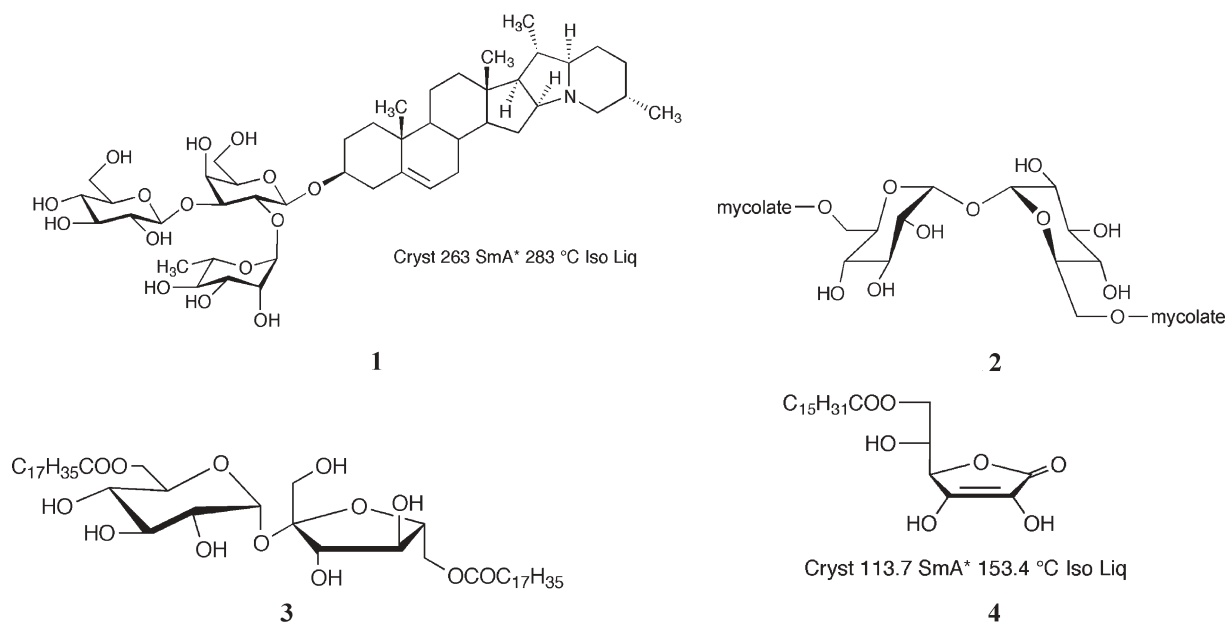[f]*Laboratoire des IMRCP, UMR CNRS 5623, Bât. 2r1, Université Paul Sabatier, 118 route de Narbonne, F-31062 Toulouse Cedex 9, France*
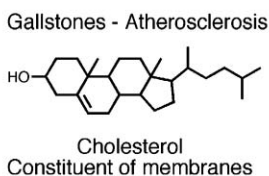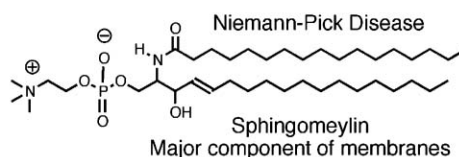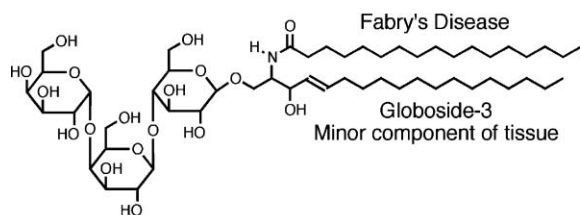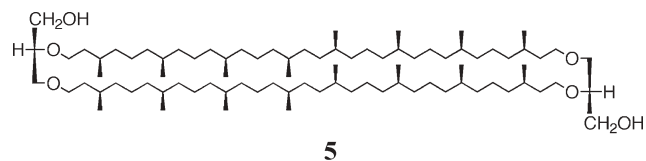
Professor John W. Goodby is Past President of the International Liquid Crystal Society and currently Chair of Materials Chemistry at the University of York. He is a member of a long term collaboration with Professors Benvegnu, Boullanger, Martin, Mackenzie Plusquellec, and Queneau and their respective research teams. Cumulatively the research grouping has focused on the self-organising and self-assembling properties of glyco- and phospho-lipids,

J. W. Goodby

and the relationship between their 'soft-matter' structures, physical properties, and biological activity.

with virulent strains of *tubercle bacilli*. Cord Factors have been shown to possess immunostimulant properties and antitumour activity, and are responsible for the bacteria forming cords in aqueous media.[2] Cord Factor also exhibits a thermotropic cubic liquid crystal phase. Bottle and Jenkins[3] showed that 6,6′-di-*O*-palmitoylsucrose (**3**), which has a similar structure to Cord Factor, exhibits biological activity. Recent research has shown that this material forms a smectic mesophase.[4] There are many other carbohydrate related systems that also exhibit liquid crystal properties, for instance, certain aliphatic derivatives of vitamin C, used as antioxidants in the food industry, exhibit thermotropic smectic A* phases,[5] see **4**.

Thus it is an interesting question to pose: are the liquid crystalline properties of these materials important in biological structures, functions, diseases and treatments?

There is a growing consciousness[6] that the observed lyotropic, and often thermotropic liquid crystallinity, of many biological materials possessing key biological functionality might be more than curious coincidence. Rather, as the survival of living systems depends on the flexibility and reformability of structures, it seems more likely that it is this combination of softness and structure of the liquid-crystalline state that determines the functionality of biological materials.

The richest sources of liquid crystals derived from living systems are found in cell membranes. Interestingly, many of these membrane components are also linked with various diseases;[7] for example, cholesterol build up is associated with gallstones and atherosclerosis. Fig. 1 shows a number of membrane lipids in relation to their place in biological systems and diseases with which they are associated. Of these, glycolipids are a particularly important class of membrane components. Cerebrosides, globosides and gangliosides are three classes of glycolipids which are often found in higher concentrations in the membranes of nerve cells. Each class is associated with a particular disease; for instance, a build up of

1

Cryst 263 SmA* 283 °C Iso Liq

2

mycolate—O

3

C$_{17}$H$_{35}$COO

4

C$_{15}$H$_{31}$COO

Cryst 113.7 SmA* 153.4 °C Iso Liq

cerebrosides in humans can lead to disorders such as Gaucher's and Krabbe's diseases.

The membranes of living organisms, other than humans, are populated by different classes of glycolipids. For example, the archaea domain is composed of a variety of extremophilic microorganisms as follows; the methanogens, halobacteria, and thermoacidophiles.[8] All three types of archaebacteria are stable to extreme environmental stress such as high temperatures, lack of oxygen *etc.* At a molecular level, the lipid components of archaea membranes are characterized by a bipolar macrocyclic architecture with two polar heads linked together by two polyisoprenoid chains which are thought to span the membrane,[9] and therefore determine the lipid layer thickness, see **5**.

5

Cell Membrane Components Biological Function and Associated Diseases

Fabry's Disease
Globoside-3
Minor component of tissue

Niemann-Pick Disease
Sphingomeylin
Major component of membranes

Gallstones - Atherosclerosis
Cholesterol
Constituent of membranes

Farber's Disease
Ceramide
Involved in sphingolipid metabolism

Tay-Sachs Disease
Gangliosides, *eg* GM2
Minor components of many tissues

Gaucher's Disease
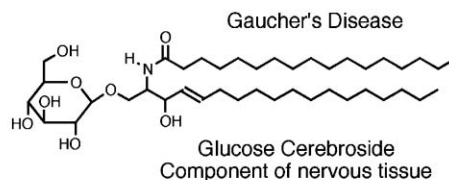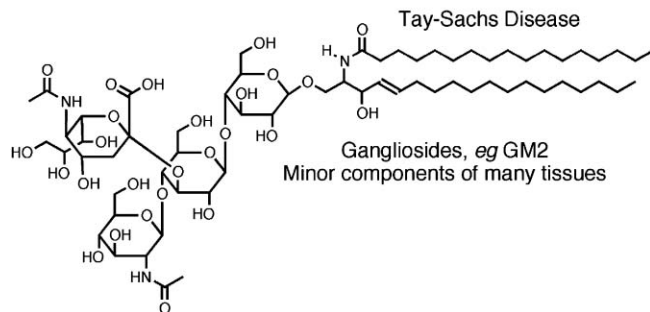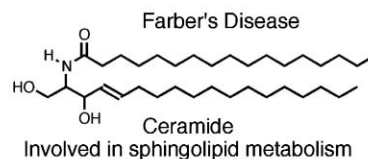Glucose Cerebroside
Component of nervous tissue

Fig. 1 Constituents of cell membranes and related diseases (after Small).[7]

Unique features of these tetraether-based lipids lie with (i) the high proportion of glycosylated lipids in the membranes of both methanogenous and sulfur depending thermophiles and (ii) the occurrence of unusual carbohydrate moieties, *i.e.* β-D-galactofuranosyl units.[8c,10] The presence of furanosyl units in such environments is a striking feature, as the glycofuranosides are much more rapidly hydrolysed than their pyranosyl counterparts.[11]

Thus phospholipids and glycolipids derived from diphytanylglycerol diethers or dibiphytanyldiglycerol tetraethers are well-adapted to the extreme environmental conditions of the three classes of archaebacteria. The ether linkages are stable over a wide range of pH, and the branching methyl groups in the isoprenoid chains help to reduce crystallisation.

Bolaphiles and macrocyclic lipids are interesting features because they effectively span the bilayer structure as shown in the cartoons in Fig. 2. This spanning adds strength to the bilayer structure, but at the same time it also reduces the mobility of the individual lipid molecules within the membrane.

Furthermore, many classes of bio-related materials, for example, surfactants, detergents, medical implants, and many materials involved in bio-processes such as intercellular recognition, also exhibit liquid crystalline properties. Also, there are many dyes and pharmaceuticals in the literature which may be liquid crystals, however, their properties remain relatively unexplored because there is a lack of recognition that liquid crystallinity could be important to their functionality.

Thus it is timely that Schwarz[12] should make the following observation. '*At the interface between chemistry, physics and biology, a new field of research has established itself during the last three decades or so, which by its followers is simply and lovingly called soft matter. Common examples of soft matter are liquid crystals, colloidal suspensions and polymer gels. These are all governed by weak intermolecular interactions, the key property leading to softness. The systems are widely used in technology, for example for computer displays, food, cosmetics and paint, because, in every case, it is essential that the material can be processed and manipulated easily. Cells and tissues, whose mechanical properties are determined mainly by polymer networks and lipid bilayers, also fall into this category.*'

2. Structures of the mesophases of liquid crystalline glycolipids

In recent years the design of chemical structures of liquid-crystalline materials has developed rapidly, and in many cases changed radically. Since Reinitzer's days[13] liquid crystals have either been classed as rod-like or disc-like, with combinations of the two leading to phasmidic liquid crystals.[14] However, the discovery that materials with bent (banana) molecular structures[15] exhibited whole new families of mesophases has led the charge towards investigating the liquid crystal properties of materials with widely varying molecular topologies – from pyramids to crosses to dendrites.[16] The mesophases formed by such individual molecular systems are created through the process of self-organisation. The formation of *supramolecular liquid crystals*, on the other hand, involves a processes of self-assembly and self-organisation, where two or more components self-assemble through various types of interaction in order to create an entity which will self-organise to form a mesophase, as shown in Fig. 3.[17]

Most simple glycolipids exhibit liquid crystal phases where the individual molecular entities of glycolipids would be very unlikely candidates to form any type of mesophase. However, glycolipids are capable of hydrogen-bonding and thus are examples of self-assembling – self-organising systems which exhibit *supermesomorphic* thermotropic phase behaviour [see reference 18 for a number of reviews on the self-organising properties of low molar mass and polymeric carbohydrate based systems]. Fig. 4 shows a cartoon of the process of self-assembly and mesophase formation for a simple glycolipid. In this case the individual molecules form a dynamically fluctuating hydrogen-bonded network. The mesophase structure can thus be considered as microphase segregated between the weakly interacting aliphatic chains and the more strongly hydrogen-bonded network.[19]

The relative cross-sectional areas of the head groups to the aliphatic chains can lead to strains on the packing of the molecules together. For example, if the cross-sectional areas of the head groups are larger than those of the aliphatic chains, then one might expect curvature to be introduced into the packing. The curvature will compete with the tendency for the materials to form layered structures. The greater the induced curvature the more likely columnar and micellar structures will be formed, as shown in Fig. 5.[20] Of course, an inverse curvature can be induced *via* the aliphatic chains having larger cross-sectional areas than the head groups.

It is possible therefore to vary molecular shape, and hence alter the packing constraints, by changing the substitution, location and number of units, of head groups with respect to aliphatic chains. In this review on glycolipids a systematic variation of head group cross-sectional area size to aliphatic
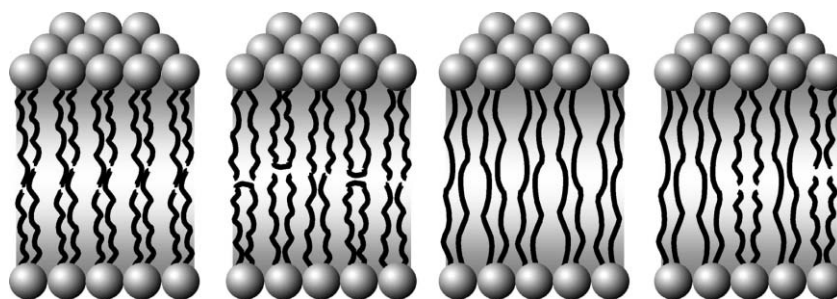

Fig. 2 Membranes of archaebacteria showing *trans*-membrane lipids
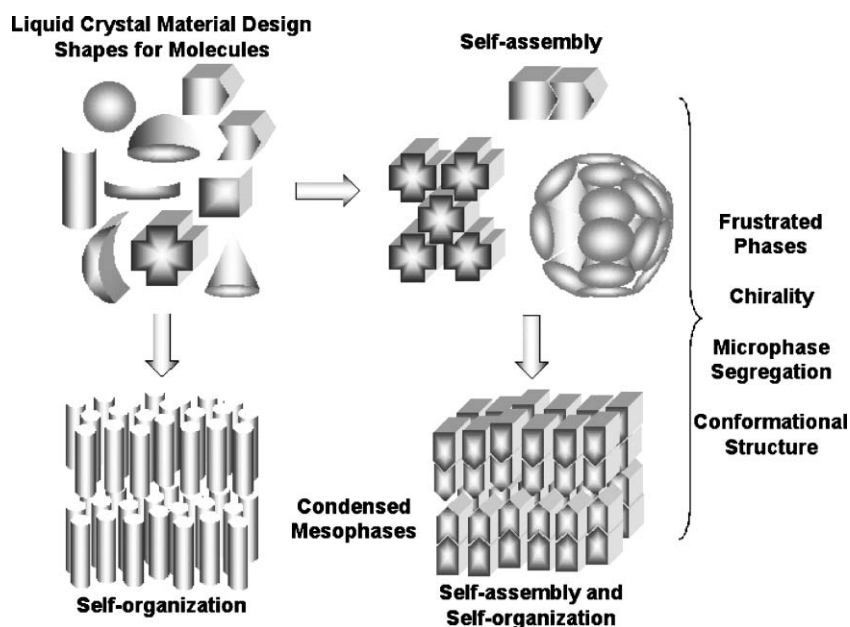
Fig. 3 The structures formed by self-organising and self-assembling liquid crystals.

cross-sectional size will therefore be investigated as a function of substitution (degree and type). The first example is for a simple glycolipid where the head group and the aliphatic chain(s) have similar sizes. Here the curvature is low, and the materials tend to form lamellar phases, as shown in Fig. 6.

A second example is where there are two head groups to one chain, or two chains to one head group. For such materials, where the molecules are depicted by the structures in Fig. 7, the overall molecular topology is wedge-shaped, *i.e.* there is a considerable difference in the volume fractions of the head and tails. Packing of wedge-like molecules can result in either the wedge-like molecules forming disc-like supra-structures, or the packing alternates to form a lamellar structure as shown in Fig. 7.[21] Where disc-like supra-structures are formed, stacking of the discs can result in the formation of a bicontinuous cubic phase or a columnar organisation, where the molecules are disorganised along the column axis. In the second case, the

columns can pack together to form rectangular or hexagonal columnar mesophases, as shown in Fig. 8.

If the degree of substitution is increased further, *i.e.* three head groups to one tail or three tails to one head group, the molecules will have conical shapes, with curvature possibly occurring in three dimensions. When such molecules pack together they will do so forming objects possessing curvature in three dimensions, *e.g.* spheres or oblates *etc.* Fig. 9 depicts the shapes of the molecules, and a spherical example of a supramolecular structure formed by the packing of the conical-shaped molecules. The supramolecular entities are shown to pack in a simple cubic array, however, body-centred and face-centred structures are also possible.

Curvature can also be induced or changed in microsegregating systems by the addition of solvents such as water or oils. These swell the head groups or tails respectively leading to change in shape and hence packing constraints. Indeed, such
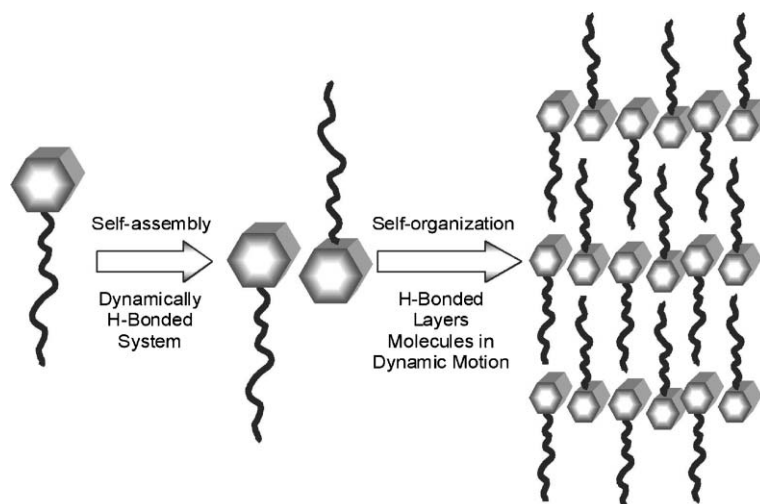

Fig. 4 A typical structure for the thermotropic smectic A phase of a glycolipid.[19]
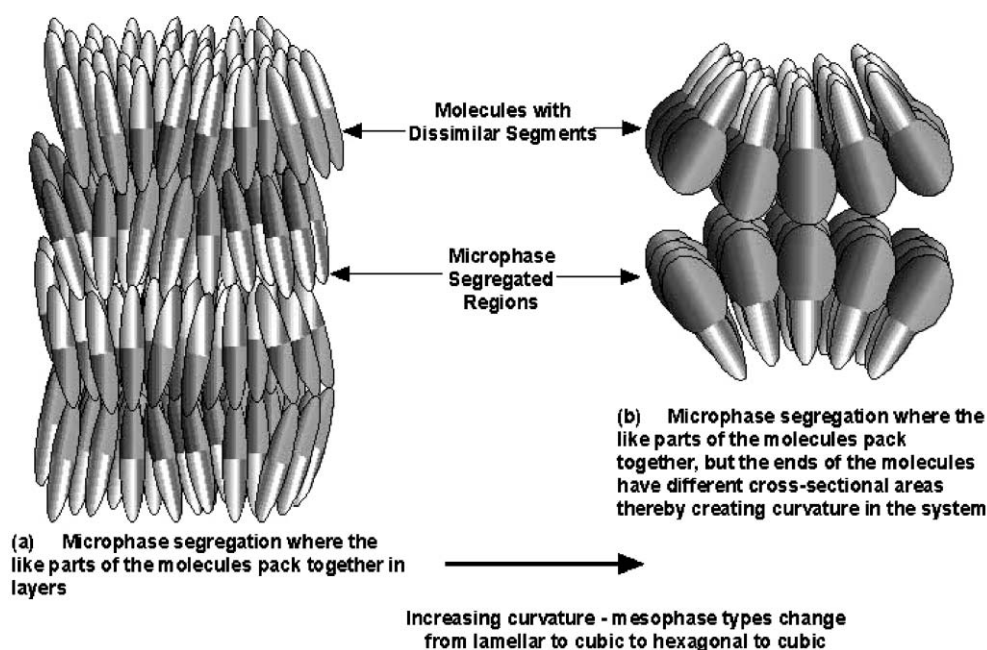
Fig. 5 Effect of curvature of packing on mesophase formation.

changes can occur as a function of concentration, and thus phase sequences can also be seen as a function of concentration as well as temperature. For example, Fig. 10 shows the change in mesophase type as a function of water concentration as a crystal of n-octyl β-D-glucopyranoside dissolves in water. A crystal of the material is placed between a glass slide and cover slip, and a droplet of water from a syringe is allowed to run under the slide by capillary action. As the crystal starts to dissolve, a ring of a lamellar phase is formed, whilst at higher concentrations sequential rings of a bicontinuous cubic and
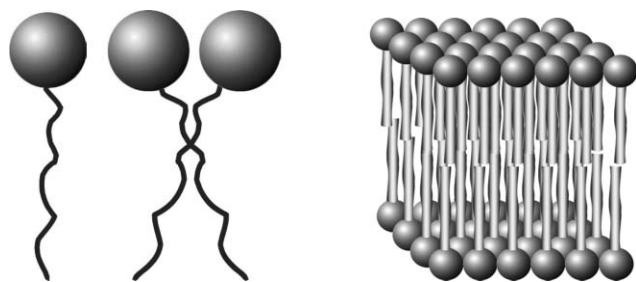

Fig. 6 Lamellar phases are formed by materials where the molecules have cylindrical shapes.
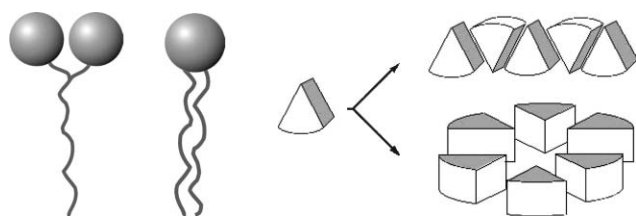

Fig. 7 Amphiphiles with wedge-like structures form either structures where the curvature of packing is compensated (top right), or where the molecules pack to give disc-like supramolecular structures.

hexagonal phases are formed respectively, as shown in the photomicrograph on the right-hand side of the figure.

One of the first families of glycolipids to be examined for both their lyotropic and thermotropic liquid-crystalline properties were indeed the n-alkyl β-D-glucopyranosides.[19,22,23] Fig. 11 shows a schematic representation of the mesophases exhibited by the octyl homologue. Upon heating the material forms a smectic A_d* phase, where the rod-like molecules are arranged in interdigitated bilayers. Three crystal states are exhibited before melting to the smectic phase occurs at 67 °C. The mesophase is then stable upon further heating to 106 °C when it transforms to the liquid. Thus the octyl-homologue shows a varied and rich polymorphism, and it can be accurately described as being amphitropic, i.e. being a thermotropic as well as a lyotropic liquid crystal.

It can be seen from structural investigations[17,18,20,24] that thermotropic phases of microsegregating systems are equally subject to the effects of curvature as lyotropic phases, and indeed the thermotropic phases mirror those of the lyotropic phases as shown in Fig. 12.

In the following sections we systematically describe the effects that molecular architecture has on liquid-crystalline stability. We investigate the effects of the number of carbohydrate residues versus the number of aliphatic chains has on mesophase formation and temperature stability for thermotropic phases. In some cases we also make this investigation as a function of water concentration in lyotropic phases. Thus we systematically investigate one head group – one chain, one head group – two chains, one head group – three chains, etc. By using this approach we develop property–structure correlations which allow us to predict the mesophase behaviour of liquid crystal glycolipids from their chemical structures. In the following narrative we also use this method for predicting the properties of bola-amphiphiles where two head groups are joined by an aliphatic system.
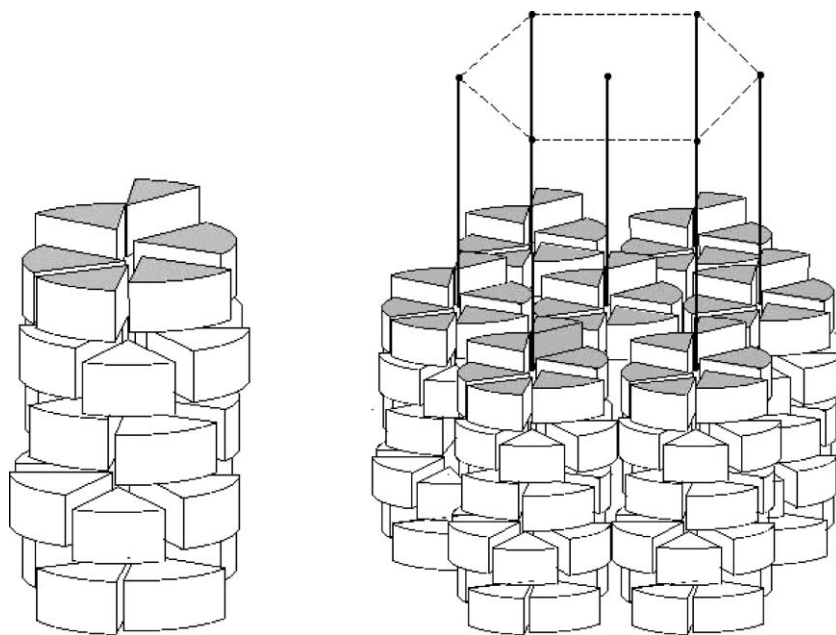
This journal is © The Royal Society of Chemistry 2007

Chem. Soc. Rev., 2007, **36**, 1971–2032 | 1975

Fig. 8 The molecules with wedge-like structures can stack to form columns where the molecules are disordered relative to the column axis (left), the columns can organise into rectangular or hexagonal arrays (right).
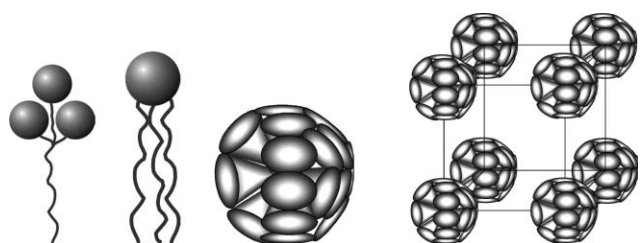

Fig. 9 Amphiphiles with conical structures (left) form structures where the curvature of packing results in the formation of a spherical supramolecular entity (centre), which self-organises to give a simple cubic mesophase (right).

The final section describes the synthesis of the materials. It is important to realise that to evaluate the liquid crystal properties of any type of material the purity of the compound

has to be high, usually >98%. The preparations described are thus the result of the best methods evaluated, and which have yielded products of high quality.

3. One head one tail

One head group – one chain may seem a simple structural architecture for an amphiphile, but for glycolipids the situation is complicated by the variation of the structures of the sugar units available for head group design, *i.e.* the head group may have an open chain structure, or a pyranose or a furanose ring
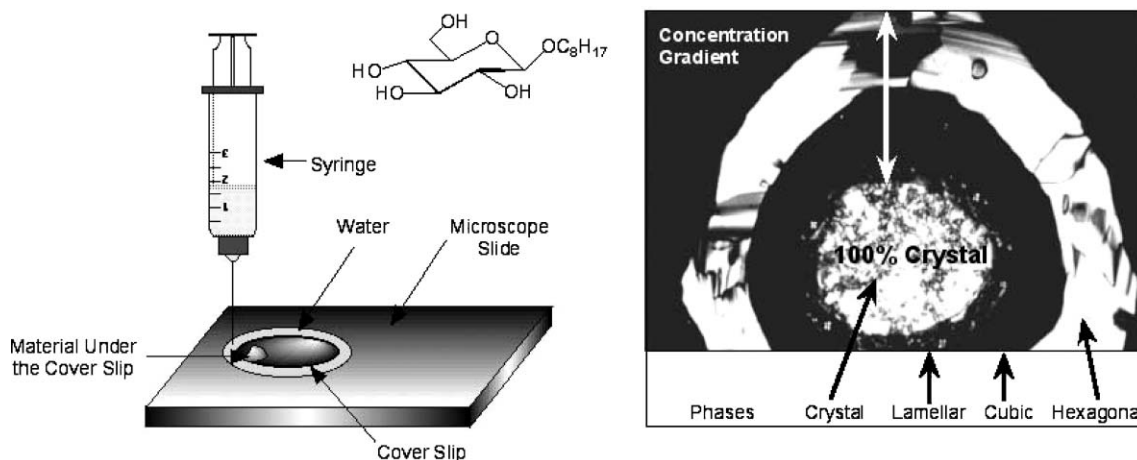

Fig. 10 The liquid crystal phases formed when a crystal of n-octyl β-D-glucopyranoside is dissolved in water, under crossed polars (×100).
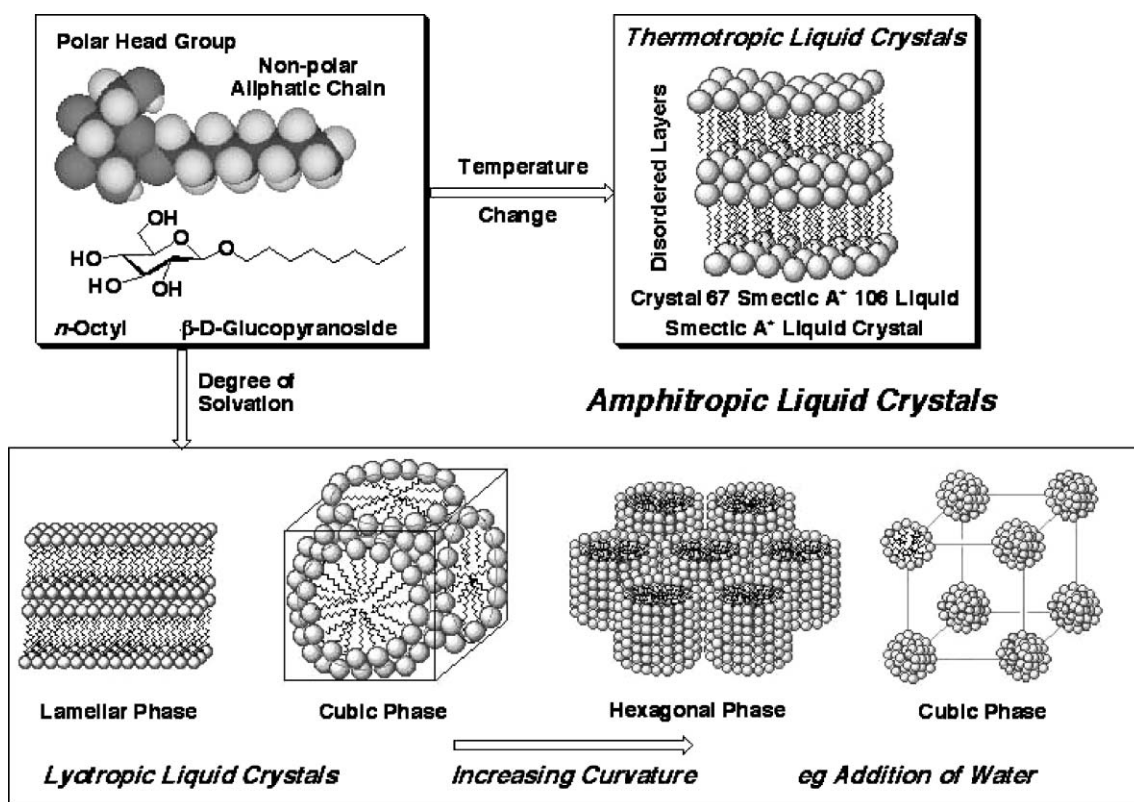
Fig. 11 Schematic structures of the thermotropic and lyotropic mesophases formed by n-octyl β-D-glucopyranoside.

structure. In the following sections, each of these structural variants will be discussed in more detail.

3.1 Non-cyclic carbohydrate systems

The simplest types of materials which have yielded the most detailed systematic property–structure correlations are the alkyl-substituted polyols. For these materials, the liquid crystal properties were investigated as a function of the aliphatic chain length, the number of hydroxyl groups and the type of linkage between the head group and the aliphatic chain.[25,63] Many of these materials were often found to exhibit both thermotropic and lyotropic phases, *i.e.* they are amphitropic liquid crystals. For systems that are composed of one aliphatic chain and one sugar/polyol head group lamellar smectic A or A* phases, depending on the stereochemistry of the material, were found to be formed *via* microphase segregation of the carbohydrate moieties with respect to the aliphatic chains. The smectic A* phase exhibits characteristic defect textures when observed using transmission optical microscopy, see Fig. 13. The focal-conic texture which was formed is characterised by hyperbolic and elliptical lines of optical discontinuity,[26] as labelled in the figure. These defects are diagnostic for the presence of a
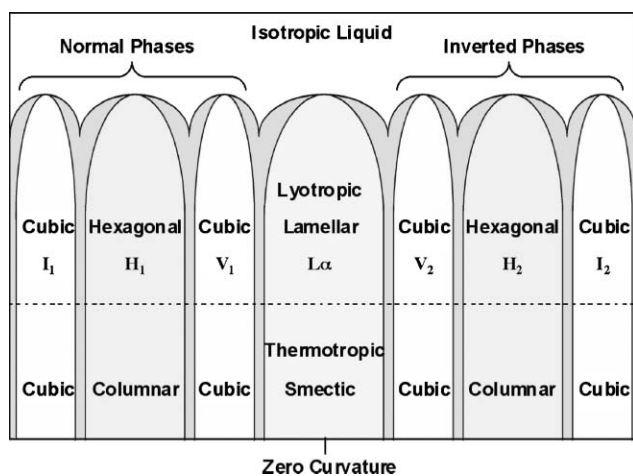

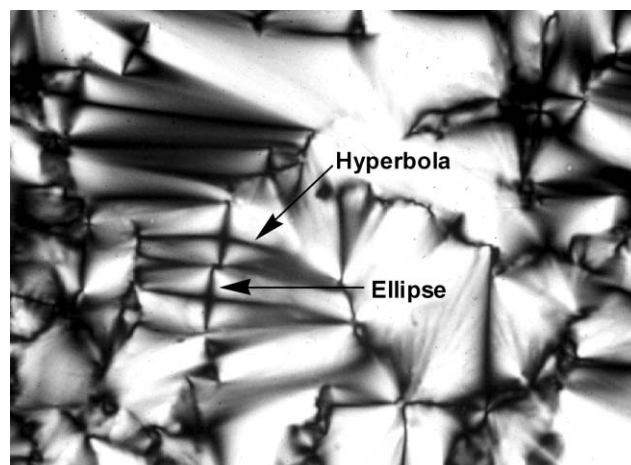**Fig. 12** Relationship between curvature and mesophase types.

Fig. 13 The focal-conic texture of the smectic A* phase of octyl β-D-glucopyranoside (×100).

This journal is © The Royal Society of Chemistry 2007

Chem. Soc. Rev., 2007, **36**, 1971–2032 | 1977

lamellar phase, and the clarity of the fan-like regions also indicate that the phase is smectic A*.

The first studies examined the effect on the clearing point of the thermotropic phases of alkyl-substituted polyols with respect to increasing the number of hydroxyl groups.[25] The synthetic pathways to these materials are described in Section 8.1. From the materials prepared (A to F in Fig. 14), it was found that the clearing points varied linearly with respect to the number of hydroxyl groups in the head group of the amphiphile, see Fig. 14 for studies on the dodecyl homologues. No change in mesophase type (i.e. calamitic to columnar) across the family of materials was found which indicates that the head groups have the same cross-sectional area as the number of CHOH groups is increased. Moreover, the results imply that there is a so-called "quantifiable amount of thermal stability" for the mesophase that is introduced into the system per each CHOH group which is incorporated into the head group of the molecular structure.[25]

In addition to showing a linear dependence of clearing point on the number of hydroxyl groups, it was also found that there was little or no effect of molecular chirality on the clearing points; compare for example compounds B and C, and, E and F in Fig. 14. In typical calamitic systems, molecular asymmetry can strongly affect mesophase behaviour, but in the case of the amphiphiles it appears that the effects that molecular asymmetry have on the packing of the head groups (and molecules) together is lost in the general disordered microphase segregated band of hydroxylated head groups in the lamellar phase.

Following on from this study, the effects on the self-organising properties caused by the sequential movement of the position of a dodecyl chain in acyclic x-O-dodecyl-(D or L)-xylitols[27] were reported, see Fig. 15. The movement of the dodecyl chain from the terminal position (1 or 5) to the inner positions 2 or 4 has the effect of increasing the bulky nature of the head group due to steric interference, and hence introducing curvature into the system by increasing the cross-sectional area of the head group. At the same time, due to the steric hindrance interfering with the motion of the aliphatic chain, the internal flexibility is reduced. However, the induced curvature is not great enough to stabilize the formation of columnar phases, but the clearing points rise due to the reduced flexibility. For the 3-substituted xylitol the head group is forked, and therefore bulky. Although no columnar phases are found, the smectic to isotropic liquid transition temperature is considerably higher in comparison to the other isomers. Thus, in spite of the increase in the bulky nature of the head group across the series 3 > 2,4 > 1,5, which should depress clearing points, the increased rigidity of the head group, due to restricted freedom of movement near to the location of the point of substitution, has the opposite and more dominant effect. This is further demonstrated by the rise in the melting points across the series, which also follows the same pattern of 3 > 2,4 > 1,5. Fig. 16 shows molecular simulations of the five isomers, demonstrating how the head group shape changes across the series of isomers.

In order to further develop systematic property–structure correlations the effects of the linking group, Z (where Z = O, S
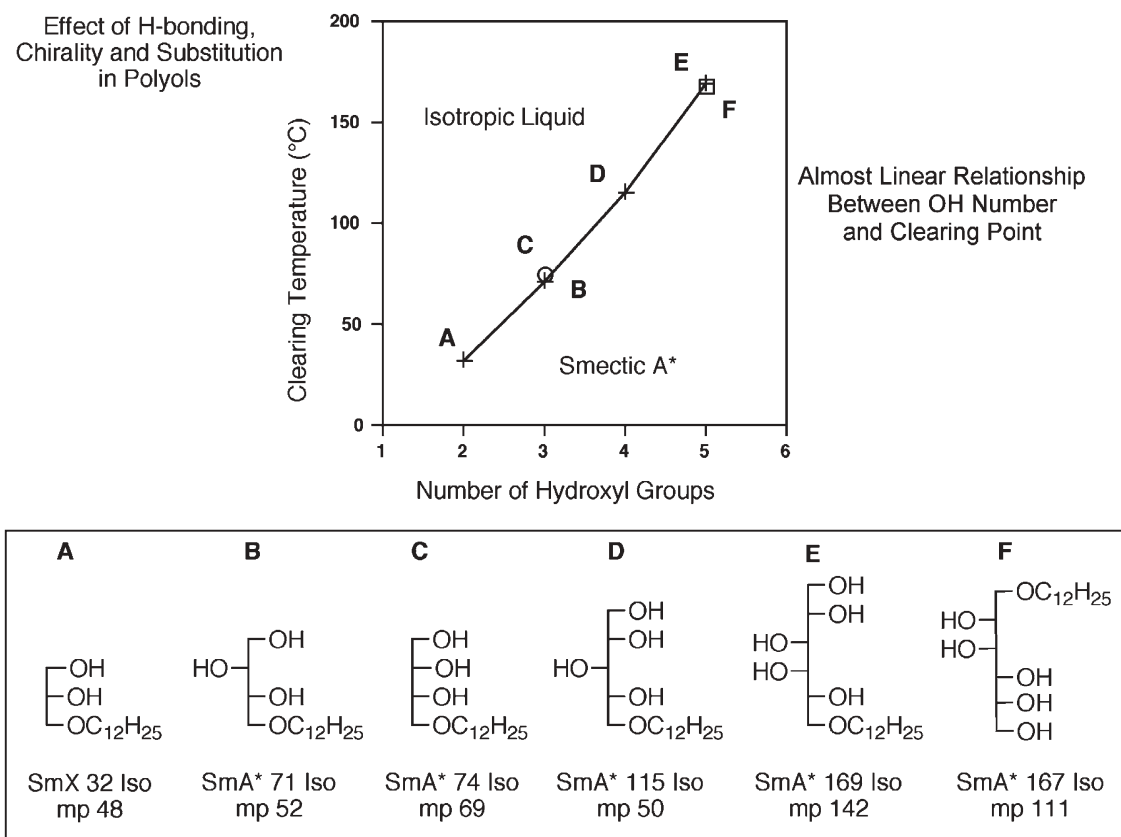

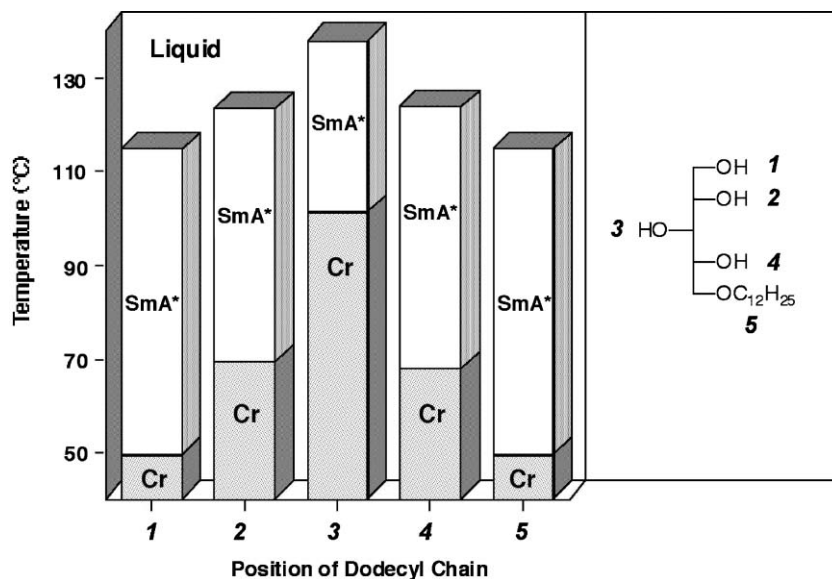**Fig. 14** Effect of the number of hydroxyl on clearing point and melting temperatures.

Fig. 15 Effect on transition temperatures caused by the sequential movement of the position of a dodecyl chain in the acyclic x-O-dodecyl-(D or L)-xylitols.
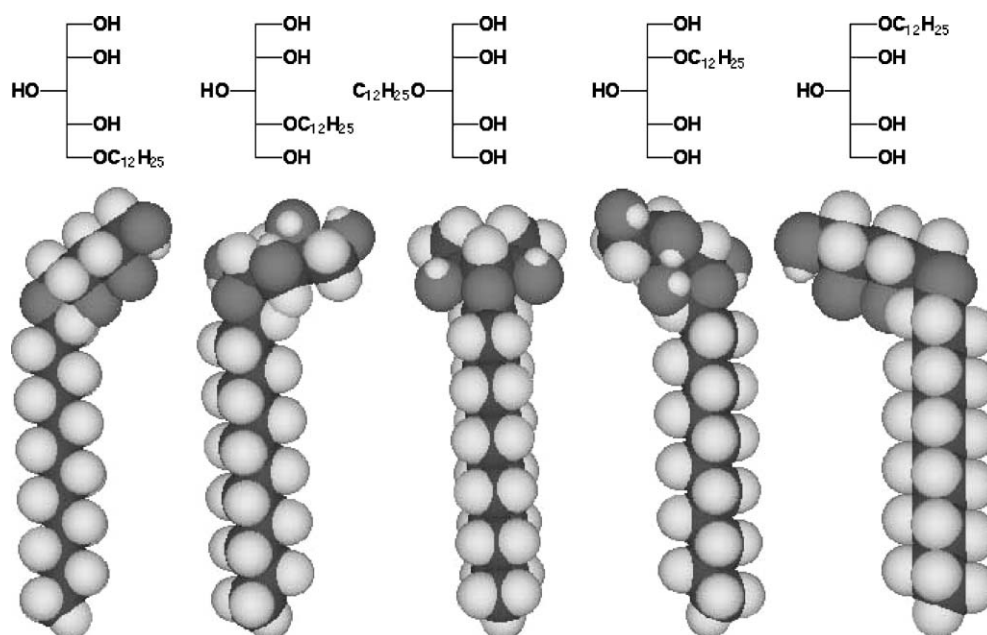

Fig. 16 Computer simulations of the acyclic x-O-dodecyl-(D or L)-xylitols in the gas phase at absolute zero. The figure shows how the cross-sectional area of the head group changes in shape as a dodecyl chain is moved sequentially from one position to the next.

or COO), positioned between the xylitol unit and the aliphatic chain in mono-substituted systems were examined: see structure **6**. Combining the literature results[28,29] on the thermotropic properties of the substituted L-xylitols, it is possible to show that the efficiency of the linking group in terms of the formation of thermotropic phases follows the pattern,[28] –SR > –OCOR > –OR.

Fig. 17 shows the variation in clearing point for the three series as a function of aliphatic chain length. The liquid crystal phases are introduced at relatively short aliphatic chain lengths (C_5); the clearing points then rise rapidly before levelling off (C_{10}). All of the materials exhibited lamellar smectic A*
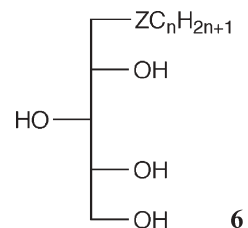
phases. The thioethers were found to have much higher clearing points than the ethers (approximately 30 °C).

Unlike the acyclic x-O-dodecyl-(D or L)-xylitols, molecular modelling (see Fig. 18) does not provide any definitive reasons
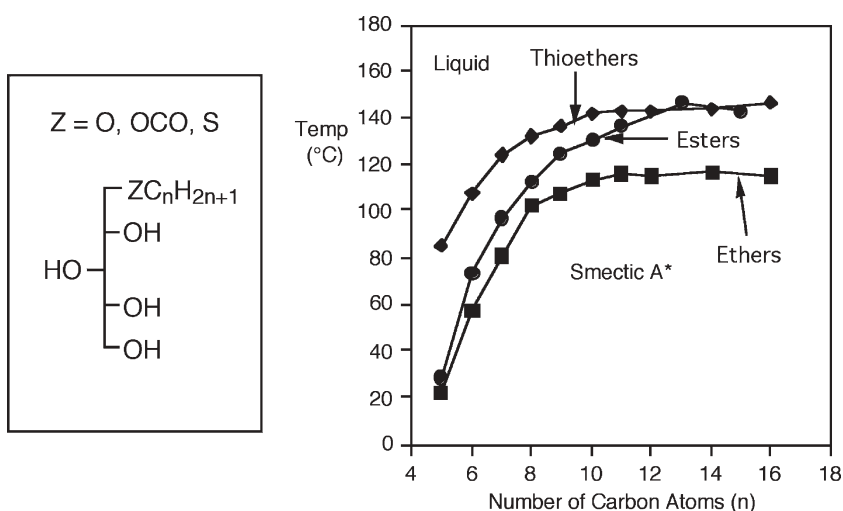
Fig. 17 The variation in transition temperatures (°C) as a function of aliphatic chain length (*n*) for the xylitols as the linking group **Z** was varied.

why the thioethers have higher clearing points than the esters or ethers, other than that sulfur is a much larger linking unit than the other two.

Surprisingly, at room temperature, the ethers form lyotropic phases more easily than the corresponding esters or the thioethers: see Table 1. The ethers also show a wider range of mesophase type (lamellar, columnar and discontinuous cubic). However, it should be emphasised that these results were only achieved at room temperature, and at higher temperatures the range of observable phases might change.

One other interesting comparison that was made was between the 6-*O*-alkyl-D-galactitols and their cyclic pyranose forms, 6-*O*-alkyl-D-galactopyranoses.[30–32] The transition temperatures (°C) were evaluated as a function of alkyl chain length. The results are shown in Fig. 19 respectively. Firstly the even members of the alicyclic systems were found to have higher clearing points, and secondly they were found to exhibit strong odd–even effects in the clearing points. The higher clearing points are related to the fact that the acyclic system has one more hydroxyl group available for H-bonding than the
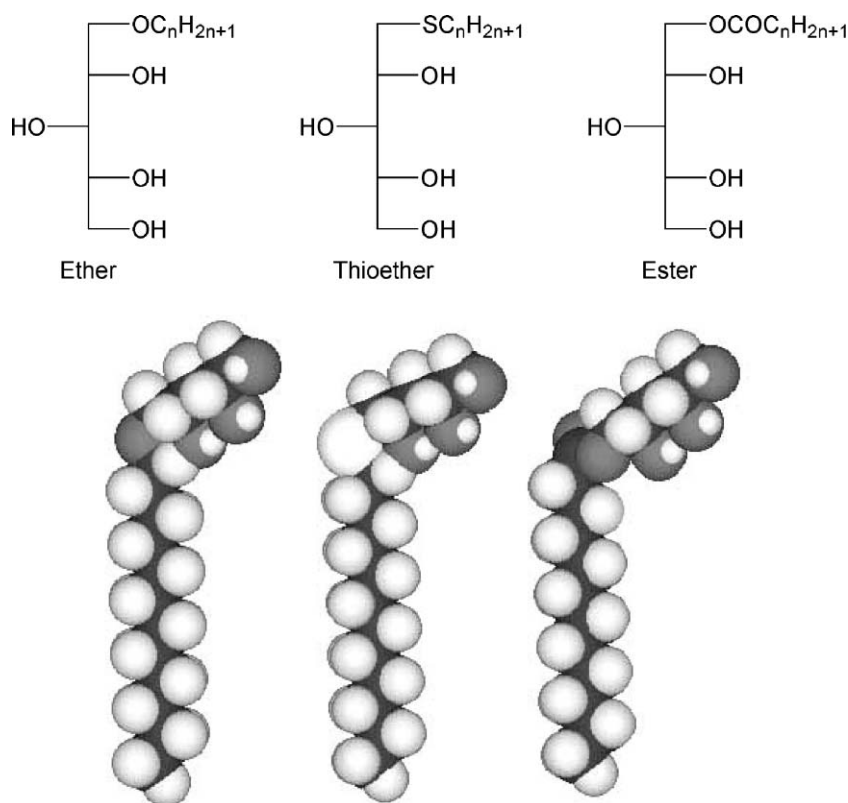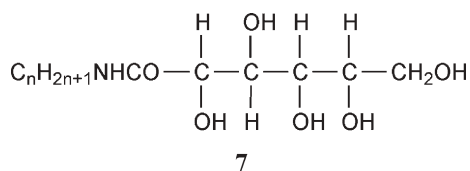

Fig. 18 Computer simulations of the thioether, ether and ester linked xylitols.

Table 1 Effect on formation of lyotropic liquid crystal phases at room temperature for the ether, ester and thioether linked xylitols as a function of terminal chain length (n)

n	Ethers	Thioethers	Esters
6	Continuously miscible	Not tested	Lamellar
7	Continuously miscible	Not tested	Lamellar
8	Lamellar	Lamellar	Not Liquid Crystal
9	Lamellar	Not Liquid Crystal	Not Liquid Crystal
10	Not Liquid Crystal	Not Liquid Crystal	Not Liquid Crystal
11	Lamellar/hexagonal/ discontinuous cubic	Not Liquid Crystal	Not tested
12	Not Liquid Crystal	Not Liquid Crystal	Not tested
14	Not Liquid Crystal	Not Liquid Crystal	Not tested
15	Not tested	Not tested	Not Liquid Crystal
16	Not Liquid Crystal	Not Liquid Crystal	Not tested

Table 2 Transition temperatures (°C) as a function of aliphatic chain length (n) for the n-alkyl gluconamides

n	Cryst 1		Cryst 2		Cryst 3		SmA*		Decomp		Iso Liq
6	•	120	—		—		—	•	156	—	•
7	•	79	•	96	•	150	•	156	•	—	
8	•	72	•	87	•	158	•	159	•	—	
9	•	84	•	99	•	159	•	175	•	—	
10	•	75	•	91	•	157	•	182	•	—	
11	•	77	•	99	•	157	•	190	•	—	
12	•	81	•	94	•	155	•	189	•	—	
18	•	111	•	151	—		—	•	197	•	—

cyclic system. It is not so clear, however, why the odd–even effect is so strong for the galactitols.

Amides have also been used as linking groups; they are of particular interest because they can introduce further sites for hydrogen bonding. The liquid crystal properties of the n-alkyl gluconamide family of materials, **7**, have been extensively investigated. The data sets produced were the first of their kind to detail the effects of changing aliphatic chain length on the thermotropic liquid-crystalline properties for open chain sugars.[33] This work followed on from the study made on the single compound, octyl D-gluconate.[34]

$$C_nH_{2n+1}NHCO - \overset{\overset{H}{|}}{C} - \overset{\overset{OH}{|}}{C} - \overset{\overset{H}{|}}{C} - \overset{\overset{H}{|}}{C} - CH_2OH$$
$$\underset{OH}{|} \quad \underset{H}{|} \quad \underset{OH}{|} \quad \underset{OH}{|}$$

7

From the classification of the mesophases formed by the gluconamides as smectic A*, it was clear that the structure of

the mesophase was composed of alternating hydrophobic and hydrophilic slabs. Consequently, this work was one of the earliest to demonstrate that microsegregation can be used as a model to support not only lyotropic, but also thermotropic mesophase formation. The temperatures of the phase transitions for the hexyl to dodecyl and octadecyl homologues are given in Table 2. It can be seen that the clearing points rise with chain length, and as the temperatures approach 200 °C decomposition becomes an ever increasing problem.

The related materials, the glucitols **8** and glucanamides **9** and **10** were subsequently prepared and examined.[35] However, these materials were mostly non-mesogenic, but those that exhibited liquid-crystalline behaviour showed the same phase types as the n-alkyl gluconamides, i.e. the mesophases were classified as smectic A*. The N-methyl group in **8**, in comparison to the gluconamides, prevents further sites for H-bonding, and moreover it also interferes with efficient packing of the molecules together, thereby suppressing mesophase formation.

There are of course many other acyclic amphiphiles that have been reported; however, the examples described serve to provide simple, but general, property–structure correlations for one head group – one chain systems.
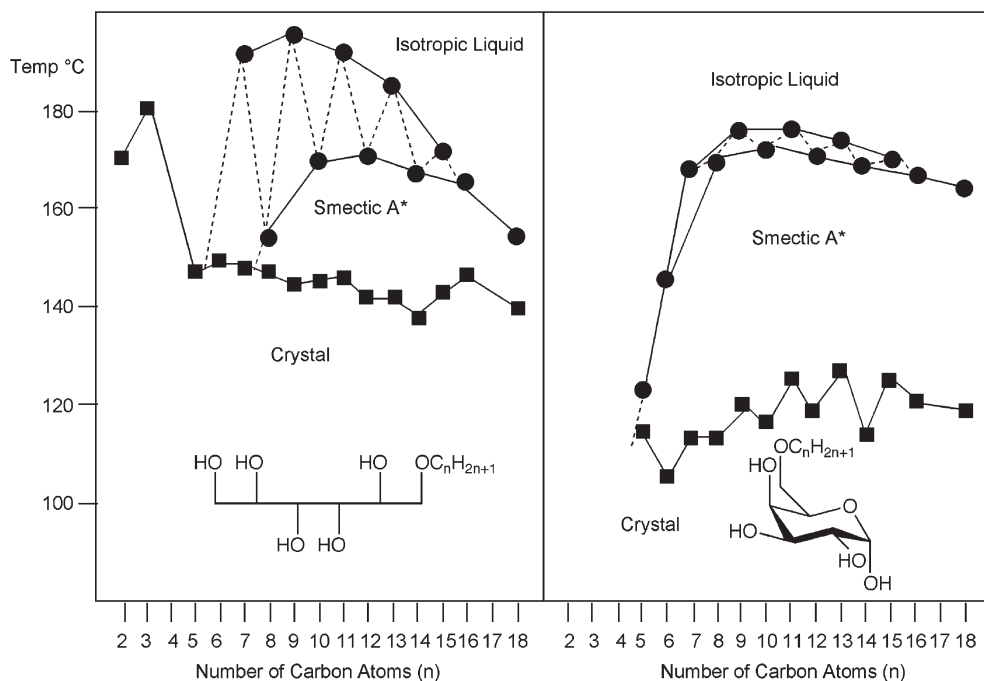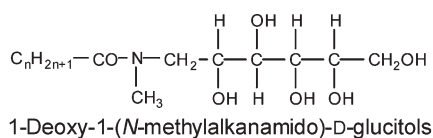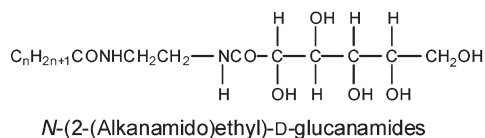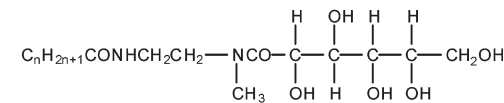

Fig. 19 The transition temperatures (°C) as a function of the aliphatic chain length (n) for the 6-O-alkyl-D-galactitols (left) and the 6-O-alkyl-D-galactopyranoses (right).

$$C_nH_{2n+1}-CO-N-CH_2-\overset{\overset{\displaystyle H}{|}}{\underset{\underset{\displaystyle OH}{|}}{C}}-\overset{\overset{\displaystyle OH}{|}}{\underset{\underset{\displaystyle H}{|}}{C}}-\overset{\overset{\displaystyle H}{|}}{\underset{\underset{\displaystyle OH}{|}}{C}}-\overset{\overset{\displaystyle H}{|}}{\underset{\underset{\displaystyle OH}{|}}{C}}-CH_2OH$$

1-Deoxy-1-(*N*-methylalkanamido)-D-glucitols

8

$$C_nH_{2n+1}CONHCH_2CH_2-NCO-\overset{\overset{\displaystyle H}{|}}{\underset{\underset{\displaystyle OH}{|}}{C}}-\overset{\overset{\displaystyle OH}{|}}{\underset{\underset{\displaystyle H}{|}}{C}}-\overset{\overset{\displaystyle H}{|}}{\underset{\underset{\displaystyle OH}{|}}{C}}-\overset{\overset{\displaystyle H}{|}}{\underset{\underset{\displaystyle OH}{|}}{C}}-CH_2OH$$

N-(2-(Alkanamido)ethyl)-D-glucanamides

9

$$C_nH_{2n+1}CONHCH_2CH_2-NCO-\overset{\overset{\displaystyle H}{|}}{\underset{\underset{\displaystyle CH_3}{|}}{C}}-\overset{\overset{\displaystyle OH}{|}}{\underset{\underset{\displaystyle H}{|}}{C}}-\overset{\overset{\displaystyle H}{|}}{\underset{\underset{\displaystyle OH}{|}}{C}}-\overset{\overset{\displaystyle H}{|}}{\underset{\underset{\displaystyle OH}{|}}{C}}-CH_2OH$$

N-(2-(*N*-methylalkanamido)ethyl)-D-glucanamides

10

3.2 Pyranose systems

As pyranose systems have cyclic structures, they are somewhat similar in molecular design to conventional thermotropic liquid crystals. In typical non-amphiphilic thermotropic liquid crystal systems, it is common to develop property–structure correlations *via* the investigation of the variation in transition temperature(s) as a function of systematic changes in molecular structure. However, unlike conventional thermotropic liquid crystals, carbohydrates can exist in a variety of structural forms which can affect transition temperatures, enthalpies of transition, and physical properties. Glucose for example, can exist in an open chain (acyclic) form, in a six membered ring (pyranose) form, or in a five membered ring (furanose). In addition, it is difficult to specify the exact stereochemistry at the 1-position (the anomeric position) because in some cases sugars invert their structures easily at the anomeric position and at best only a ratio of the amount of α-substitution to β-substitution can be given. This is particularly true for situations where the 1-position is unsubstituted. Thus, it is possible to give a number of transition temperatures for a compound described, for example, as simply octyl glucoside. In Fig. 20 the thermotropic transition temperatures are given for the α- and β-substituted pyranose and furanose

forms of octyl glucoside.[36] It can be seen from this figure that the pyranose forms have higher clearing temperatures, with the α form being higher than the β for the pyranoside, whereas the order is reversed for the furanosides. Unlike conventional thermotropic systems, this observation does not herald the introduction of a property–structure correlation because the order of clearing temperatures α-pyranoside > β-pyranoside > β-furanoside > α-furanoside, does not necessarily translate to other sugar systems. Consequently it is very difficult to develop property–structure correlations for the thermotropic properties of substituted sugars.

Unfortunately, systematic studies for cyclic glycolipids with respect to the relationship between the position of substitution of an aliphatic chain and thermotropic behaviour are relatively few. One such comparison has been completed for the thermotropic properties of the x-*O*–dodecyl α,β-D-glucopyranoses by Miethchen and other researchers.[19,23,24] Miethchen *et al* demonstrated the effect on clearing point temperatures as a dodecyl chain is moved sequentially from one position to the next in substituted D-glucopyranose systems:- see Fig. 21.

In Fig. 21, the dodecyl chain is moved from the 1- to 6-position; however, the ratio of α to β anomer for this series of materials varies from one member to the next, except for the glucopyranoside homologue where either 100% α or 100% β anomer is present. Despite the variation of the anomeric purity across the series, there is still a wide range in clearing points from 140 to 167.2 °C, which is also influenced by the position of substitution.

Interestingly, the mesophase exhibited by all of the homologues is the same; *i.e.* smectic A_d* where the molecules have an interdigitated arrangement within the layers and where the layer thickness to molecular length has a ratio of 1.4 : 1. The fact that the mesophase type is lamellar suggests the shapes of the molecules, for each of the members of the series, are rod-like, with the carbohydrate head group having a similar cross-sectional area to that of the aliphatic chain.

The systematic study of the liquid crystal properties in the alkyl β-D-glucopyranosides observed as a function of aliphatic chain length reveals some interesting comparisons. Evaluation of the thermotropic properties shows that the clearing points rise steeply as the chain length is increased (see Fig. 22) whereas the melting points remain relatively constant.[23] As the chain length is increased the number of crystal phases rises. Throughout the series of compounds the only liquid crystal phase observed is the smectic A* phase. When the materials
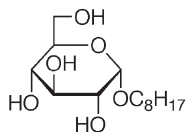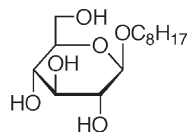
Alkyl D-Glucofuranosides
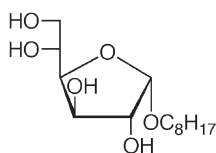
Cryst 51 SmA* 60.6 °C Iso Liq
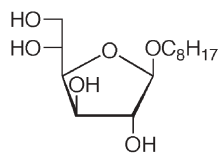
Cryst 61 SmA* 99.2 °C Iso Liq

Alkyl D-Glucopyranosides

Cryst 72.3 SmA* 116.3 °C Iso Liq

Cryst 67.1 SmA* 106.4 °C Iso Liq

Fig. 20 Comparison of the mesophase behaviour and transition temperatures for the α- and β-octyl D-glucofuranosides with the α- and β-octyl D-glucopyranosides.
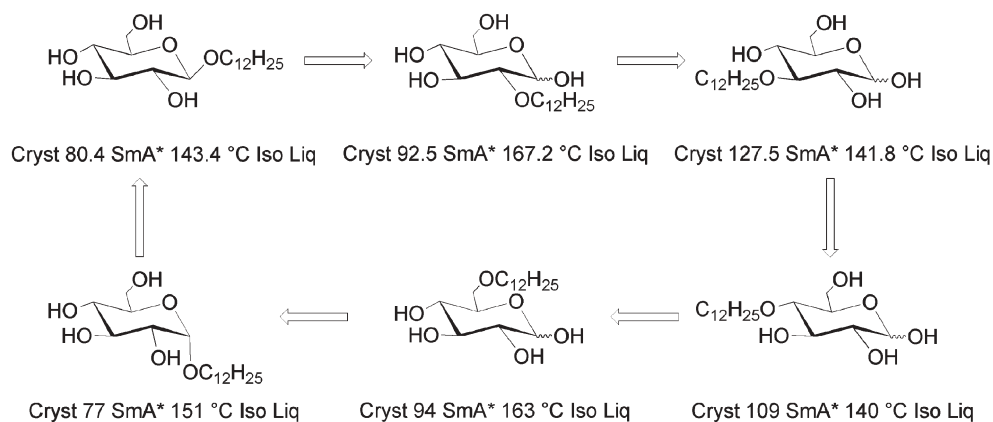
Fig. 21 Effect of position of substitution of a dodecyl aliphatic chain on the liquid crystal properties of the x-*O*-dodecyl α,β-D-glucopyranoses and glucopyranosides.

are investigated for their lyotropic phase behaviour, meso-phases other than the lamellar phase are introduced into the phase sequences.

The lyotropic phase behaviour, at room temperature, was evaluated for four of the homologues using the solvation method described earlier. Fig. 23 shows the solvation of a crystal of each of the materials. The heptyl homologue only exhibits a lamellar phase, whereas the octyl homologue exhibited lamellar, bicontinuous cubic, and columnar phases. The decyl homologue was found to exhibit lamellar and micellar cubic phases. By inserting a λ wave-plate into the microscope, the Becker line separating the isotropic liquid from the cubic phase was observed. The dodecyl material did not exhibit lyotropic phases. Thus this study demonstrates that the even homologues of the alkyl β-D-glucopyranosides have a greater tendency to exhibit thermotropic liquid crystal phases in comparison to lyotropic phases. However, the range of

lyotropic phases observed (lamellar, bicontinuous cubic, hexagonal and cubic phases) was greater than the range found for the thermotropic phases (SmA*). At longer aliphatic chain
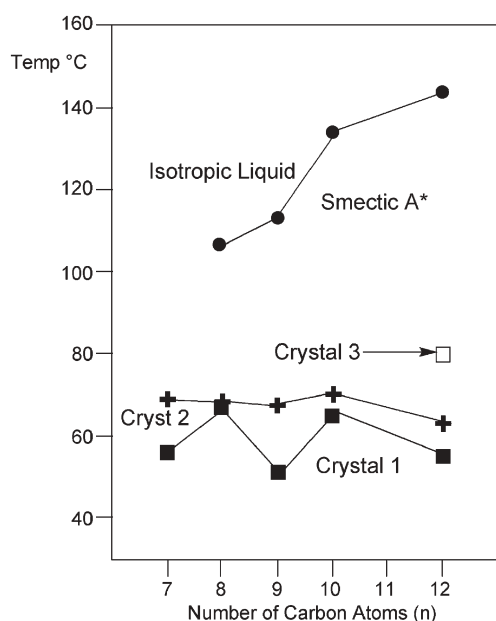

Fig. 22 The transition temperatures (°C) as a function of the aliphatic chain length (*n*) for the alkyl β-D-glucopyranosides.
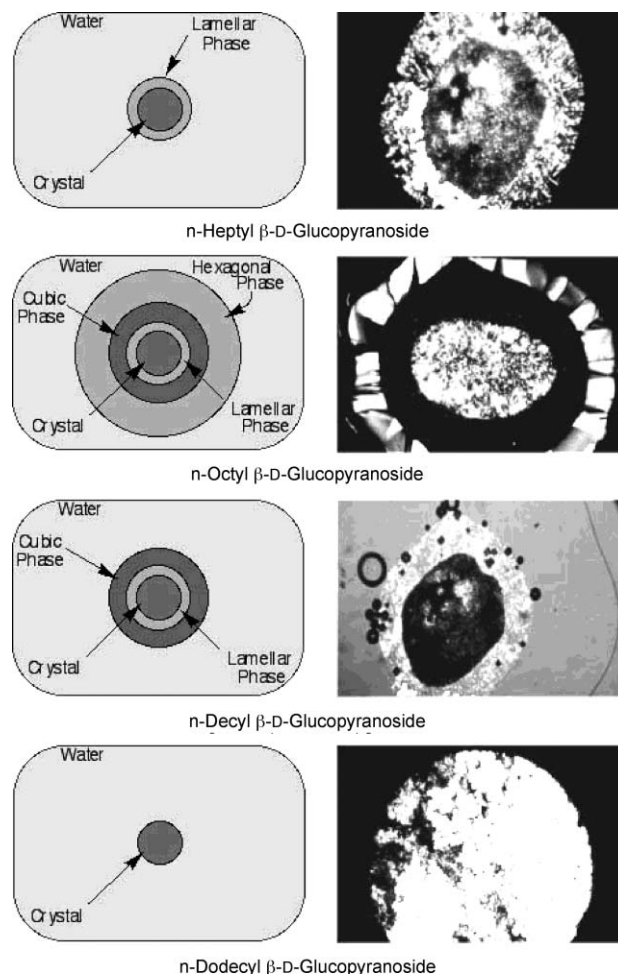

Fig. 23 The solvation of crystals of four alkyl β-D-glucopyranosides in water. The left-hand cartoons depict the results of solvation, whereas the right hand photomicrographs were taken under crossed polars (× 100), except for the decyl homologue where a λ wave-plate was inserted.

This journal is © The Royal Society of Chemistry 2007

Chem. Soc. Rev., 2007, **36**, 1971–2032 | 1983

lengths, the glycolipids are not conducive to exhibiting lyotropic phases, even upon heating, suggesting that glycolipids in membranes are only moderately solvated by water.

As with the acyclic systems, studies have been performed on linking groups between the sugar moiety and the aliphatic chain. Linkages involving sulfur in comparison to oxygen have been made for a variety of different sugars. One example is shown for the 6-substituted galactopyranoses. As with the acyclic systems the 6-*S*-n-alkyl-6-thio-α-D-galactopyranoses have higher clearing points than the 6-*O*-n-alkyl-α-D-galactopyranose equivalents:- see Fig. 24.[37] Again the mesophase observed is smectic A*.

Many other linking groups have been investigated for pyranose systems. For example, the (*N*-alkylcarbamoyl)methyl α-D-glucopyranosides, **11**, exhibit smectic A* phases as expected.[38] The syntheses for these materials are described in Section 8.2. The melting points are in the range of 63 to 100 °C, and the clearing points reach levels of just below 200 °C:- see Table 3. Smectic phases are injected into the homologous series starting at an aliphatic chain length of between eight to nine carbon atoms. Thus the liquid crystal properties of this series of materials are very similar to others where the head-group possesses a pyranose ring structure with one aliphatic chain attached to it. Across a number of series investigated it appears that the liquid crystal phase sequences in glucopyranosides and
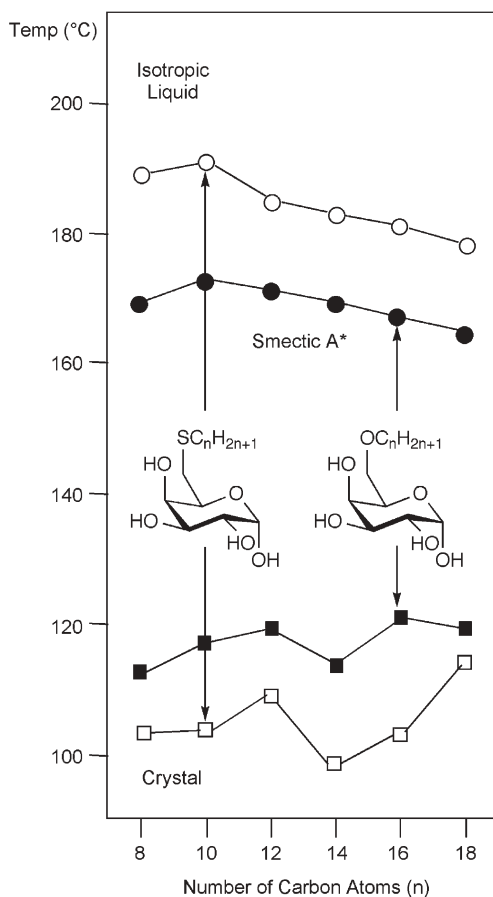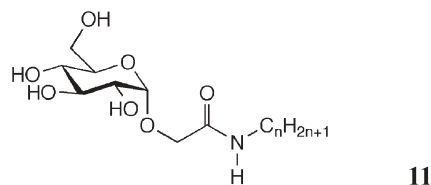
Table 3 Transition temperatures (°C) for the (*N*-alkylcarbamoyl)-methyl α-D-glucopyranosides as a function of aliphatic chain length

n	Cryst		SmA*		Iso Liq
6	•	63	—	—	•
8	•	74	—	—	•
10	•	81	•	94	•
14	•	89	•	122	•
15	•	92	•	178	•
16	•	100	•	192	•

associated transition temperatures are relatively insensitive to linking groups and position of substitution of aliphatic chains.

11

For the carbamoyl systems, steroidal examples were also reported as shown by structures **12** to **15**. All compounds were found to decompose at high temperatures (>230 °C). The cholestanyl derivatives, **12** and **13**, were shown to melt to smectic A* phases at temperatures of 202 and 181 °C respectively. However, the cholesteryl derivatives decomposed at temperatures above 230 °C without exhibiting any mesophases. Because of decomposition it was difficult to ascertain if any mesophase formation occurred on cooling.

Cryst 202 SmA* >230 °C Decomp

12
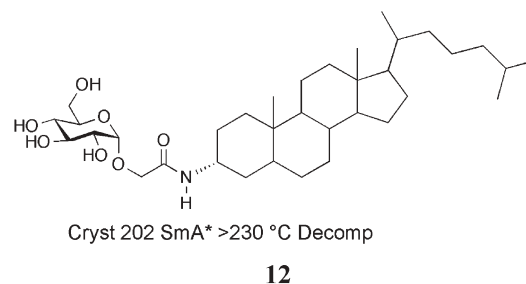
Simulations of the structures of the cholestanyl compounds allowed for speculative modelling of the lamellar phase, as shown in Fig. 25. Here the steroid units pack tightly together, but because of their bulky nature the sugar units cannot pack closely together. This leads to interdigitation of the sugar units between the layers. This type of structuring could lead to the formation of an intercalated smectic phase[39] where the local orientational ordering within the layers passes from one layer to the next.

One of the families of glycolipids that has not often been reported on, is the fructosides. D-Fructose is one of the most naturally abundant carbohydrates. It appears generally as a β-furanosyl residue in sucrose or in plant and bacterial polysaccharides.[40] Inulins and levans, which provide respective examples of β-(1,2)- and β-(2,6)-glycosidic linkages between fructofuranose moieties, possess interesting biofunctional properties and are involved, for instance, in defence mechanisms against microorganisms or as food reservoirs.[41] As a consequence of their biological importance, various enzymatic

Fig. 24 Comparison of the clearing and melting points (°C) of the 6-*S*-n-alkyl-6-thio-α-D-galactopyranoses and the 6-*O*-n-alkyl-α-D-galactopyranoses as a function of aliphatic chain length (*n*).

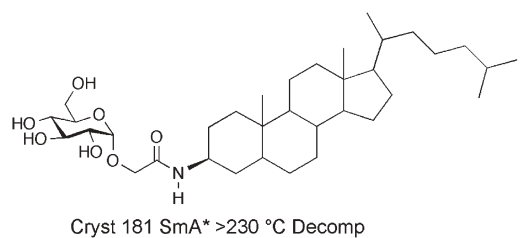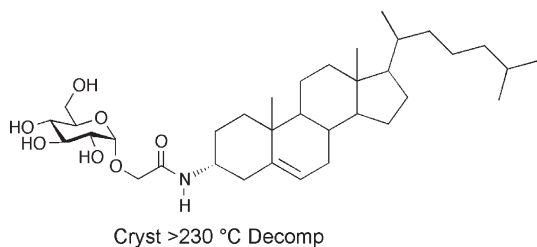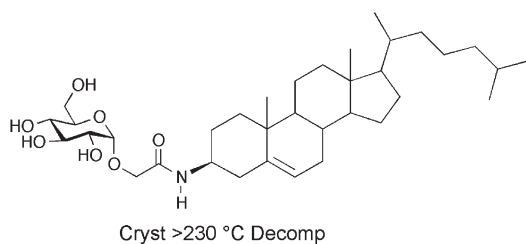Cryst 181 SmA* >230 °C Decomp

13

Cryst >230 °C Decomp
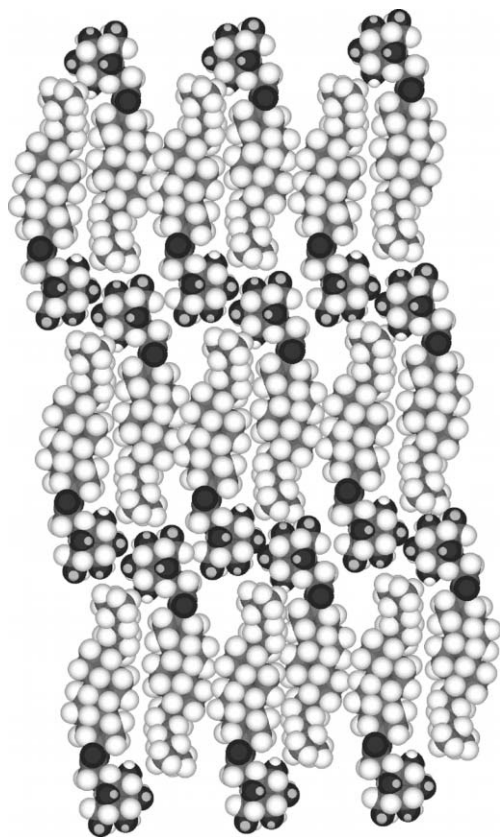
14

Cryst >230 °C Decomp

15

Fig. 25 Proposed packing of the layers in the smectic A* phase of the compound **12**.

and chemical methods have been proposed for the synthesis of fructofuranosyl derivatives:- see Section 8.3.

Generally, glycosidic amphiphiles of fructose readily self-assemble and self-organise to give a variety of thermotropic and lyotropic liquid crystal phases, and they find applications as surfactants or as specialised non-ionic detergents, especially for the solubilisation and the extraction of membrane proteins.[42]

The even homologues of the alkyl β-D-fructopyranosides, **16**, were prepared[43] so that their liquid crystal properties could be compared with the alkyl β-D-glucopyranosides. The clearing points determined by thermal polarizing optical microscopy and melting points measured by DSC on the first heating cycle are shown together in Table 4 as a function of the alkyl chain length (n).
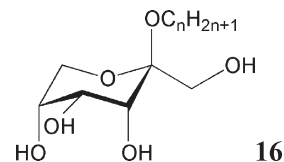
The appearance of a smectic A* phase only begins for the dodecyl β-D-fructopyranoside, and then disappears before the octadecyl analogue is reached. On cooling from the smectic A* phase for the C_{12}, C_{14} and C_{16} homologues, or the isotropic liquid for the remaining compounds, a novel mesophase was found. The thermal stability of the new phase, X, initially increases with chain length only to marginally decrease from the decyl homologue onwards. Finally, the melting points do not seem to be affected much by the length of the alkyl substituent, with the exception of the C_{18} member. Fig. 26 depicts these property–structure correlations as a function of alkyl chain length.

The mesophase formed directly from the isotropic liquid for the C_{12}, C_{14} and C_{16} homologues was classified as smectic A* by miscibility studies with the standard material octyl β-D-glucopyranoside. For the new phase, X, which was exhibited by all of the materials, mesophase classification was attempted by examination of the defect textures observed on cooling from the preceding phase (smectic A* or isotropic liquid). Taking the tetradecyl homologue as an example, upon cooling from either the homeotropic or focal-conic smectic A* phase, worm-like filaments or ribbons slowly separated from the smectic A* regions and coalesced in the bulk to form a fan-like texture with a large number, of what appeared to be, edge dislocations with associated high energy walls in the vicinity of

Table 4 The transition temperatures (°C) as a function of chain length (n) for the alkyl β-D-fructopyranosides

n	Cryst	X		SmA*		Iso Liq
6	124.3	•	124.4	—	—	•
8	128.5	•	131.0	—	—	•
10	129.1	•	133.3	—	—	•
12	128.6	•	131.6	•	132.7	•
14	130.0	•	131.0	•	136.5	•
16	129.6	•	129.9	•	135.8	•
18	114.5	•	128.2	—	—	•

This journal is © The Royal Society of Chemistry 2007

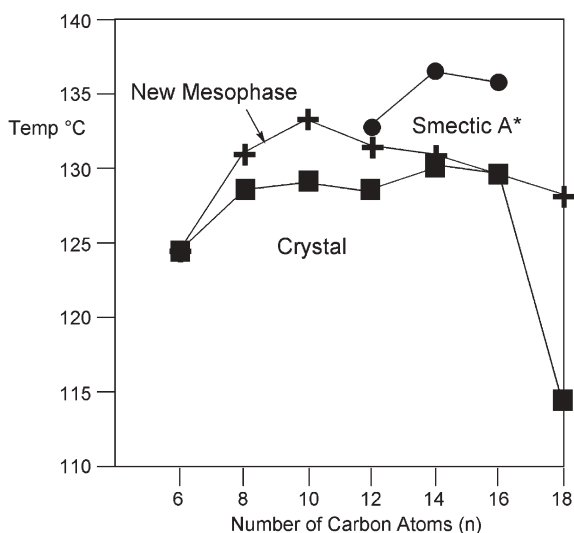*Chem. Soc. Rev.*, 2007, **36**, 1971–2032 | 1985

Fig. 26 The transition temperatures (°C) as a function of chain length (*n*) for the alkyl β-D-fructopyranosides.

the defect cores:- see Fig. 27. No hyperbolic or elliptical discontinuities[26] were observed indicating that the X-phase does not have a lamellar structure. In addition, no surface treatment was capable of inducing a homeotropic texture for the X phase. Indeed in paramorphotic formation from the smectic A* phase, the destruction of the homeotropic texture at the transition to the X phase strongly suggests that the X phase is not lamellar in character. Furthermore, the X phase was found to be difficult to shear, indicating that it has a much higher viscosity than the layered smectic A* phase.

The presence of the banded fan-like defects for the X phase indicated that it could have a columnar structure where the molecules are ordered along the column axes.[44] Columnar mesophases generally have structures based on either rectangular or hexagonal packing of the columns. Hexagonal phases can exhibit both homeotropic and homogeneous textures, whereas the textures associated with a rectangular phase tend to be birefringent. Thus, as the X phase did not exhibit a homeotropic texture, it was thought to be most likely a rectangular columnar phase.

X-ray diffraction was used to elucidate the structure of the X phase further. The (100) reflection of the tetradecyl analogue
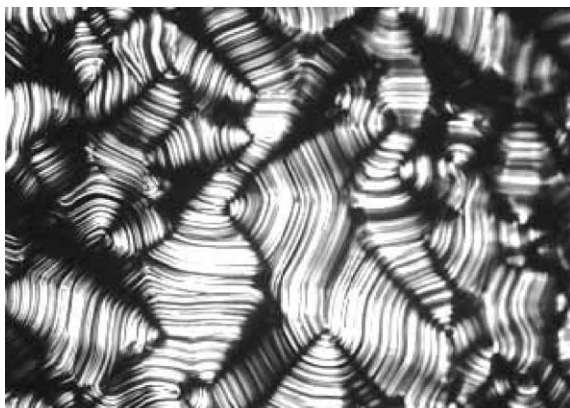
was examined upon cooling at 133.3 in the SmA* and at 125.8 °C in the novel X mesophase (with supercooling):- see Fig. 28. The peak width in the smectic A* phase was found to be effectively resolution limited (FWHM = 1.31×10^{-3} Å^{-1}), whereas the same reflection in the X phase was shown to be much wider at some $6\times$ resolution (FWHM = 8.3×10^{-3} Å^{-1}), indicating a short-range reflection plane order with a correlation length of *ca.* 230 Å (*ca* 8 × smectic A* bilayers). The correlation length was estimated on the assumption that correlations decayed exponentially, which was thought to be reasonable since the diffraction peaks had Lorentzian forms. The short-range correlation length for the layer ordering was thought to support the possibility of a composite columnar structure that retains local, finite-sized, smectic-A* regions as one of its structural components.

A $Q_{\parallel}$ scan at 125.8 °C in the X phase confirmed the absence of a (110) reflection. The $Q_{\parallel}$ scan also showed that, like the (100) reflection, the (200) reflection was not resolution-limited. If it is assumed that the composite columnar structure is composed of layered sub-units, which are responsible for the observed broad (100) and (200) reflections, then there could exist additional diffraction features at lower $Q_{\parallel}$ wave vectors associated with a 2D ordering of larger columnar sub-units. However, no further peaks were observed from the experiments. This implied that if a 2D structure with a large unit cell existed, then the scattering is either weak or the unit cell has a size larger than 0.13 μm.

In summary, the X-ray diffraction studies did not rule out the possibility of a columnar-type structure for the X phase, although higher order reflections would be expected as well as those due to the (100) plane.[45] If the X-phase is columnar, however, the columns cannot be arranged in a simple 2-D lattice, unless the dimensions of the lattice are extremely large. This suggests that if a columnar structure is present, then the columns will be packed in a disordered way. To date, the structure of the X phase has not been fully elucidated. However, it is interesting to note that the fructosides provide
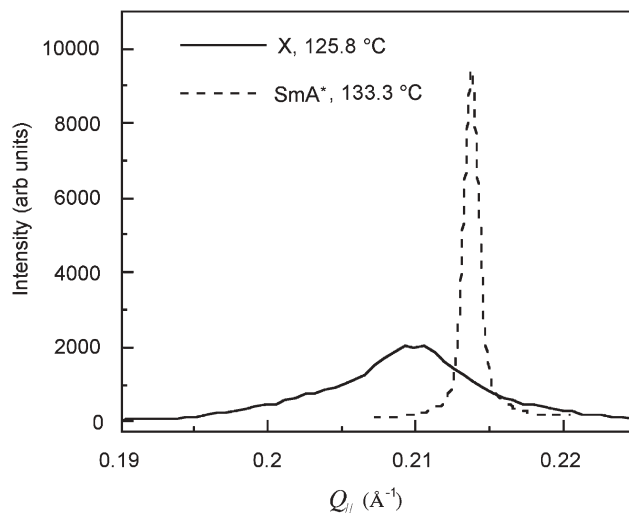

Fig. 28 Primary reflections of tetradecyl β-D-fructopyranoside upon cooling at 133.3 and 125.8 °C (with supercooling). Notice the increase in FWHM in the X phase.

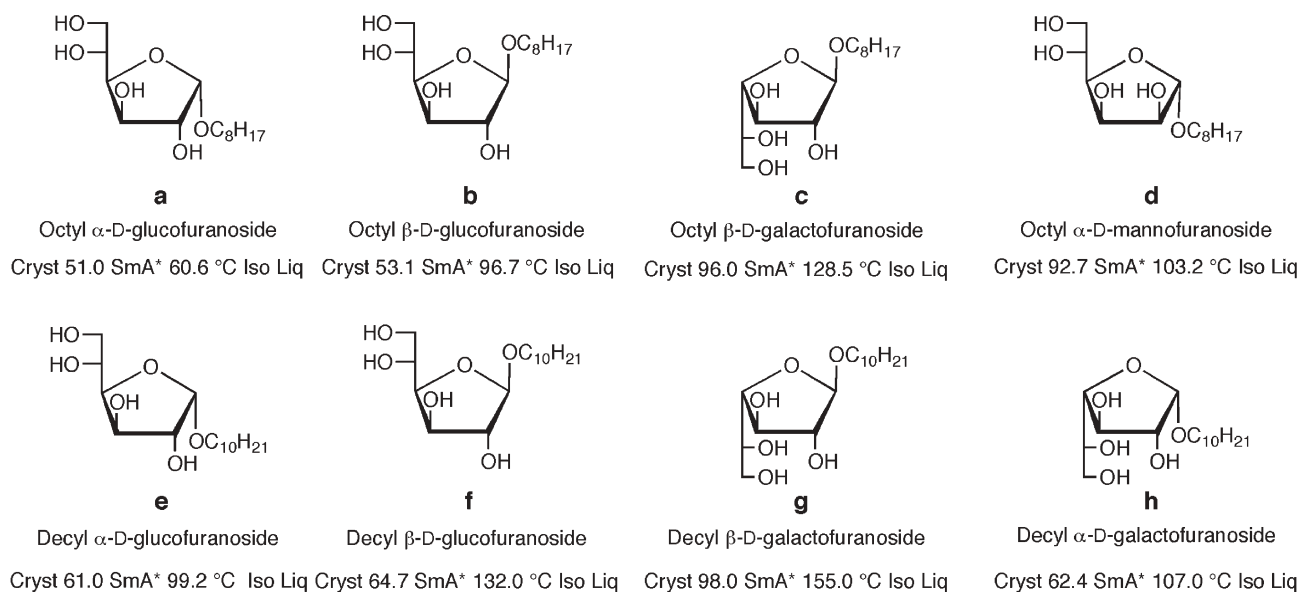**Fig. 27** The defect texture of the novel mesophase X (×100).

Fig. 29 The transition temperatures (°C) for a number of related glycofuranosides.

examples of very different mesomorphic behaviour in comparison to the gluco- and galacto-pyranosides.

3.3 Furanose systems

In the following section the transition temperatures and the properties of eight furanosides, in their neat forms, will be described.[36] The materials were prepared by novel and efficient synthetic routes, as described in Section 8.3 unlike those reported by other researchers using traditional multistep synthetic pathways.[46,47] The results obtained for the transition temperatures are given in Fig. 29.
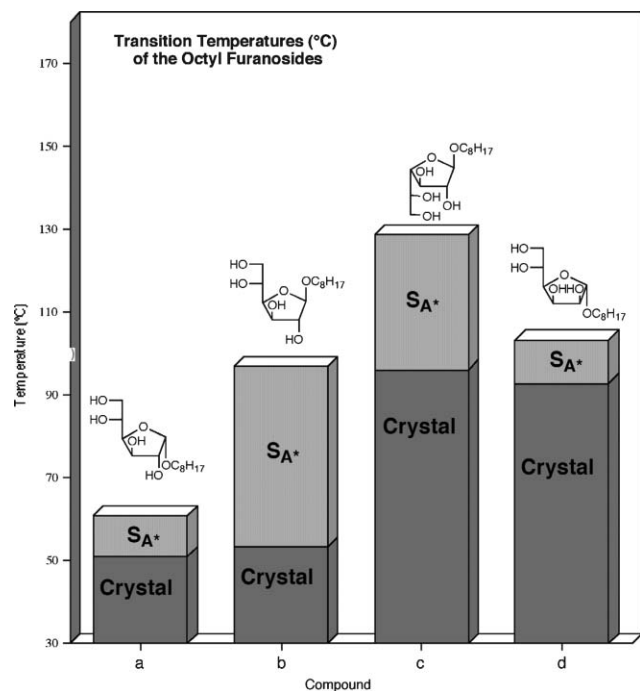
Fig. 29 groups the materials into two sets based on alkyl chain length; the top row shows the octyl derivatives and the bottom row the related decyl derivatives. For both the octyl and decyl derivatives, the α-glucofuranoside (a and e) have the lowest values for the clearing point transition, whereas the octyl β-anomer, b, has a comparable clearing point to the octyl α-mannofuranoside, d. However, in both groups the β-substituted galactofuranosides (c and g) have the highest clearing point temperatures. Fig. 30 shows the variation in clearing and melting point temperatures for the octyl derivatives.

A number of miscibility studies were carried out in order to establish the identities of the thermotropic mesophases exhibited by the furanosides. For example, Fig. 31 shows a selection of miscibility studies carried out using the previously classified material octyl β-D-glucopyranoside as the standard.[19] In this figure co-miscibilities between the liquid crystal

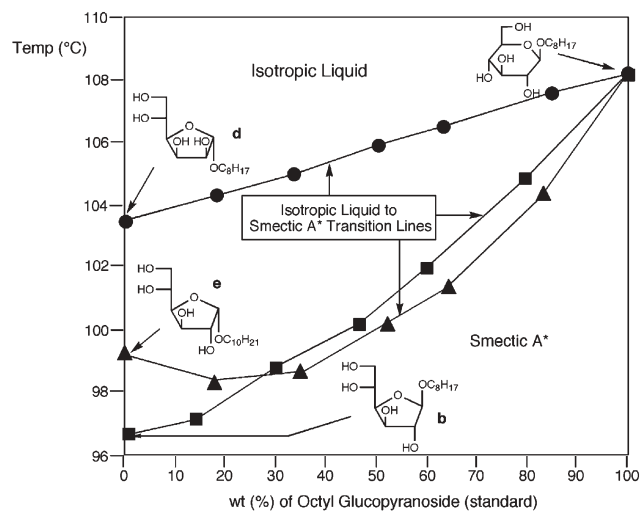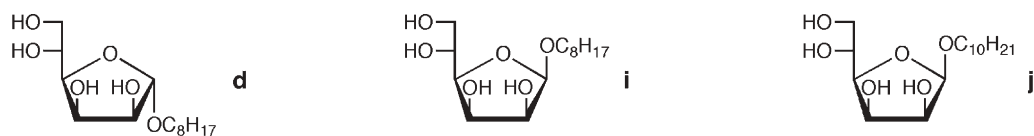Fig. 30 The variation in clearing and melting point temperatures (°C) for the octyl derivatives, compounds a to d.

Fig. 31 Miscibility phase diagram between compounds b, d, and e and the standard material n-octyl D-glucopyranoside (wt%).

This journal is © The Royal Society of Chemistry 2007

Chem. Soc. Rev., 2007, 36, 1971–2032 | 1987

Fig. 32 Transition temperatures (°C) of some related alkyl mannofuranosides.

phases of octyl β-D-glucofuranoside, **b**, octyl α-D-manno-furanoside, **d**, and decyl α-D-glucofuranoside, **e**, were established with the smectic A$_d$* phase of the standard material. Thus, the thermotropic phases of the three compounds are found to have the same identity, and are all classified as smectic A$_d$*.

Although complete families of glycofuranosides are not available for full structure–property correlations to be developed, some further comparisons can be made, for example, between the melting behaviours of α- and β- mannofuranosides. Fig. 32 shows the structures and transition temperatures of three related mannofuranosides, **d**, **i** and **j**.[48] The results show that when the aliphatic chain is positioned so that it does not sterically interfere with the hydroxyl moieties (α-anomer) then the transition temperatures are higher than when steric hindrance occurs (β-anomers), *i.e.*, the availability of hydroxyl moieties for the purposes of hydrogen bonding with neighbouring molecules markedly affects the stabilities of liquid crystal phases.

Investigations into the lyotropic phases were carried out for compounds **a** to **h**. Interestingly, only the octyl derivatives exhibited lyotropic behaviour. Of the octyl substituted systems, the galactofuranoside did not show any lyotropic phases. The α-anomers of mannofuranosides and glucofuranosides were found to exhibit hexagonal and lamellar phases respectively, however, the textures of these phases appeared to be difficult to characterise because they were bound closely to dissolving crystals. The β-anomer of glucofuranoside was found to exhibit rich polymorphism in that it exhibited lamellar, cubic and hexagonal phases as a function of increasing water concentration.

It is interesting to note that the lyotropic phase behaviour does not match the thermotropic properties. None of the decyl homologues showed a lyotropic phase upon the addition of water at room temperature. It was suggested that this was because of the insolubility of the longer aliphatic chain in water. For the octyl derivatives, the β-glucofuranoside exhibits the larger number of mesophases when mixed with water. This fact was thought to be related to the non-linear nature of its structure, *i.e.*, the hydroxyl groups of the carbohydrate are exposed to enable hydrogen bonding with water, and the diameter of the polar head group is large with respect to the cross-sectional area of the aliphatic chains. Hence, its ability to form curved structures is improved, and therefore, the β-glucofuranoside exhibits cubic and hexagonal structures in addition to lamellar phases, whereas the galactoside did not exhibit any lyotropic behaviour.

Surface tension (γ) and critical micellar concentrations (CMCs) of the alkyl glycofuranosides **a-g** were determined by tensiometric measurements; the results for which are shown in Table 5. The furanosides generally possess very interesting surfactant properties. The alkyl glycosides, and octyl glucofuranoside, **a** in Fig. 29, in particular, were able to reduce the surface tension of pure water (69 mN m^{-1} at 46 °C, and 72 mN m^{-1} at 20 °C) by more than 40 mN m^{-1}. Thus, the surface tension values above the critical micellar concentration varied between 25 and 30, whereas those obtained for the tautomeric pyranosic compounds are generally greater than 30 mN m^{-1}.[49] Furanosides are therefore more efficient surfactants than the corresponding pyranosides.

Furthermore, the interfacial areas, *A*, for each of the compounds were found to be similar to those of the known octyl and decyl glycopyranosides.[49] This result shows that the tautomeric form of the polar head group and the anomeric configuration have a low influence on this parameter. In addition, the values for the critical micellar concentrations obtained for the furanosides were generally lower than those of the pyranosides.[49] This result probably reflects a greater destructuring effect of the furanosides on the three-dimensional structure of water.[50] Consequently, the shape of the glucoside moiety seems to have a great influence on the micellization for amphiphiles of similar chain lengths and polarities, and this effect could constitute a new factor for modulating surfactant properties.

3.4 Derivatives of sucrose

Although the family of mesogenic glycolipids, which have molecular architectures composed of either a pyranose, furanose, or acyclic monosaccharide units and a single alkyl chain, is growing, the number of mesogenic glycolipids that have head groups that possess two or more sugar units bonded to each other in a linear or branched fashion remains relatively small. For example, most mesogenic disaccharide compounds synthesised have been derived from reducing disaccharides such as maltose and lactose.[23d,51] Dodecyl β-D-maltoside, **17**, and tetradecyl β-D-lactoside, **18**, were each found to exhibit a bilayer smectic A*$_d$ phase.

Table 5 Micellization parameters for glycofuranosides **a** to **g**

Compound	CMC/mM	γCMC/mNm^{-1}	A/Å^2	T/°C
Octyl Derivatives				
a	7.5	25.5	51	20
b	9.4	30.2	44	20
c	6.1	28.9	57	46
d	4.9	28.0	54	46
Decyl Derivatives				
e	0.85	28.0	39	20
f	1.06	26.4	49	46
g	—	—	33	46

Cryst 80 SmA*_d 244 °C Iso Liq

17

Cryst 183 SmA*_d 246 °C Iso Liq

18
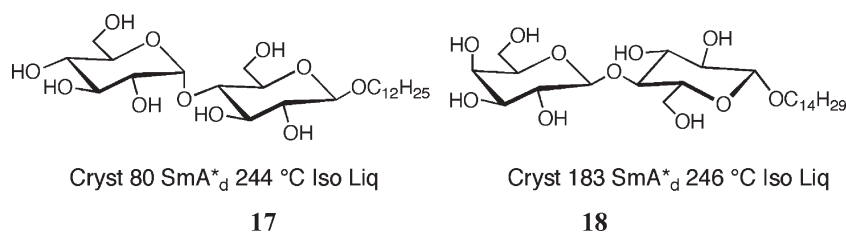
n-Dodecyl α-gentiobioside **19**, on the other hand, was found to exhibit a cubic phase.[52] The position of both the alkyl chain and the linkage between the two sugar units engenders a non-linear molecular structure. Therefore, in this case the material self-organises to give a cubic phase, where curvature of the local molecular packing is present.

Cryst 75 Cub 162 °C Iso Liq

19
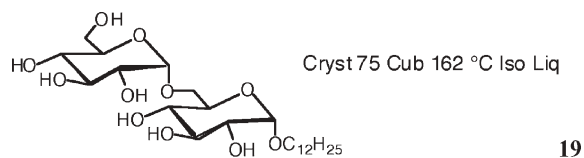
In a similar way, a dodecyl aliphatic chain was sequentially moved from one position to the next for the mono-*O*-(2-hydroxydodecyl)-sucrose family of materials (see Fig. 33), and the liquid crystal behaviour of the materials were examined.[53a] Sucrose itself provides a unique opportunity to prepare (see section 8.4) and study the combination of a pyranose and a furanose ring system. Comparisons have already been made on furanose and pyranose based glycolipids (discussed earlier) which have a single sugar unit in the head group, and have shown that the clearing points of the α and β anomers have an inverted relationship with respect to the ring type of the sugar moiety.[19,36]
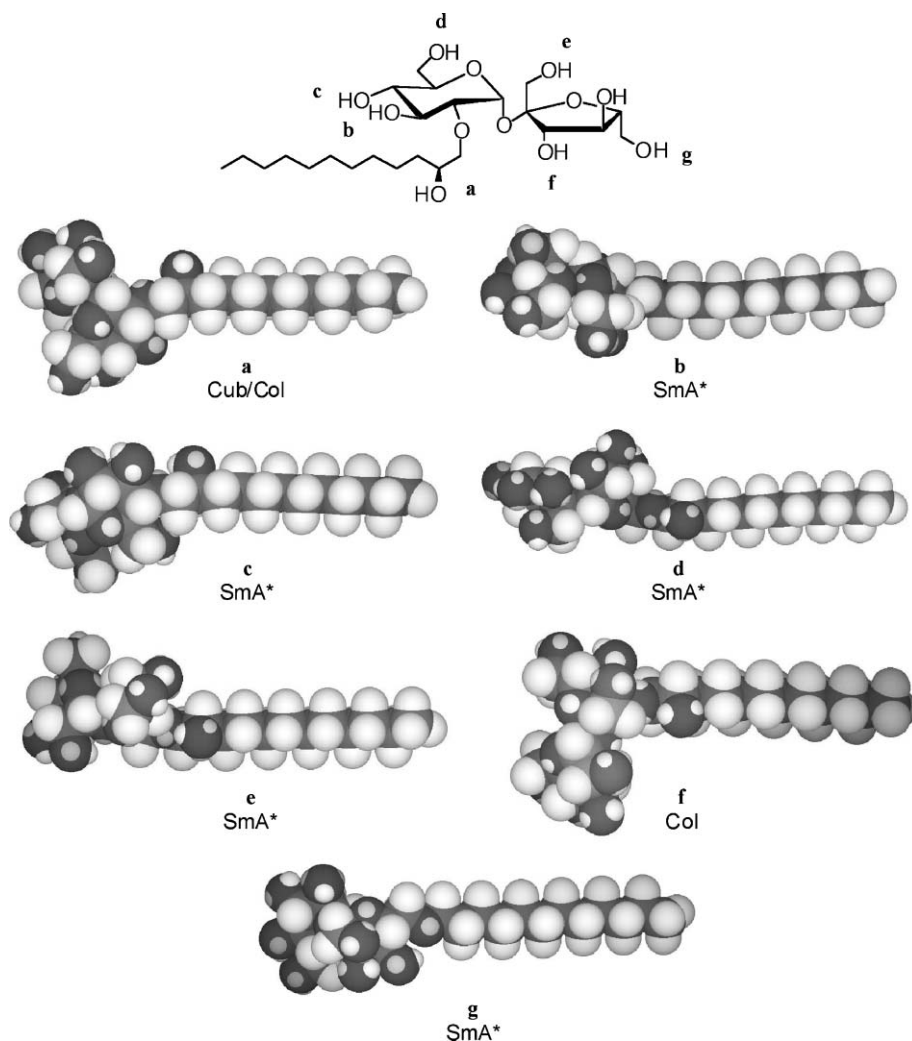

Fig. 33 Effect of substitution on the molecular shape of the mono-*O*-(2-hydroxydodecyl)-sucroses, (oxygen dark grey, carbon mid-grey, hydrogen white).

This journal is © The Royal Society of Chemistry 2007

Chem. Soc. Rev., 2007, **36**, 1971–2032 | 1989

Fig. 33 shows the structure of the family of sucrose ethers examined.[53a] The dodecyl chain was sequentially moved from position **a** to **g** and the liquid crystal properties of the materials were examined by microscopy, differential scanning calorimetry and miscibility studies. Molecular modelling was used to examine the molecular shapes of the homologues. Where the aliphatic chain is attached to positions **b**–**e**, and **g** the shape of each associated molecular structure is rod-like; however, for positions **a** and **f**, the molecular structures become T-shaped with the cross-sectional area of the head group being larger than that of the aliphatic chain. Consequently, with **a** and **f** having wedge-like structures they exhibit cubic and columnar phases respectively. Fig. 34 shows the textures and structures of sucroses **a** and **d**.

The changeover from one type of phase to another, *i.e.* lamellar to columnar, also involves a large change in clearing point temperatures. The columnar and cubic phases tend to occur at much lower temperatures, approximately 50 °C lower relative to the lamellar phase. Fig. 35 shows how the melting points and phase transition temperatures vary for homologues **a** to **g**.

The balance between the formation of lamellar and columnar and cubic structure is finely tuned. For example, the difference between axial and equatorial substitution, or even whether or not a hydroxyl group is axial or equatorial can be enough to tip the balance in favour of one phase or another. A report by Laurent *et al.*[54] on the synthesis (Section 8.5) of systems with one head group and two aliphatic chains showed by optical microscopy, differential scanning calorimetry and
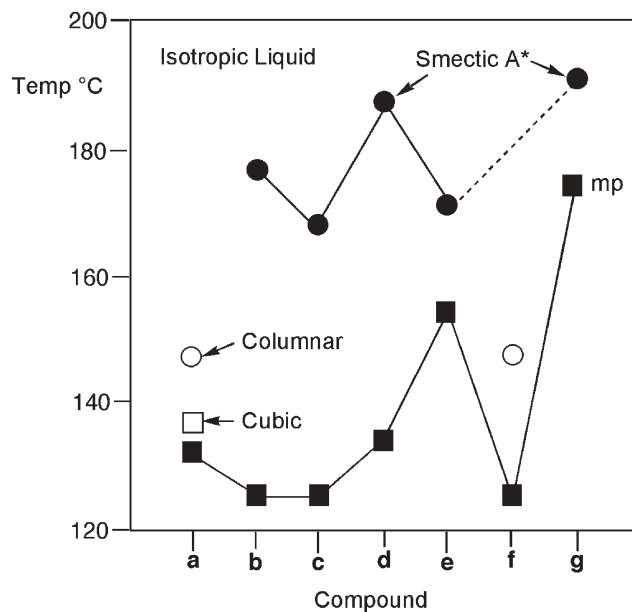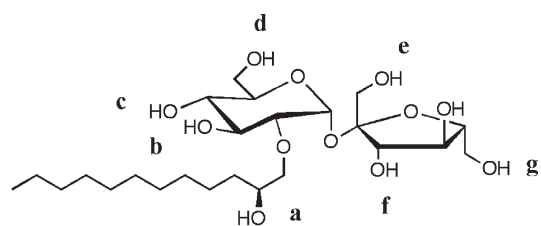

Fig. 35 The relative clearing points (°C) for the mono-*O*-(2-hydroxydodecyl)sucroses.
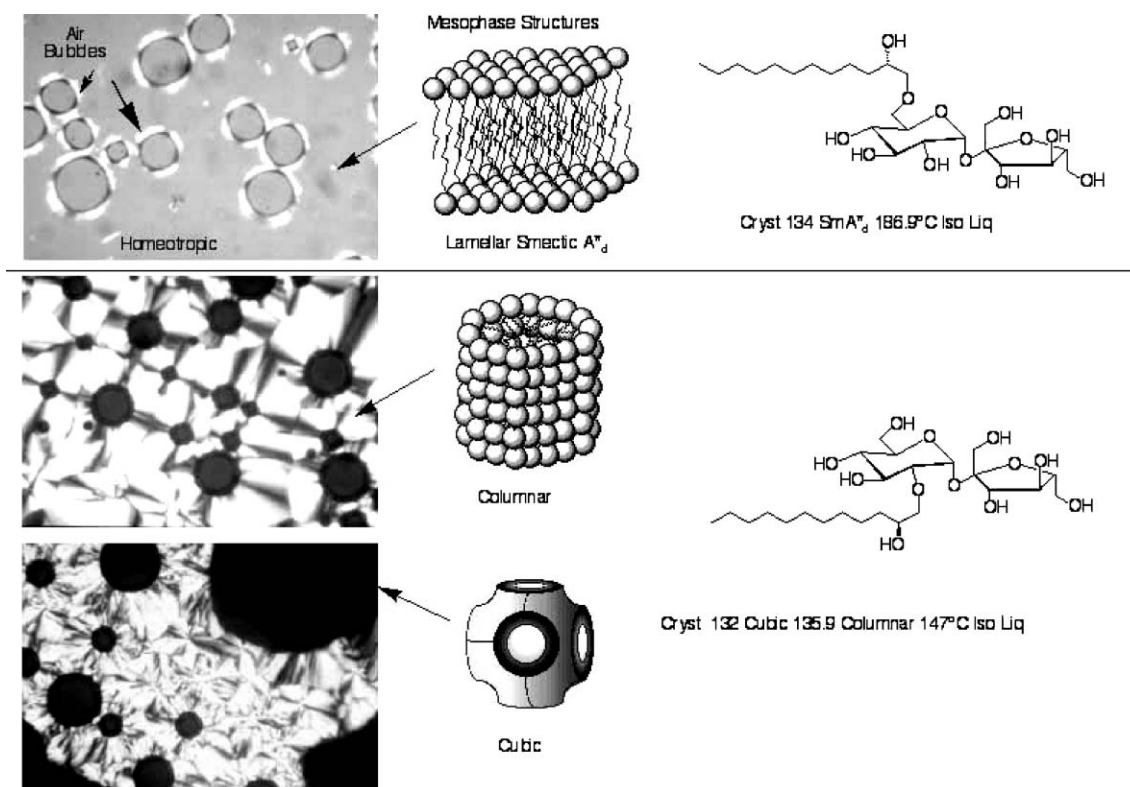

Fig. 34 The textures and structures of sucroses **a** (bottom) and **d** (top).

X-ray diffraction that 4-(4′-*N,N*-didodecylaminophenylazo)-phenyl β-D-glucopyranoside exhibited a columnar phase, whereas 4-(4′-*N,N*-didodecylaminophenylazo)phenyl β-D-galactopyranoside possessed a lamellar phase. It was envisaged for the glucose derivative that curvature is induced within layers, which is localised into a columnar structure, because the glucose derivative has the smaller head group relative to the cross-sectional area of the chains than the galactose derivative does:- see Fig. 36.

Another possibility of stabilising columnar or cubic phases over lamellar phases in sucrose systems is to change the length of the aliphatic chain(s). For a material which has a head group that has a larger cross-sectional area relative to the aliphatic chain, then as the chain is increased in length, lamellar phases become more stable because the curvature in the packing of the molecules is reduced, *i.e.*, the molecules become less wedge-shaped. However, for systems that have a larger cross-sectional area for the hydrophobic region relative to the head group, the longer the aliphatic chain(s) the more stable the columnar and cubic phases become. Molinier *et al.*[53b] demonstrated the effect of aliphatic chain length by comparing the liquid crystal properties of 6-*O*-octanoylsucrose (**20**), with 6-*O*-octadecanoylsucrose (**21**). Molecular simulations show that the sucrose head groups form intramolecular hydrogen bonds, thereby exposing the remaining hydroxyl groups on the outer surface of the head, as shown by the space-filling models in Fig. 37. The models show that, for the shorter chain length, the overall molecular structure is wedge-shaped, whereas for the octadecanoyl homologue the overall structure is more rod-like. Hence, at shorter chain lengths columnar (and potentially cubic) phases are more stable, whereas at longer aliphatic chain lengths the lamellar phase is the more stable. It is also important to note from Fig. 37 that the clearing point for the lamellar phase is over 100 °C higher than that for the columnar phase, which is in keeping with the results obtained for the mono-*O*-(2-hydroxydodecyl)-sucrose family of materials described earlier.

Intra-molecular hydrogen-bonding can thus affect the molecular shape and topology, thereby influencing the self-assembly and self-organisational properties. Molinier *et al.*[53b] went on to investigate the liquid crystal properties of three families of materials, the 6-, 6′-, and 1′-*O*-alkanoylsucroses. For all three families, simulations show that intra-molecular hydrogen-bonding is a low energy configuration which leads to the formation of quasi-macrocyclic structures, as shown in Fig. 38. By forming cyclic structures, the sucrose head groups have the maximum number of hydroxyl groups exposed on the top surface of the heads away from the aliphatic chains. In this way the head groups can be easily solvated with water to form lyotropic systems.

The formation of macrocycles for the three families also leads to the possibility of creating cavities within the molecular structures. The macrocycles have either 5 or 6 oxygen atoms in their ring structures, which would allow for complexation of various ions. When these systems form columnar phases, with the head groups located at the surfaces of the columns and the aliphatic chains towards the interior, the macrocyclic rings/cavities will overlap, or stack, one on top of another, thereby forming tubes, or ion channels, through the structure as shown in Fig. 39.
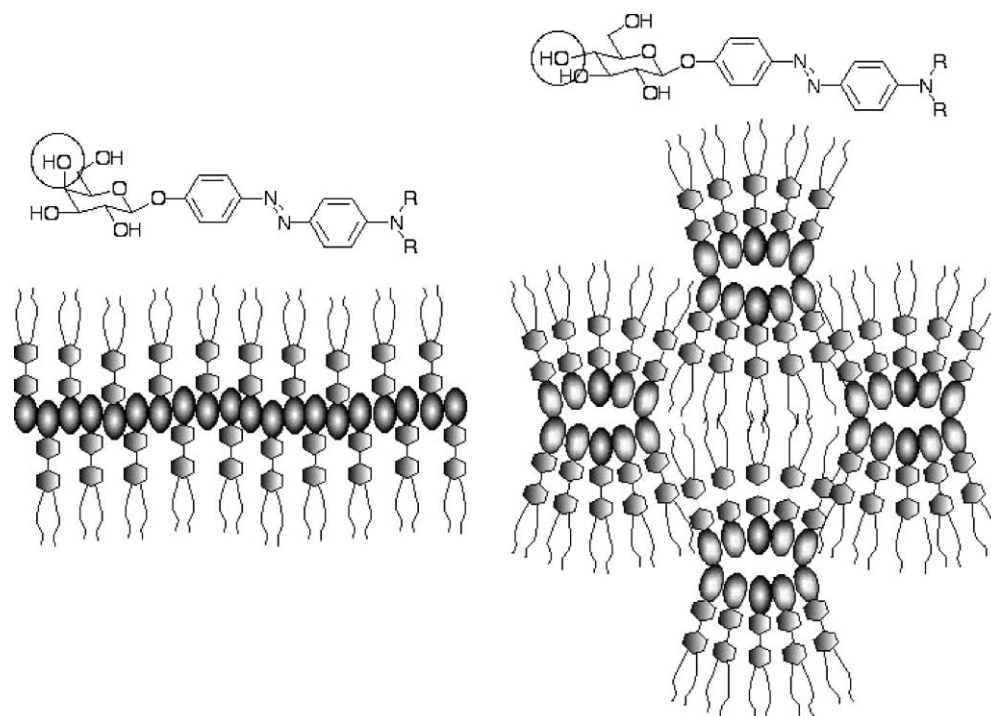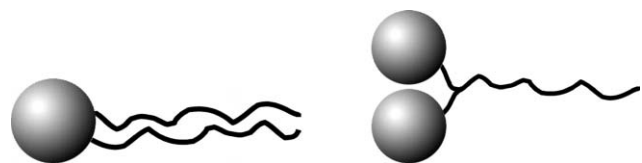

Fig. 36 Columnar mesophase formation for the glucose with respect to the formation of the lamellar mesophase for galactose derivatives for the 4-(4′-*N,N*′-didodecylaminophenylazo)phenyl β-D-glycosides.

This journal is © The Royal Society of Chemistry 2007

Chem. Soc. Rev., 2007, **36**, 1971–2032 | 1991

4. One head two tails, two heads one tail

In this section we will devote most of our discussions to materials that have direct biological relevance. However, most of the work previously reported is on the materials in aqueous media, whereas we will focus more on thermotropic liquid crystalline properties. The first systems described are cerebrosides which are commercially available in their natural and synthetic forms from Sigma.[5] Synthetic mimics of cerebrosides
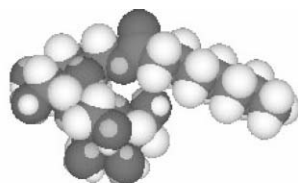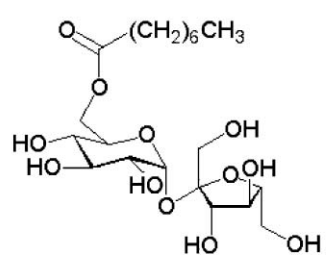
Soft solid - Columnar 95.6 Iso Liq

20
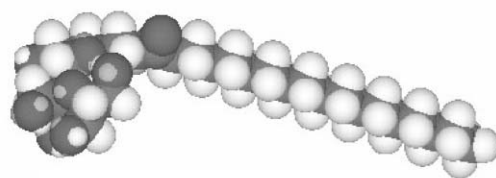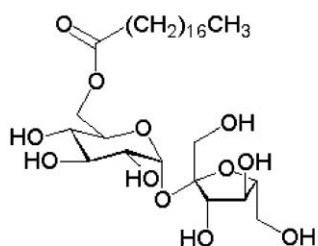
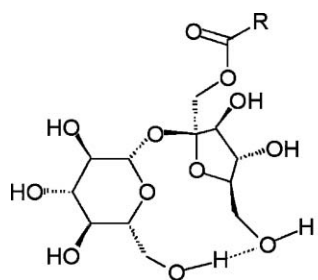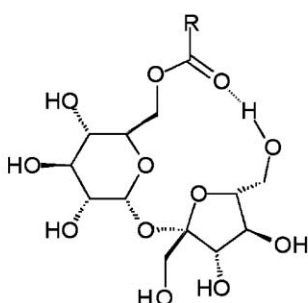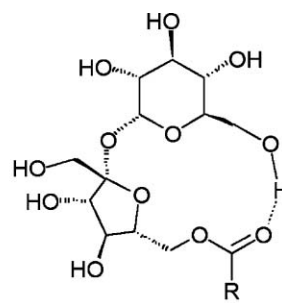**Cryst 39.3 SmA* 212 Iso Liq**

21

Fig. 37 Comparison of the molecular shapes for the octanoyl **20** and octadecanoyl **21** monosubstituted sucrose fatty acid esters, (oxygen dark grey, carbon mid-grey, hydrogen white).
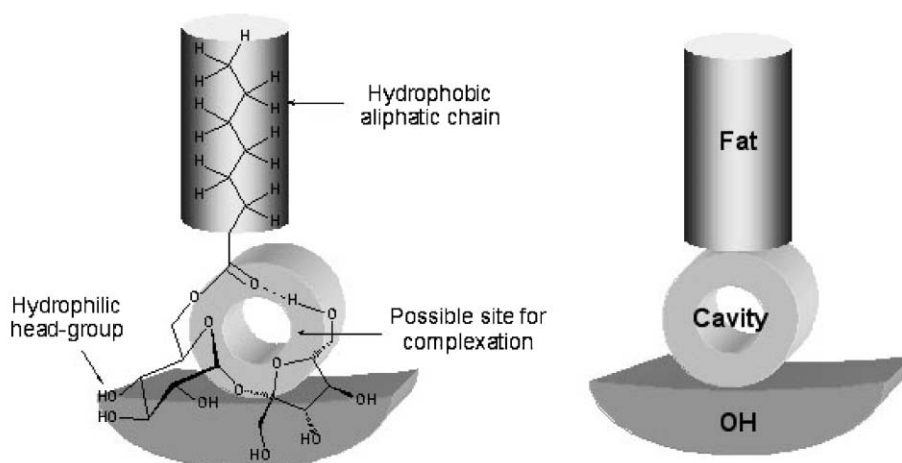
(1') **(6)** **(6')**

Fig. 38 Intra-molecular H-bonding results in cyclic systems where the hydroxyl groups are exposed on the outer surface of the head-groups.
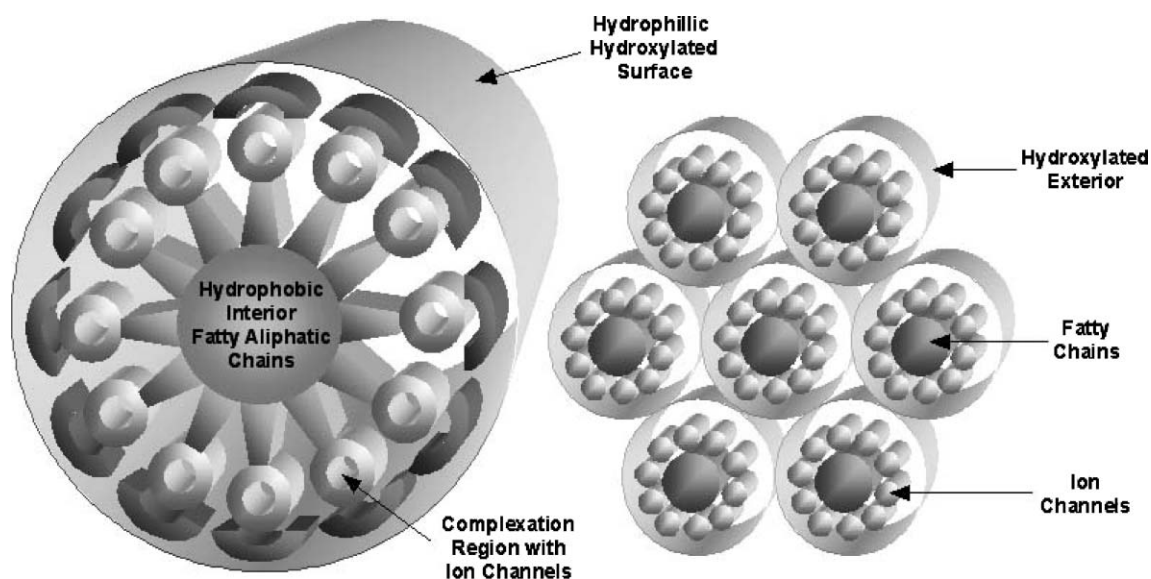
Fig. 39 Columnar stacking of the intra-molecular macrocyclic sugar systems. When the columns pack together they form a hexagonal columnar phase.

have also been reported in the literature and their preparations are discussed in Section 8.6. The second system that will be examined are the lipids of methanogenic and halophilic archaebacteria, which are characterized by high proportions of diether-type components with a 2,3-diphytanyl-sn-glycerol backbone. We will examine the liquid crystal properties of synthetic N,N-bis-(D-mannitolyl)dodecylamide which has two head groups and one tail, and the unusual structural properties of disubstituted sucrose esters.

4.1 Cerebrosides

Naturally occurring cerebrosides are usually isolated from animal sources, such as cattle. For example, galactose cerebrosides, which are typical examples of cerebrosides, are prevalent in the myelin membranes of nerve fibres (axons) found in brain tissue. The depletion of cerebrosides through de-myelination is associated with diseases such as multiple sclerosis (MS). Interestingly, some of the very earliest investigations of liquid crystals also involved the study of myelin,[6] and some of the textures observed for bioactive liquid crystals have been termed myelin fingers.

Cerebrosides are glycosphingolipids, where the sugar residue is either galactose or glucose. For example, psychosine (**22**), (1-β-D-galactosphingosine) is a glycolipid that has one head group and one tail, and exhibits a lamellar smectic A* phase.[5]

Cryst 106.2 SmA* 211.1 °C Iso Liq

22
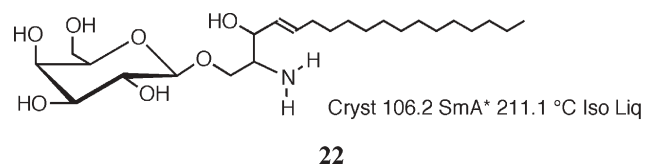
However, in gluco- and galactocerebrosides, two aliphatic chains are present, as shown in Fig. 40. Thus the molecules have wedge-like structures, and as a consequence they self-organise to give thermotropic columnar structures.[5,55] Quite

often these types of materials also exhibit lyotropic columnar phases on the addition of water. However, the lyotropic columnar structure is inverted relative to that of the thermotropic phases, as upon the addition of water, the head groups swell and their cross-sections become larger than those of the aliphatic tails.

The liquid crystal properties of the commercially available stearoyl, palmitoyl, oleoyl and nervonoyl galactocerebrosides derived from bovine brain have been previously reported:[5,55] see Fig. 41. These materials provide the opportunity to compare the effects of having a double bond in both of the terminal chains *versus* having one of the chains being fully hydrogenated. All four were found to exhibit hexagonal columnar phases over very wide temperature ranges: see the texture in Fig. 42(a). The materials were found to have high clearing temperatures, and thus they exhibit relatively stable mesophases. Interestingly, the stearoyl and oleoyl members of the series have almost identical clearing points indicating that unsaturation in at least one of the terminal aliphatic chains does not markedly affect the self-organising properties of the materials. Where the two chains are only slightly different in length, ± 2 carbon atoms (symmetrical), *e.g.*, for the palmitoyl derivative, higher clearing points were realized, whereas typically if the chains have considerably different lengths (asymmetrical) then the melting points are much lower, *e.g.*, stearoyl.

Differential scanning calorimetry showed complex melting from the solid state to the liquid crystal state, with many solid–solid transitions occurring. In addition to exhibiting thermotropic liquid crystal phases, the materials were also found to exhibit lyotropic hexagonal phases through the addition of water.

One experiment employing a water concentration gradient was also used to investigate the miscibility of the thermotropic hexagonal phase of the palmitoyl compound, **23**, with water. The microscopic texture of the concentration gradient is shown in Fig. 42(b), with the dry specimen on the right-hand side and the high water concentration on the left-hand side of the

This journal is © The Royal Society of Chemistry 2007

Chem. Soc. Rev., 2007, **36**, 1971–2032 | 1993
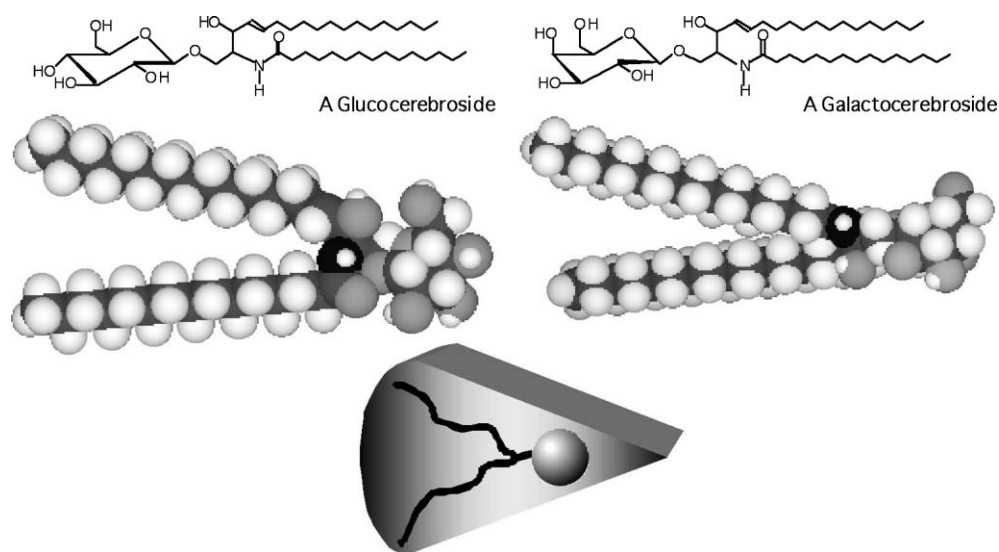
Fig. 40 Structures of gluco- and galacto-cerebrosides.

Palmitoyl   Cryst 146.6 Col 185.7 °C Iso Liq

Oleoyl   Cryst 128.3 Col 176.5 °C Iso Liq

Stearoyl   Cryst 91.2 Col 178.5 °C Iso Liq

Nervonoyl   Cryst 138.4 Col 186.6 °C Iso Liq
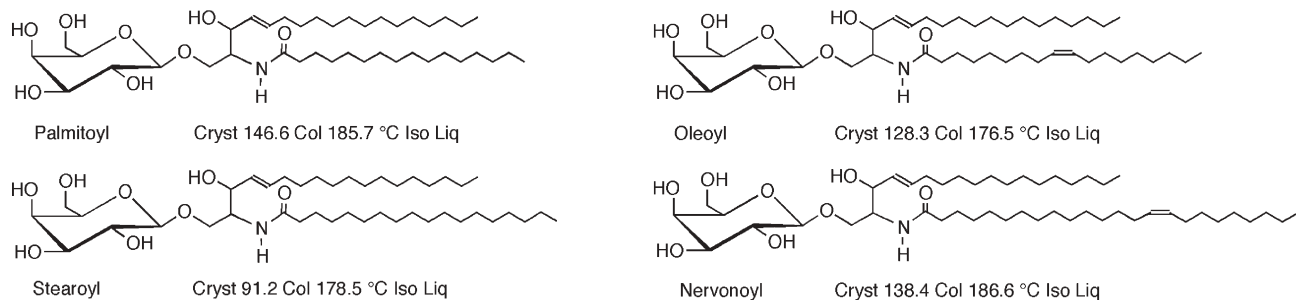
Fig. 41 The liquid-crystalline properties of four naturally occurring cerebrosides.

(a)   (b)
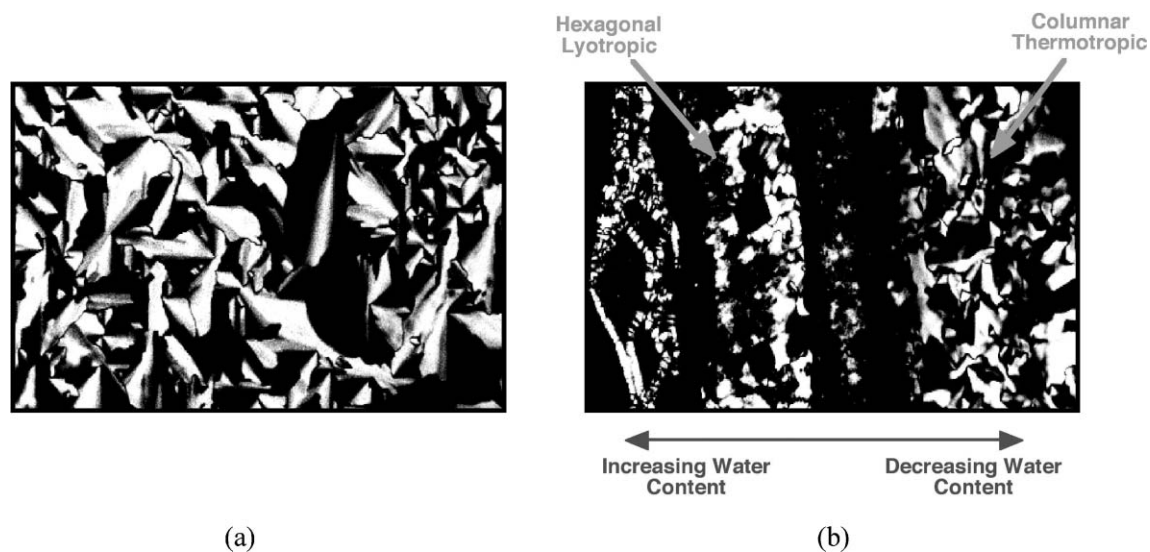
Fig. 42 (a) The texture of the thermotropic columnar phase of compound 23, and (b) the contact between the thermotropic columnar phase (right) and water, yielding a hexagonal columnar phase (left).

picture. The photomicrograph shows that the columnar thermotropic phase and the columnar lyotropic phase do not appear to be continuously miscible, and the formation of other phases which correspond to cubic phases (black regions) and the lamellar phase (light region down the center of the photomicrograph) occur between the hexagonal phases. This indicates that the two hexagonal columnar phases have inverted structures relative to one another.

23
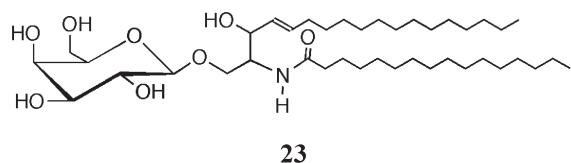
In order to confirm the presence of thermotropic hexagonal phases, X-ray diffraction studies on the galactocerebrosides were made. The intensities of the reflections were however, found to be extremely weak even when using a synchrotron radiation source for the studies. However, the related material cerebroside sulfate, **24**, which was characterized by microscopy as exhibiting a hexagonal columnar phase, was found to give a high quality diffraction pattern when examined X-ray diffraction. The reflections as a function of temperature: see Fig. 43, are in the ratio of $1 : \sqrt{3} : \sqrt{4}$ confirming the presence of a hexagonal columnar phase.[55]

cerebroside sulfate

Cryst 88.8 Col >204 °C Decomp

24
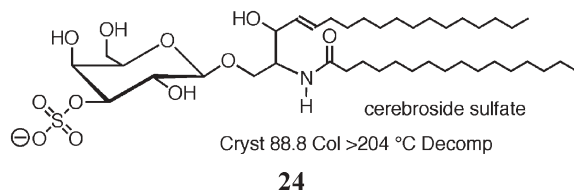
As with the naturally occurring cerebrosides, the synthetic D,L-dihydro analogues were also found to exhibit columnar mesophases. The melting and isotropization points are shown in Tables 6 and 7 for the C_{15}, C_{17} and C_{23} homologues of the gluco- and galacto-cerebrosides respectively.

It is interesting to note that for these materials, the melting points are much lower than those for the naturally occurring materials. This means that the liquid crystal phases are exhibited over much wider temperature ranges. Moreover, there is virtually no change in the isotropization temperature with respect to change in the sugar unit (*i.e.* galactose *versus*
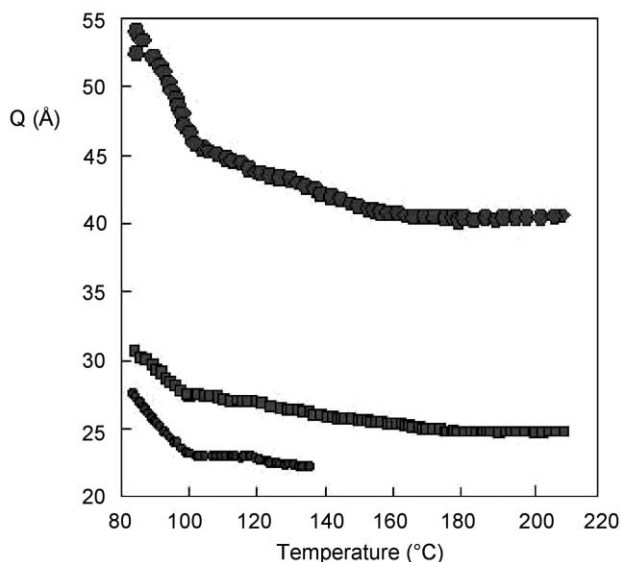

Fig. 43 *Q* spacing (Å) as a function of temperature for compound **24**.

Table 6 Transition temperatures (°C) as a function of chain length (n) for the alkanoyl-D,L-dihydroglucocerebrosides

n	Cryst		Col		Iso Liq
15	•	94.7	•	184.5	•
17	•	108.1	•	191.1	•
23	•	95.6	•	193.1	•

Table 7 Transition temperatures (°C) as a function of chain length (n) for the alkanoyl-DL-dihydrogalactocerebrosides

n	Cryst		Col		Iso Liq
15	•	95.3	•	185.5	•
17	•	91.3	•	193.2	•
23	•	102.1	•	193.0	•

glucose), again demonstrating that the polar head group does not greatly affect the mesomorphic properties. Unlike the 4-(4′-N,N-didodecylaminophenylazo)phenyl β-D-glycosides described earlier,[54] in this case it appears, that the self-organization is relatively insensitive to stereochemical structure in the head group. This may be due the curvature of packing being greater for the cerebrosides in comparison to the 4-(4′-N,N-didodecylaminophenylazo)phenyl β-D-glycosides, because the overall molecular lengths are shorter in relation to the cross-sectional areas of the aliphatic chains.

Synthetic cerebroside mimics have also been prepared, and their liquid crystal properties have been investigated and the results compared to the natural and synthetic sources described above.[55] The structures, melting transitions and the isotropization points are given for the seven novel cerebroside mimics as shown in Fig. 44.

One advantage of creating cerebroside mimics is that the lengths and types of the two aliphatic chains can be varied independently of one another, whereas for naturally occurring cerebrosides one of the chains is of a fixed length and type. Varying the two chain lengths does, however, reveal some interesting results. For example, only four of the materials shown in Fig. 44 are liquid crystalline, *i.e.* **26** to **29**. Of these, **27** and **29** exhibit enantiotropic phases, whereas the other two, **26** and **28**, are monotropic. Where mesophases are exhibited, they were found to be columnar.

Interestingly, the materials that were non-mesogenic possessed either one or two short aliphatic chains, and created an unsuitable hydrophilic/hydrophobic balance. Similarly, when the chains are of a similar length, mesomorphism is again suppressed due to the relatively symmetrical molecular structure inducing higher melting points. For materials with long aliphatic chains attached to the amide unit, *e.g.* C_{16}, the transition temperature to the solid state is reduced and the clearing point is raised leading to stabilization of the liquid
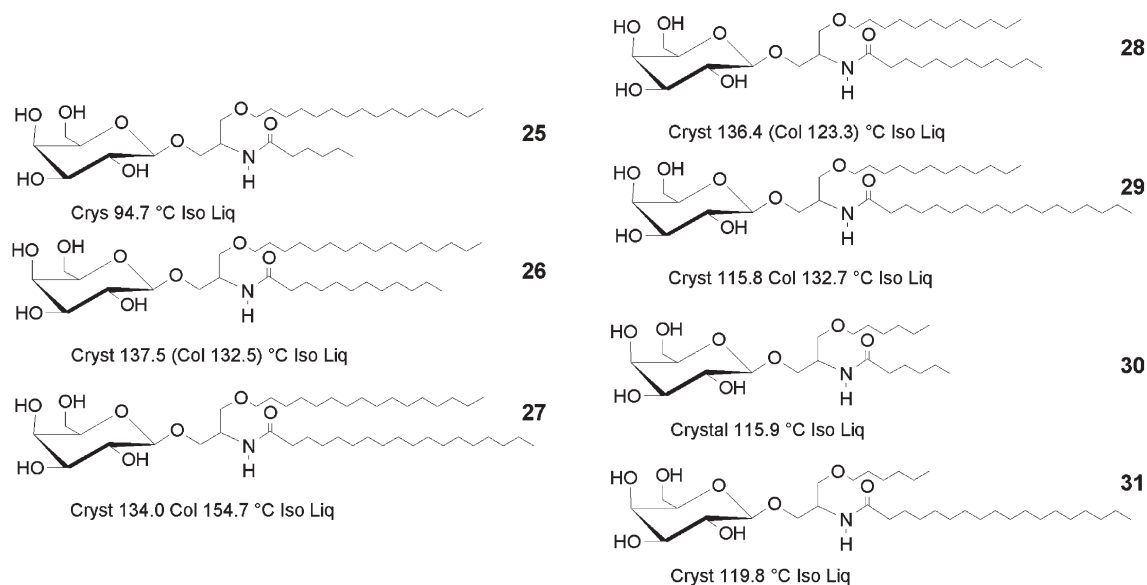
This journal is © The Royal Society of Chemistry 2007

Chem. Soc. Rev., 2007, **36**, 1971–2032 | 1995

Fig. 44 Transition temperatures (°C) of some cerebroside mimics.

25 — Crys 94.7 °C Iso Liq

26 — Cryst 137.5 (Col 132.5) °C Iso Liq

27 — Cryst 134.0 Col 154.7 °C Iso Liq

28 — Cryst 136.4 (Col 123.3) °C Iso Liq

29 — Cryst 115.8 Col 132.7 °C Iso Liq

30 — Crystal 115.9 °C Iso Liq

31 — Cryst 119.8 °C Iso Liq

crystal state. Overall the clearing points were considerably lower than those found for the natural and synthetic cerebrosides described earlier.

For these materials, some of the effects of chirality on the self-assembly–self-organisation processes were investigated. For example, the thermotropic properties of the diastereoisomers **32** and **33** were investigated. The materials exhibit columnar phases, with the difference in the clearing points of 3.6 °C being due to the diastereochemical purities of the materials. This indicates that the effects associated with the attachment of one terminal chain are limited. The melting point differences, on the other hand, are very large, as might be expected for diastereoisomers. These results demonstrate that the self-organising liquid-crystalline state is more tolerant of changes to the chirality of the system than is the solid state, or is indeed self-assembly itself.
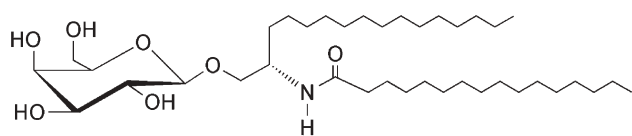
Cryst 153 Col 155.5 °C Iso Liq   Recryst 132.6 °C

32
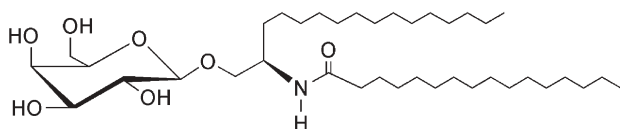
Cryst 133.4 Col 151.9 °C Iso Liq   Recryst 94.4 °C

33

Similar results have been found in the case of threitol and erythritol substituted systems, described earlier in this review, where the stereochemistry inversion occurs in the head group.[25] Again very little difference in the isotropization temperatures occurs (within experimental error a distinction between the two diastereomers cannot be determined), that is in contrast to the melting points which are substantially different.

Overall, the degrees of unsaturation in the aliphatic chains and changes to the stereochemistry of the system do not markedly affect the liquid crystalline phase behaviour; however they effect large changes with respect to the solid state.

Other interesting naturally occurring materials and synthetic mimics include the diacyl derivatives of galactosylglycerols, **34**. Up to 75% of the total lipid content of plant chloroplast membranes consist of galactoglycerolipids,[56] many of which are being investigated today in the developments of biodiesel fuel. The glucoglycerolipids, such as the α-D-glucopyranosyl-diacylglycerols, **35**, have been investigated in detail with respect to their liquid crystal properties. These materials were originally reported as exhibiting smectic A* phases. However, at a later date the classification of their mesophase properties was changed to columnar in keeping with the cerebrosides described above. Table 8 gives the transition temperatures for the C_{12} to C_{20} homologues; however, because of the uncertainty of the reported mesophase type, the liquid crystal phase is unclassified (i.e., X).

4.2 Glycolipids associated with archaebacteria

The lipids of methanogenic and halophilic archaebacteria are characterized at a molecular level by saturated isoprenoid chains (see Fig. 45), attached to glycerol by ether linkages with an sn-2 stereochemistry opposite to that of conventional mesophilic lipids. Polar groups at the sn-1 position of these lipids include various phosphate derivatives and unusual glycosyl units based on furanosidic moieties. In particular, glycosidic headgroups in *Methanospirillum hungatei*, a methanogen species, consist of repetitious moieties in which the first sugar attached to glycerol is β-D-galactofuranoside (β-Galf) and the second either β-Galf or α-D-glucopyranoside.[9,57] The
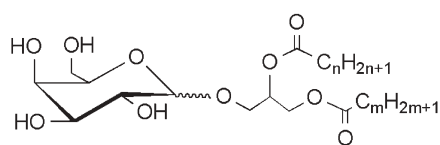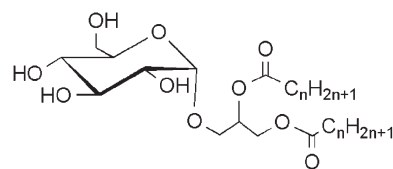
Table 8 Transition temperatures (°C) as a function of chain length (*n*) for the α-D-glucopyranosyl-diacylglycerols, **35**

n	Cryst		X		Iso Liq
12	•	40–44	•	120–122	•
13	•	58–60	•	128–130	•
14	•	67–69	•	129–131	•
15	•	67–71	•	139–140	•
16	•	76–77	•	142–143	•
17	•	79–81	•	143–144	•
18	•	80–82	•	144–145	•
19	•	81–83	•	145–146	•
20	•	89–91	•	141–142	•

presence of β-D-galactofuranose is a striking feature since D-galactose as well as other hexoses appears only in the pyranose cyclic form in mammalian glycolipids and glycoproteins.[9,57] Some model amphiphiles have been synthesized in order to investigate the ability of diether-types of lipid to provide stable vesicles or planar membranes in water. The synthetic molecules contain either linear alkyl chains or phytanyl residues linked to glycerophosphate derivatives. Upon sonication, these compounds furnish well-defined liposomes that are particularly useful for the long-term storage of inorganic salts and protein stability.[58]

Here we describe the evaluation of the liquid-crystalline properties of some synthetic diether-type glycolipids bearing one furanosyl head group, which were prepared as described in Section 8.7.[58,59] Thus we describe the properties of seven materials, **a** to **g** in Fig. 46, possessing: (i) polar head groups selected from the following; β-D-galactofuranose, β-D-glucofuranose, and α-D-mannofuranose; (ii) optically pure (*R* or *S*) or racemic glycerol isomers; (iii) phytanyl, dihydrocitronellyl and/or straight alkyl chains, the phytanyl group being used to mimic the isoprenic chains found in the lipids of archaeal membranes.

All of the compounds **a** to **g** were found to exhibit columnar phases.[60] It is interesting to note that only the glycolipid **e**, bearing two linear saturated chains, exhibits a defined melting point in addition to the clearing point. All of the other glycosides with two methyl branched aliphatic moieties exhibit no detectable melting points, instead they all form glassy phases at very low temperatures. The lack of a melting point transition could be explained by the steric hindrance of the methyl groups to ordered packing of the hydrocarbon residues. Thus, these materials are in their liquid crystal phases at room temperature and can be cooled down to −50 °C without recrystallisation occurring. On cooling, compound **f**, which possesses mixed linear and branched chains and with a *sn*-2 stereochemistry for the glycerol unit, was found to give a glass transition below −25 °C. The clearing point enthalpies for all compounds were found to be relatively small (<1 Jg⁻¹) in comparison with the values obtained for carbohydrates with a single lipophilic chain (around 5 Jg⁻¹). These results indicate that, near to the transition from the isotropic liquid state to the columnar phase, the structure of the liquid and mesophase are similar.

Classification of the mesophases formed by the archaeal lipid mimics was achieved by optical microscopy: see Fig. 47. The lack of elliptical and hyperbolic disclinations and the presence of a homeotropic texture in the photomicrograph indicate that the phase has a hexagonal disordered columnar structure. Thus the wedge-shaped molecules pack together to form disc-like structures which then stack into columns. The resulting liquid-like columns are packed into a hexagonal array.

In order to determine if the aliphatic chains are located on the outer or the inner surfaces of the columns, the lyotropic phase properties were investigated. The thermotropic columnar phase was not continuously miscible with water, and
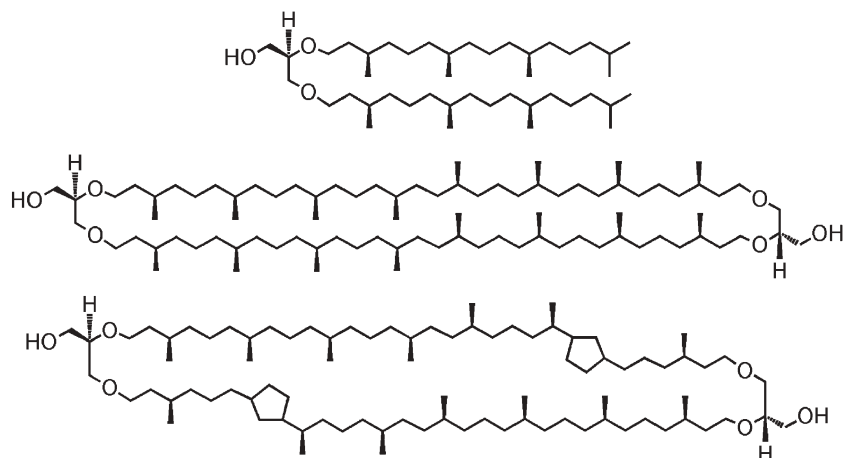

Fig. 45 Isoprenic chains of the lipids of archaeal membranes.

a   Col 64.4 Iso Liq   b   Col 53.9 Iso Liq

c   Col 70 Iso Liq   d   Col 69.6 Iso Liq

e   Cryst 75.4 Col 124.8 °C Iso Liq   f   Col 102.5 Iso Liq
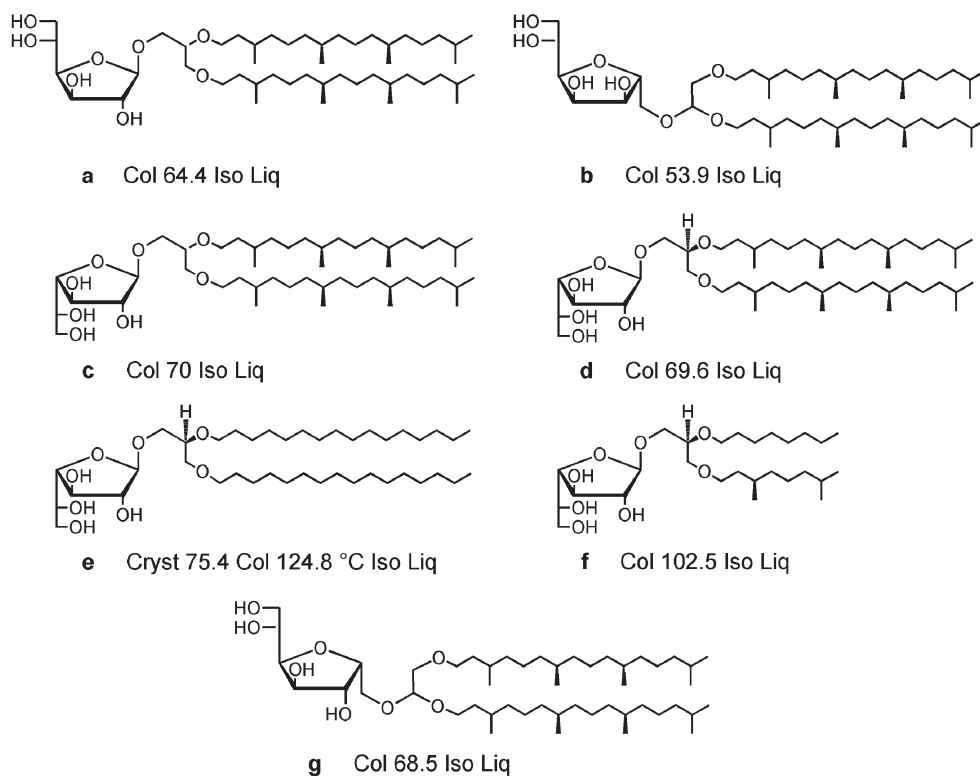
g   Col 68.5 Iso Liq

Fig. 46 Liquid crystalline properties of a variety of synthetic diether-type glycolipids.

lyotropic phase formation was obtained only after heating the samples above their clearing points: see Fig. 48. At this point a hexagonal liquid-crystalline domain formed. Thus below the clearing point the water did not penetrate into the thermotropic columnar phase, but in the liquid state at higher temperatures, penetration rapidly occurred resulting in the formation of a lyotropic columnar phase with an inverse structure relative to the thermotropic phase, as shown in Fig. 49. This very simple, but elegant experiment demonstrates that in the thermotropic phase the aliphatic chains are located on the exterior of the columns, thus the lyotropic and thermotropic phases have inverted structures relative to one another. The structure of the thermotropic phase of the archaeal lipid mimics is shown in Fig. 50.
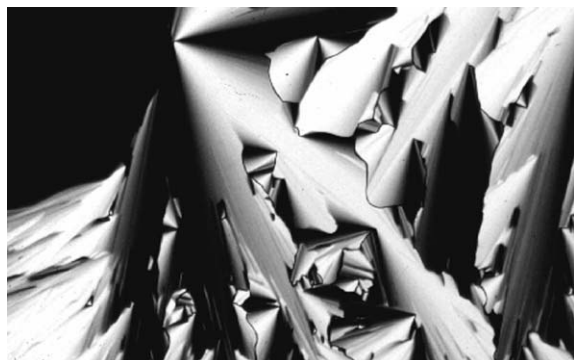
4.3 Systems with two heads and one chain

There are relatively few mesomorphic materials that have structures where the head group has two separately identifiable sugar groups attached to a single aliphatic chain. Material **36** which possesses two β-glucopyranoside units is one such example.[52,61] These cyclic polar groups are large enough so as to induce curvature in three dimensions, and thereby induce the formation of a micellar cubic phase.

Other examples of materials with this type of molecular design include the N,N'-bis-(D-mannitolyl)alkylamides, **37**, which have acyclic sugar units. These materials were prepared as described in Section 8.8. For these materials the total head group size is smaller than for compounds of type **36**, but still large enough to induce curvature into the molecular packing. Therefore, it should not be surprising that these materials were found to exhibit columnar phases, as listed for various homologues in Table 9.[62]
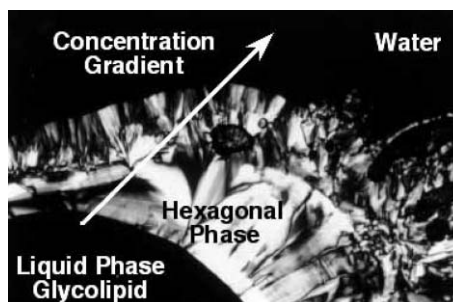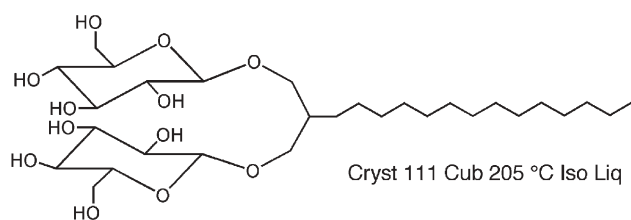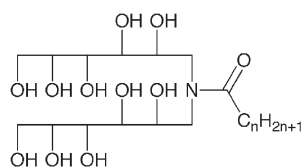

Fig. 47 Texture of the columnar phase of a synthetic diether-type glycolipid under crossed polars.

Fig. 48 Photomicrograph of the glycolipid–water interface at a temperature of 75 °C with the glycolipid in the liquid state.

Cryst 111 Cub 205 °C Iso Liq

36

37

Optical microscopy again was used to identify the mesophase exhibited by the mannitolyl materials. For example, the mesophase for the *N,N'*-bis-(D-mannitolyl)dodecylamide, *i.e.* the C_{11} homologue, showed no tendency to form a homeotropic texture, nor did it exhibit focal-conic defects. Instead a fan texture, typical of a columnar phase, was formed: see Fig. 51.

In order to investigate the effects of curvature in these systems further, a binary phase diagram for mixtures of *N,N'*-bis-(D-mannitolyl)dodecylamide with octadecanoyl D-galactocerebroside was reported. As described earlier, the galactocerebroside exhibits a columnar phase with a structure where the polar head groups are located towards the inside parts of the columns and the aliphatic chains at the outside,
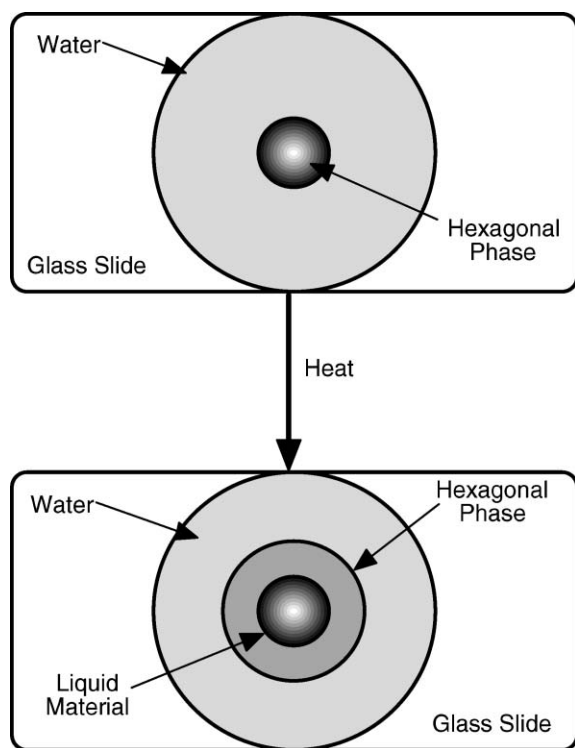

Fig. 49 Demonstration of how lyotropic mesophase formation can be used to determine the structure of a thermotropic liquid crystal phase through examining the effects of solvation.

whereas for the mannitolyl compound the structure of the columnar phase is inverted. Fig. 52 shows the phase diagram for the binary mixtures. It was found that as the phase diagram was traversed as a function of concentration, the columnar phase gave way to cubic, which in turn gave way to lamellar; the process was then repeated in reverse with lamellar giving cubic and cubic giving columnar. Thus induced curvatures of the two compounds compensate as a function of concentration, as one material induces positive curvature and the other gives negative; see Fig. 53.[63] The phase diagram therefore resembles that often obtained for lyotropic systems.

4.4 Disubstituted sucrose esters

In a recent report the liquid-crystalline properties of disubstituted sucrose esters have been described.[4,64] The preparation and characterisation of the 1',6'- and the 6,6'-disubstituted esters are discussed in Section 8.4. Bottle and Jenkins[3] previously reported on the synthesis and the biological activity of 6,6'-di-*O*-palmitoylsucrose, which was found to possess immunostimulant properties. However, they did not investigate the melting behaviour of the material. Further examples of the 1',6'- and 6,6'-families are listed in Table 10. As the molecular structures for these materials possess two aliphatic chains that are not adjacently attached to the sucrose unit, the materials will tend to exhibit smectic A* phases as predicted. This is particularly the case with the 6,6'-family where the molecules tend to have linear shapes.

We will focus first on the liquid crystalline behaviour of 6,6'-di-*O*-octadecanoylsucrose, **38**, because the compound was found to have quite remarkable structural properties. The variation of the layer spacing as a function of temperature was found to be unexpectedly large. The layer spacing, *d*, is shown in Fig. 54 as a radially integrated diffraction pattern taken over a wide temperature range.

Cryst 109.8 SmA* 164.3 °C Iso Liq Recryst 70 °C

38
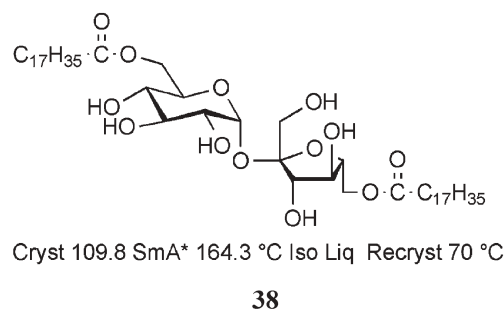
An intense small angle reflection was observed in the isotropic phase, as shown by the light grey curves in Fig. 54. This indicates pre-transitional effects occurring in the liquid, which might be related to the formation of clusters of molecules where intermolecular hydrogen bonding is present.

When cooling down into the smectic A* phase (dark lines) the second order reflection (002) can be seen, which grows more intense as the temperature falls. At higher temperatures the fundamental (001) reflection was fitted by a Lorentzian distribution function, taken from the widths of the peak intensity values at half the peak height. This indicates the presence of *short-range* positional order. At lower temperatures ($T < 100$ °C) the shape of the reflection changes to a
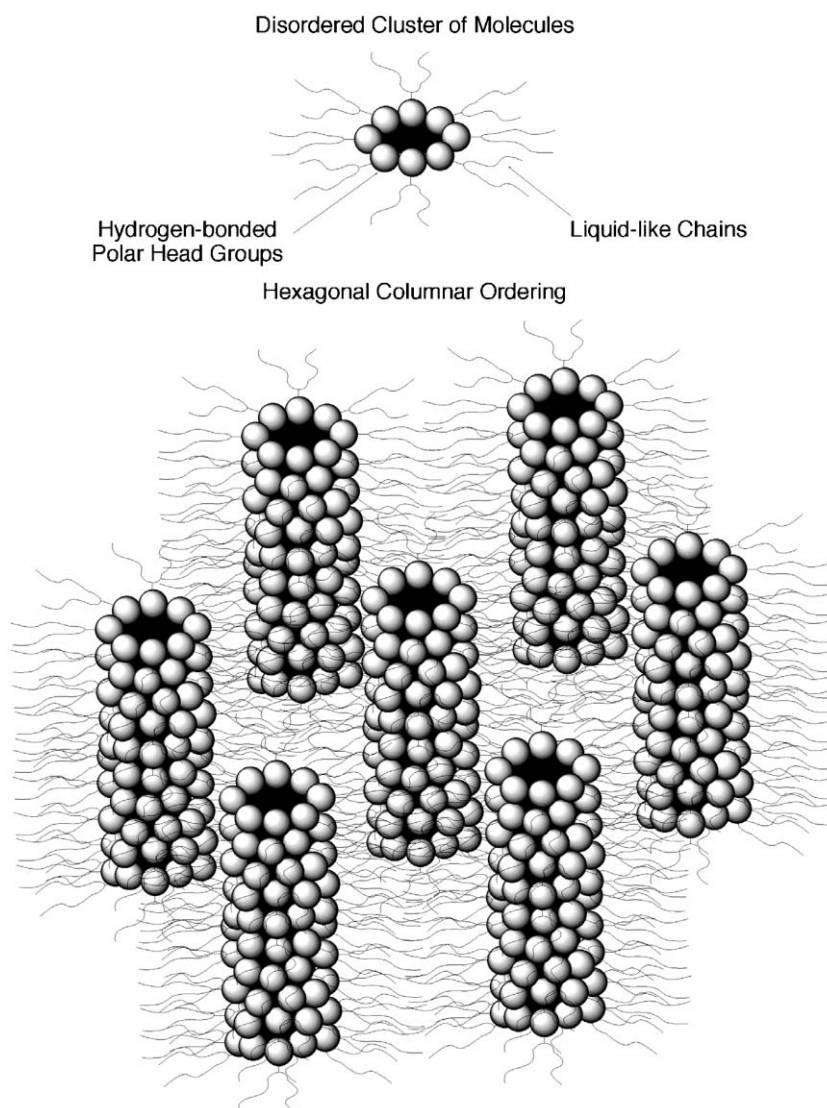
This journal is © The Royal Society of Chemistry 2007

Chem. Soc. Rev., 2007, **36**, 1971–2032 | 1999

Fig. 50 Structure of the hexagonal disordered columnar phase of the archaeal lipid mimics with the liquid-like aliphatic chains located on the exteriors of the columns.

Gaussian distribution function, indicating an increase in the extent of the positional order. In this temperature range third and fourth order reflections were also observed, indicating that the layers become better defined. The change in shape of the diffraction patterns for the fundamental reflections at $T = 105\ ^\circ$C (Lorentzian) and $T = 95\ ^\circ$C (Gaussian) is illustrated in Fig. 55.

A strong temperature dependence of the layer spacing was also observed in the smectic phase, with the d-values ranging

Table 9 Transition temperatures ($^\circ$C) as a function of chain length (n) for the N,N–bis-(D-mannitolyl)alkylamides

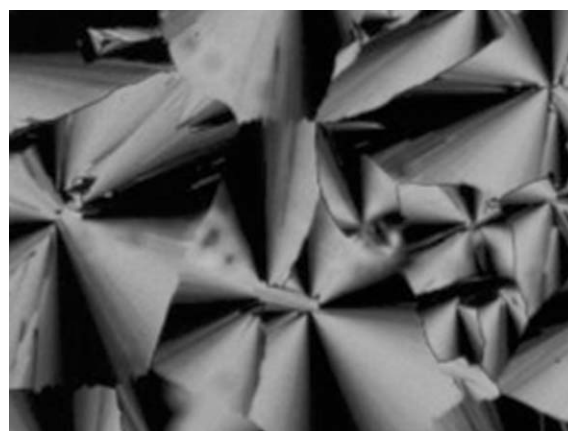| n	mp	Col		Iso Liq
8	104.1	•	144.3	•
9	145.6	•	157.5	•
11	148.9	•	170.2	•
13	147.8	•	183.0	•

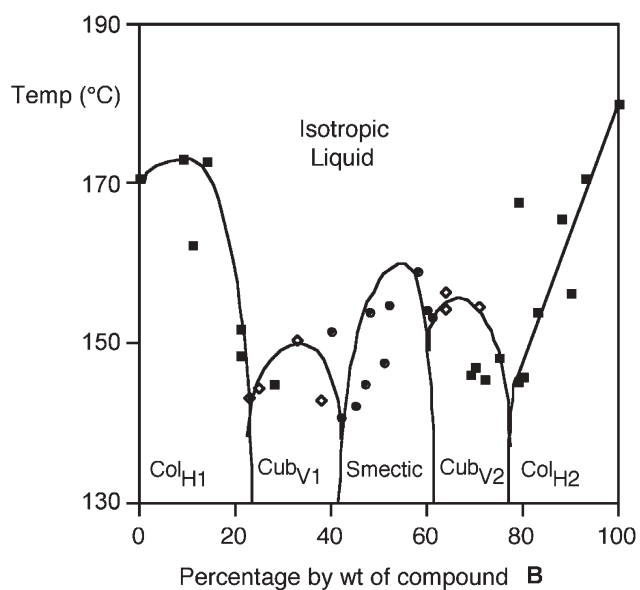**Fig. 51** The fan texture of the columnar phase of N,N'-bis-(D-mannitolyl)dodecylamide.

Fig. 52 Miscibility phase diagram (wt%) as a function of temperature (°C) between *N*,*N*-bis-(D-mannitolyl)dodecylamide (A) and octadecanoyl D-galactocerebroside (B).

from 35 to 50 Å; see Fig. 56. It is interesting that the *d*-spacing changes continuously in the smectic phase and on into the isotropic liquid. Crystallization is observed between 70 and 75 °C, where the layer spacing (d_{001}) and the correlation length (ξ_{001}) become virtually temperature independent. Where the peak shape changes from Gaussian to Lorentzian ($T = 100$ °C), a local minimum in the correlation length (half-width of the reflection peak) is observed.

At low temperatures the layer spacing approaches 48 Å. Molecular modelling gave a length of the minimized extended molecular conformation of 54.8 Å. At high temperatures the layer spacing approaches 36 Å, whereas modelling of a folded molecular conformation gives a value of 31.6 Å. Thus, one explanation given for the transformation in the smectic A* phase was that the molecules are interdigitated at high temperature, and the extent of the interdigitation reduces with temperature as the phase becomes more ordered. Thus, it appears from the *d*-spacing measurements that there was a continuous transformation from an intercalated SmA_c^* to a non-intercalated SmA_1^* structuring of the layers. The transformation from the intercalated to the non-intercalated phase was thought to be related to the change in Gaussian to Lorentzian line-shape associated with the correlation length.

An alternative explanation given was that the molecules have folded conformations, and at high temperatures the folded molecules pack in interdigitated bilayers, *i.e.* as in the SmA_d^* phase.[65] As the temperature is lowered the interdigitation is reduced and eventually the phase has only weak interdigitation, as in the SmA_2^* phase: see Fig. 57. The change over from one form of smectic A* phase to the other may not be detected from the X-ray layer spacings, but it is possible that such a transition might be seen through examination of the correlation length.

The change in the correlation length is also associated with an increase in the number of reflections seen in the radial scans. At high temperatures only the first and second order reflections are seen, whereas at low temperatures the number of reflections increases to the fourth reflection. This suggests that the layers are becoming better defined at lower temperatures in the smectic A* phase. The increased layer
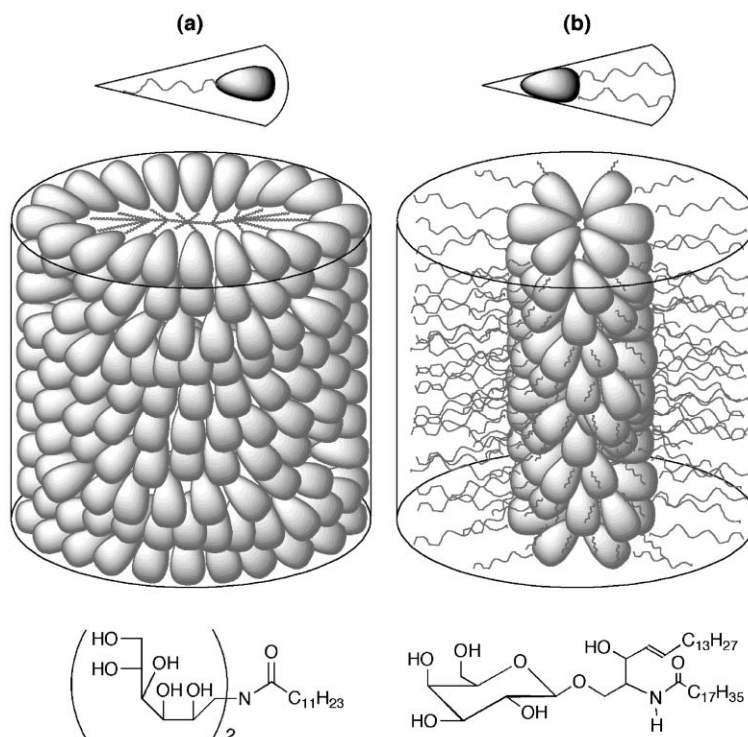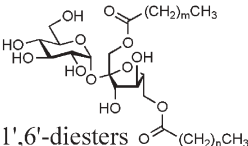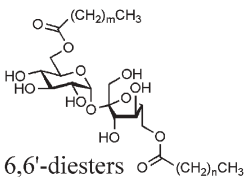

Fig. 53 Comparison between columnar mesophases with positive and negative curvatures.

This journal is © The Royal Society of Chemistry 2007

Chem. Soc. Rev., 2007, **36**, 1971–2032 | 2001

Table 10 Transition temperatures (°C) of the saturated fatty acid sucrose diesters determined by thermal polarized light microscopy as a function of aliphatic chain lengths

Compound Structure	Chain lengths	Compd Number	Transition temperatures/°C
1',6'-diesters	$m = n = 10$ $m = 10$ $n = 14$	A B	Cryst 42.1 SmA* 120 Iso Liq Cryst $\sim$ 30 SmA* 115.9 Iso Liq
6,6'-diesters	$m = n = 6$ $m = n = 8$ $m = n = 10$ $m = n = 14$ $m = n = 16$ $m = 10$ $n = 14$ + $m = 14$ $n = 10$	C d e f g h	Soft solid – SmA* 146.3 Iso Liq[a] Cryst $\sim$ 90 SmA* 163.0 Iso Liq Cryst 87.3 SmA* 170.8 Iso Liq Cryst 106.6 SmA* 167.8 Iso Liq Cryst 109.7 SmA* 164.3 Iso Liq Cryst 84.7 SmA* 167.8 Iso Liq

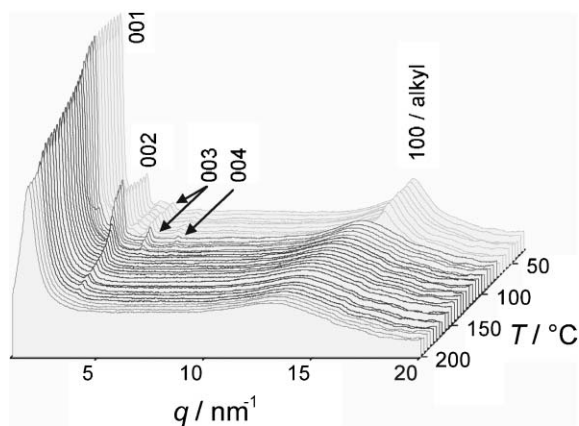[a] A melting point could not be established by microscopy or DSC.

Fig. 54 Radially integrated diffraction pattern (intensity using a logarithmic scale in arbitrary units) of 6,6'-di-*O*-octadecanoylsucrose, **38**, taken over a temperature range of 40–200 °C.
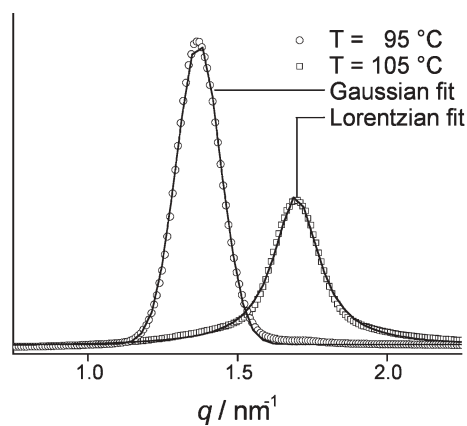

Fig. 55 Lorentzian and Gaussian fits to the diffraction data at temperatures of 105 and 95 °C respectively for 6,6'-di-*O*-octadecanoyl-sucrose, **38**.

definition may be a result of the sugar units packing more strongly together due to extensive hydrogen bonding interactions. The second model is probably more likely to give well-defined layers in comparison to the first model described above, because the second arrangement allows for flexible interactions both between and within the layers, whereas the interlayer ordering for the first model has a greater dependency on the interfacial interactions between the aliphatic chains.

Whichever model is applied, such a substantial change in the layer spacing in a smectic A* phase as a function of temperature has not been observed before in conventional thermotropic liquid crystals, and smectic A* polymorphism has not been observed before in sugar-based mesogens.

A comparison of the layer spacings as a function of temperature for the octanoyl, hexadecanoyl, and octadecanoyl (**c**, **f** and **g** in Table 10) homologues is given in Fig. 58. This figure clearly demonstrates, for the materials with shorter aliphatic chains, that the layer spacing is relatively independent of temperature, whereas the longer chain lengths show very
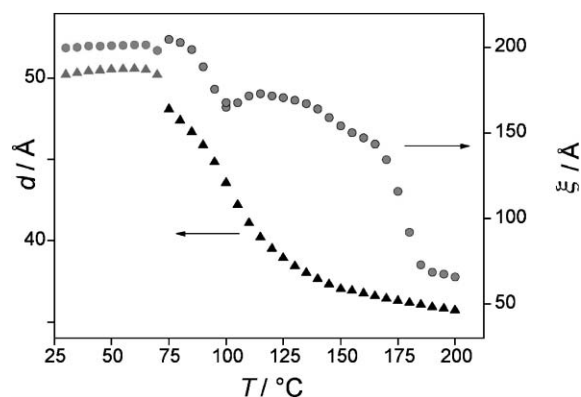

Fig. 56 Temperature-dependence of the layer spacing, d_{001}, and the correlation length, ξ_{001}, for 6,6'-di-*O*-octadecanoylsucrose, **38**.
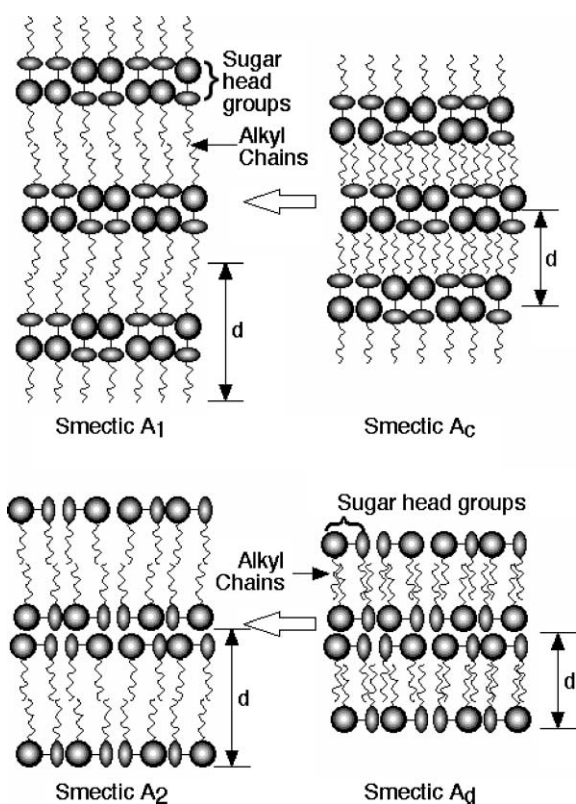
Fig. 57 The intercalated to non-intercalated transformation for the fully extended molecular model (top), and the interdigitated to non-interdigitated transformation for the folded molecular model (bottom). For each drawing the left-hand side represents the lower temperature structure.

large temperature dependencies. In addition, for the longer chains the layer ordering persists well into the liquid phase.

5. One head three tails, three heads one tail
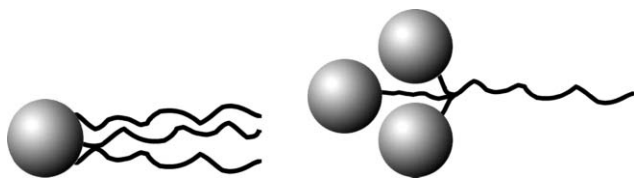
In order to investigate the effects of curvature on mesophase formation in thermotropic phases a range of pentaerythritol

derivatives **39**, **40** and **41**, were synthesised (Section 8.9),[66a] see also.[66b] It is known for lyotropic liquid crystal phases that as the curvature is varied from negative to positive, there is a passage from cubic-hexagonal-cubic-lamellar-cubic-hexagonal-cubic phases across the phase diagram as the solvent type and concentration are changed. However, for thermotropic liquid crystal phases, the same type of curvature dependent sequence has not been fully realised. Thus various homologues of the three series of compounds were made and their liquid crystal properties investigated (see Tables 11 to 13). Thus by mixing the families **39** with **40** it was hoped that the 'lyotropic phase diagram' would be emulated for the thermotropic phases.

The relative shapes of the molecules were investigated *via* computer simulations. For the purposes of comparison, Fig. 59 shows the minimised structures for the dodecyl homologues of series, **39**, **40** and **41** respectively.

For series **39**, the compounds are composed of three chains and one carbohydrate unit, and thus have wedge-like shapes with the sugar units at the apices of the wedges. Consequently these materials were expected to exhibit cubic and columnar mesophases with inverted structures. Thus the proposed type of columnar phase exhibited by series **39** was a hexagonal columnar phase with the individual molecules disordered up and down the column axis as shown in Fig. 60.

In the columnar phase the materials were expected to adopt a relatively flat conformation to enable them to self-organise into a cylindrical columnar arrangement. However, at higher temperatures, where the molecules have increased dynamical motion leading to conical shapes, several of the homologues of series **39** were also found to exhibit cubic mesophases. From the analyses of the liquid crystal properties of systems that have similar shapes to series **39**, it was deduced that the cubic mesophase was a micellar cubic phase. The curvature introduced into the system through the splay of the three chains for the compounds in series **39** is thought to be sufficient to support the formation of this type of mesophase.

For materials of type **41**, the structures of the cubic mesophases are essentially the inverse of those of type **39** compounds. The galactose units are this time located towards the exterior of the micelle and the aliphatic chains are towards the centre, as shown in Fig. 61.

For series **40**, with structures half way between series **39** and **41**, it was found that the head groups were of a similar cross-sectional size to those of the aliphatic chains. Thus when the molecules pack together they formed
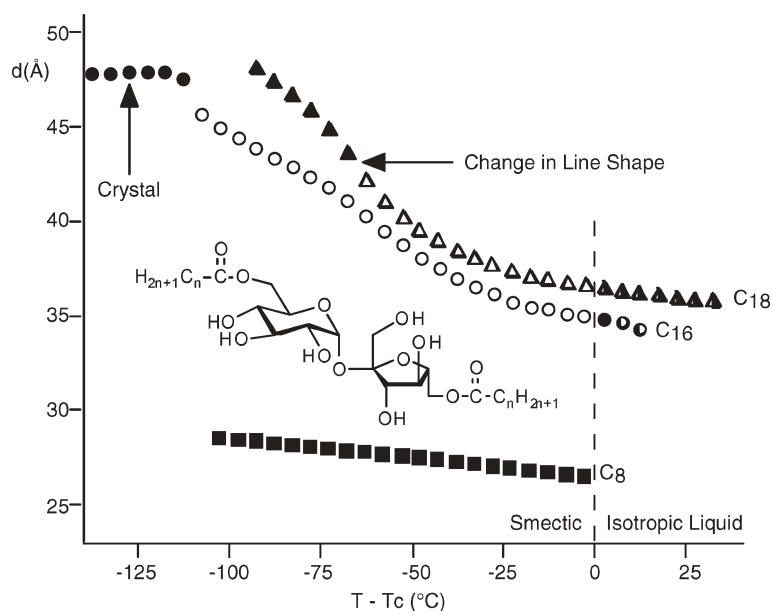

39   **40**   **41**
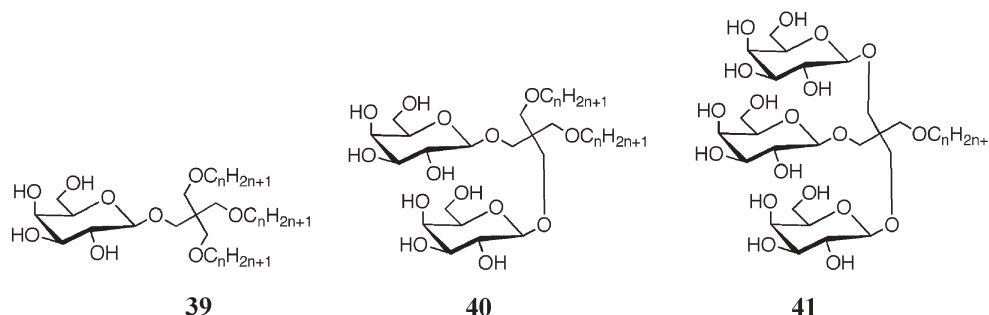
Fig. 58 The layer spacing as a function of the reduced temperature ($T - T$c) °C from the clearing point for the octanoyl, hexadecanoyl, and octadecanoyl (**c**, **f** and **g** in Table 9) homologues.

Table 11 Transition temperatures (°C) for a family of compounds of type **39**

n	Cr		Col		Cub		Iso Liq
6	a	—	•	62.3	—	—	•
7	•	44.0	•	72.1	•	82.3	•
9	•	36.0	•	59.4	•	76.2	•
10	•	37.0	•	53.3	•	63.8	•
11	•	30.0	•	38.3	•	43.4	•
12	•	37.5	(•	32.0)	—	—	•
14	•	52.7	—	—	—	—	•
16	•	58.2	—	—	—	—	•

a Material in its condensed or amorphous phase at room temperature.

Table 12 Transition temperatures (°C) for a family of compounds of type **40**.

n	Cr		SmA*a*		Iso Liq
6	a	—	•	156.2	•
12	•	53.3	•	203.1	•
14	•	46.9	•	202.2	•
16	•	41.7	•	202.2	•

a Material in its condensed or amorphous phase at room temperature.

Table 13 Transition temperatures (°C) for a family of compounds of type **41**

n	Cr		Cub		Iso Liq
12	•	91.6	•	204.0	•
16	•	150.0	•	>200.0	a

a decomposition.

39   **40**   **41**

Fig. 59 Minimised structures of the dodecyl homologues of series **39**, **40** and **41** respectively
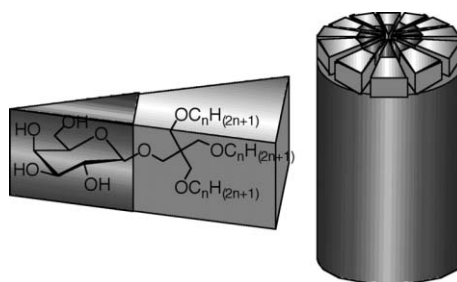
Fig. 60 The columnar structure of the hexagonal columnar phase formed by series **39**.

lamellar smectic A* phases as expected. Fig. 62 shows the packing structure of the lamellar phase for the di-dodecyl homologue.

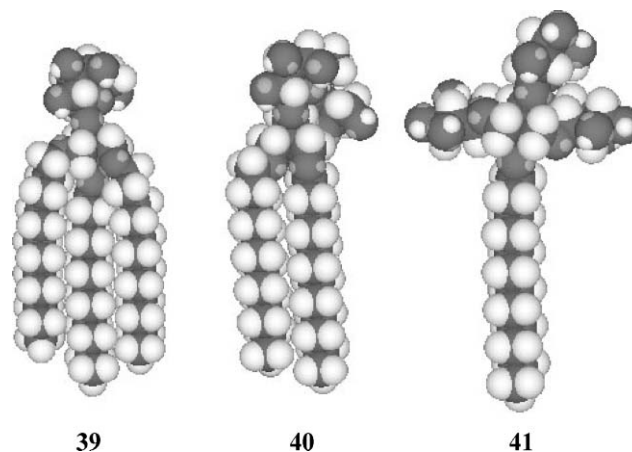From these studies and those made previously it can be seen that molecular shape and microphase segregation, the related curvature of packing and the volume fraction have similar impacts on thermotropic phases as they do for lyotropic
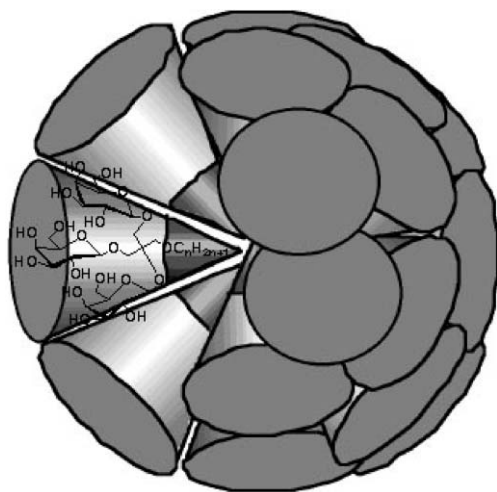
Fig. 61 Packing of cone-shaped conformational volumes of the molecules for the cubic phases of series **41**.
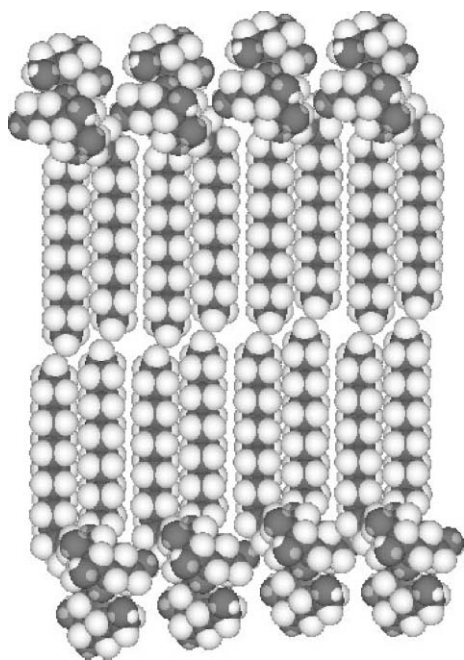

Fig. 62 The packing structure of the molecules into a lamellar phase for the di-dodecyl homologue of series **40**.

systems. This finding was tested further *via* mixing of materials derived from series **39** with those from series **41**. By doing so a lamellar phase would be expected to be obtained in the 50–50 region of the phase diagram, and indeed this was found to be the case, when a contact preparation is made between the dodecyl homologues a lamellar phase appears in the centre of the texture.

In a similar way, a range of amphiphilic polyhydroxy compounds where the structure has been partially systematically varied was also reported. This family of materials, shown in Fig. 63, exhibit a range of thermotropic mesophases, from discontinuous through to columnar phases. Thus the sequence of phases replicates those found in lyotropic and diblock copolymer systems.[67]

## 6. Heads joined by chains – bolaphiles

Bolaphiles are essentially systems where two head groups are linked together by one or more aliphatic chains. Thus in this section we first briefly examine some simple bolaphiles before moving on to more complex materials that have direct relevance to naturally occurring materials, such as those found in archaebacteria.

α,ω-Dihydroxyalkanes are possibly the simplest form of bolaphiles, but these materials are not liquid crystalline. However, the tetraols given by structure **42** are liquid crystalline. Surprisingly these materials exhibit smectic polymorphism, with most of the family shown in Table 14 exhibiting smectic C phases. A smaller number of homologues possess smectic A phases as well. X-ray diffraction shows that the molecules in the smectic C phase are tilted at an angle 28° with respect to the layer planes. The layers are composed of compounds with their diol units located at the exterior of the layers and the aliphatic chains spanning the layers. The diols form a hydrogen bonded network at the layer interfaces, thus it is only the aliphatic chains that appear tilted.[68]

42
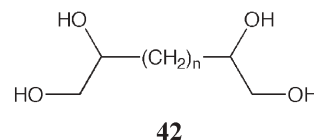
It is interesting that if heteroatoms are introduced into the aliphatic chain, different mesophase sequences are observed. For example, compounds of structure **43**, which are very similar in structure to **42**, appear to exhibit more ordered soft crystal phases, *i.e.* crystal B and crystal G.[69]
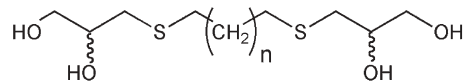
n = 9 Iso Liq 98 Crystal B 45 °C Crystal G

n = 11 Iso Liq 99 Crystal B 40 °C Crystal G

43

When sugar units are appended at the ends of the aliphatic chain, the types of mesophase formed become more varied and in many cases mesophases of unknown structure are obtained, *e.g.* see compounds of structure **44** which have acyclic sugar moieties.

For cyclic systems, however, there is a return to typical smectic A* properties: see structure **45**. The cross-sectional areas of the aliphatic chains are similar to the head groups, so there is little curvature associated with the packing of the molecules together. It is also interesting that although the clearing points for the bolaphiles are similar to those of the equivalent one-head-one-tail homologues, the melting points tend to be higher. This observation is contrary to
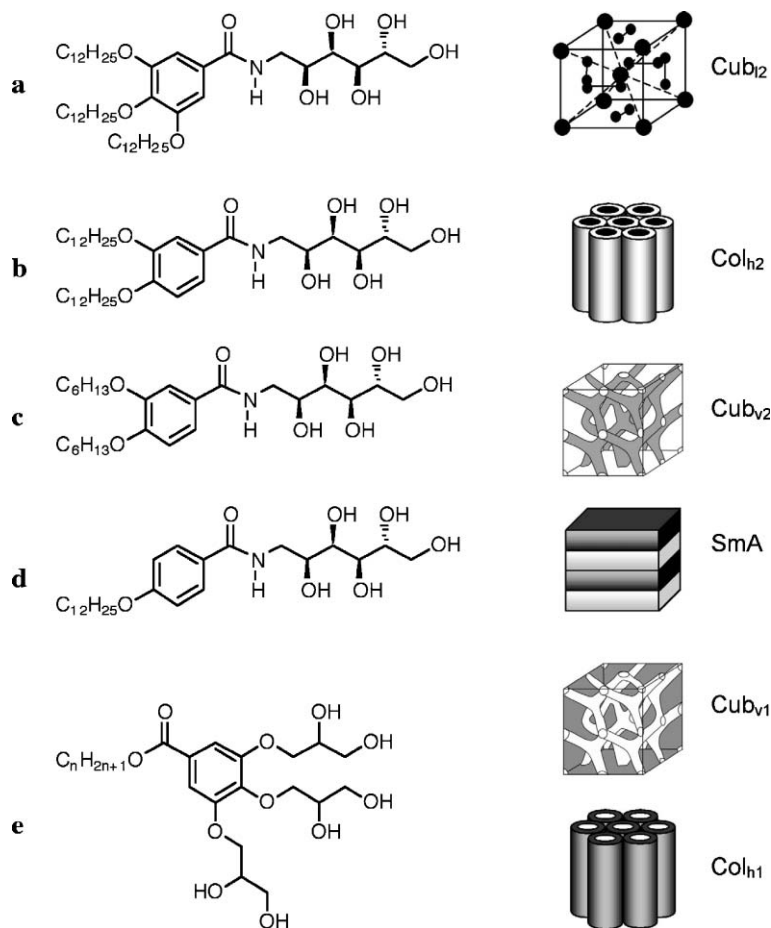
Fig. 63 Dependence of mesophase structure on molecular structure and the effect of microphase segregation (after Tschierske).[67]
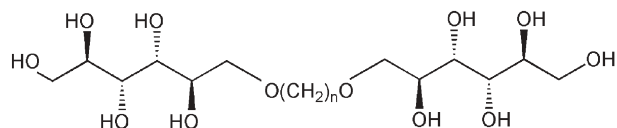
n = 16 Iso Liq 196 M 149 °C Cryst

n = 22 Iso Liq 208 M 130 °C Cryst

44

previous reviews of carbohydrate liquid crystals which have stated that the stabilities of bolaamphiphile mesophases are remarkably increased compared to simple amphiphiles of half the length.
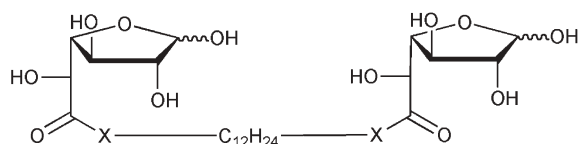
X = O Iso Liq (137) SmA* 144 °C Cryst

X = N Iso Liq (145) SmA* 165 °C Cryst

45

7. Complex bolaphiles – quasi-macrocycles
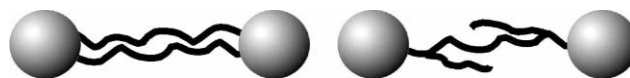
As noted in the introduction, of particular interest in this section is the molecular topology of lipids derived from

Table 14 Transition temperatures (°C) as a function of methylene chain length for the tetra-ols of general structure **42**

n	Cryst		SmC		SmA		Iso Liq
4	•	79	—		—		•
5	•	77	(•	36)	—		•
6	•	101	(•	75)	—		•
7	•	118	(•	90)	—		•
8	•	114	(•	110)	—		•
9	•	110	•	115	—		•
10	•	85	•	124	—		•
11	•	101	•	127	•	128	•
12	•	87	•	132	•	134	•
13	•	90	•	131	•	136	•
14	•	79	•	134	•	137	•
15	•	89	•	135	•	139	•
16	•	84	•	138	•	142	•
17	•	61	•	139	•	143	•
18	•	87	•	140	•	143	•
20	•	111	•	140	•	141	•

46

47 Col115.2 °C Iso Liq

48 Col 117.6 °C Iso Liq

49 Col 118.4 °C Iso Liq
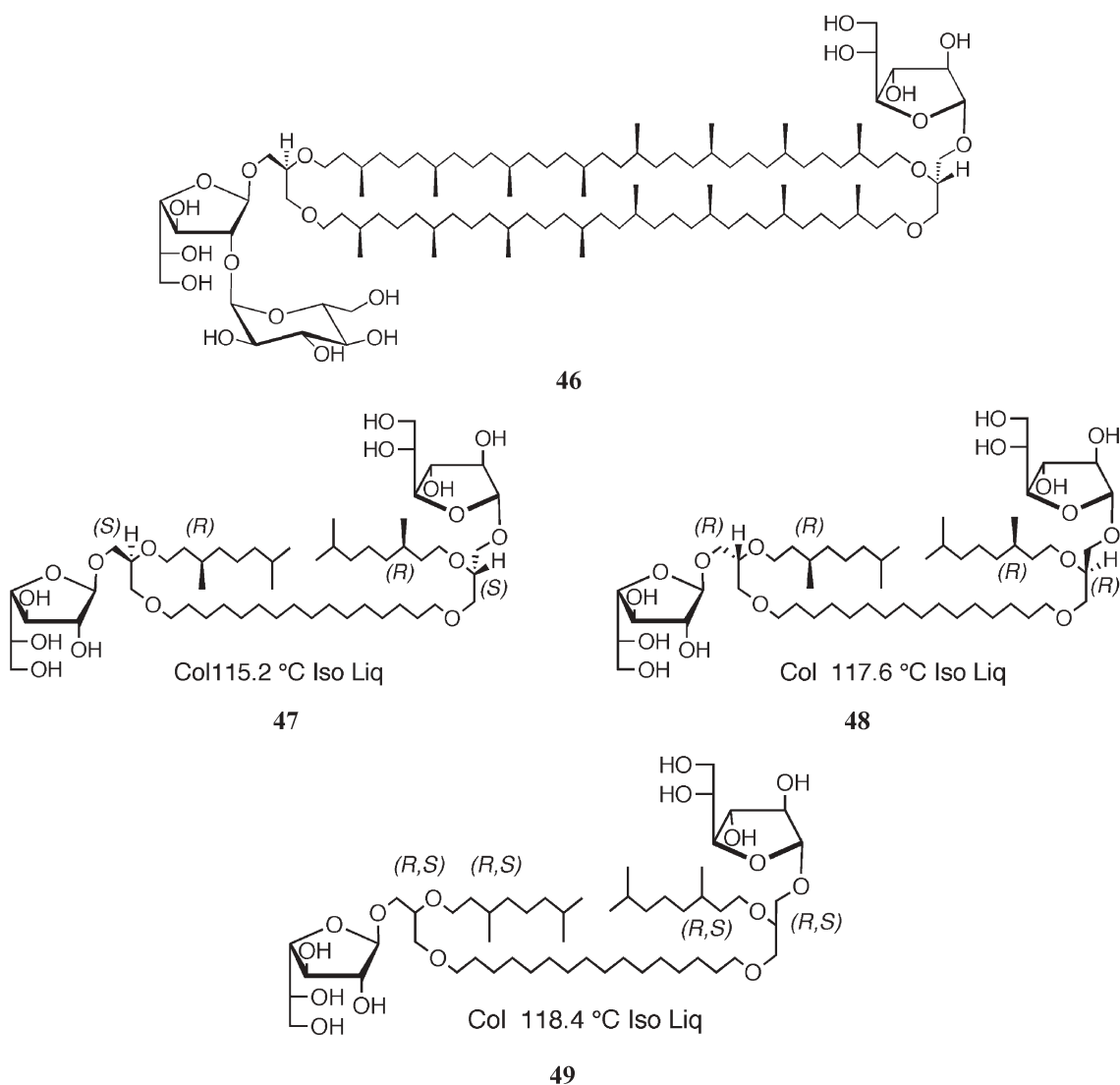
thermophilic archaea. The bolaphiles of archaebacteria are often characterized by a bipolar architecture with two polar heads linked together by two C_{40} polyisoprenoid chains which are thought to span the membrane, and therefore determine the lipid layer thickness. For example, compound **46** is a bolaphile derived from *Methanospirillum hungatei*, which is a methanogen species of bacteria.[70]

However, in spite of the growing attention to archaeal glycolipid structure and function, very few studies have been reported so far that elucidate the relationships between the molecular structure of monomeric glycolipids and the architecture of their supramolecular aggregates. This is in part due to the difficulty of obtaining sufficient amounts of chemically pure compounds from natural sources or by synthetic methods. Nevertheless, some synthetic approaches to mimics of archaeal lipids, such as **46**, have been made, as described in Section 8.10.[59,71,72] For example, the diastereo-isomeric materials **47** to **49** were prepared as mimics where there was the added advantage that the effects of molecular topology on supramolecular architecture could be investigated.

The high temperature mesophases of the materials **47**–**49** were characterised from their classical defect textures as being disordered columnar hexagonal phases (Col$_{hd}$): see Fig. 64.[44] The fan-like domains shown in the figure exhibited no banding and were smooth indicating that the positions of the molecules in the phase are disordered.
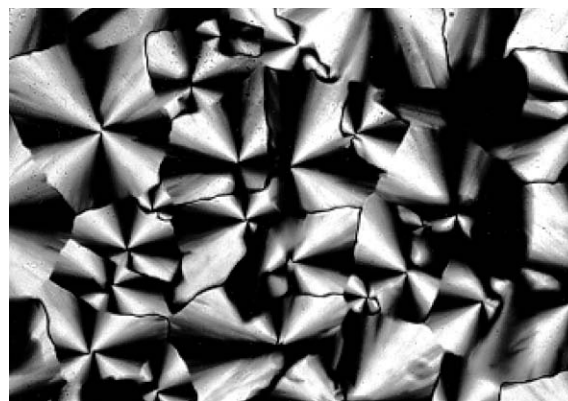

Fig. 64 The thermotropic phase of compound **49** seen between crossed polars.

This journal is © The Royal Society of Chemistry 2007

Chem. Soc. Rev., 2007, **36**, 1971–2032 | 2007

The clearing point temperatures for the three compounds do not vary much as a function of change in stereochemistry. In fact, given the small variations in purity and the experimental error in the measurements of the clearing temperatures, the isotropization points were effectively found to be the same for all three. Interestingly, the liquid crystal phase of each compound was found to supercool quite substantially to temperatures well below 0 °C. Recrystallisation was in fact not often observed, and instead it was replaced by the formation of a glassy state.

Two models were postulated for the structures of the columnar phase, one where the aliphatic chains are on the exterior and the sugar moieties are in the inside of the columns, and one where the aliphatic chains are in the interior and the sugar moieties are on the outside. However, it was found that the controlled addition of water to the neat phase showed that the thermotropic columnar phase is not continuously miscible with water. This apparent lack of miscibility with water indicated that the aliphatic chains must be located towards the exterior of the columnar structure, as shown in Fig. 65. For this structure to be stable, the molecules need to be bent double, see Fig. 66, and have hairpin-like conformational structures. The molecular folding allows for the chains to be located towards the exterior of the columnar structure and the sugar units to be in the interior.

To further elucidate the structures of the mesophases, compound 47 was investigated further by X-ray diffraction.[71] Interestingly, after leaving the material at room temperature for a few days, X-ray scattering detected a further mesophase which gave six reflections in the spacing ratios $\sqrt{6}/\sqrt{8}/\sqrt{14}/\sqrt{16}/$

$\sqrt{20}/\sqrt{22}$ corresponding to the reflections hkl = 211, 220, 321, 400, 420, 332 of a cubic phase, space group 230 (Q230) of 73.8 Å lattice dimension, a value which is approximately twice the molecular length from head group to head group. The cubic phase Q230 has been often observed in lipid systems; it consists of two 3D networks of one polarity separated by a continuous medium of opposite polarity. In the wide angle region, a broad band characteristic of fluid chains was found at 4.8 Å, as well as an additional band centred around 8 Å.

X-ray diffraction also detected a thermotropic phase transition at 70 °C, with the corresponding XRS displaying only one slightly broad scattering reflection corresponding to a value of 30 Å. This was found to correspond to the hexagonal columnar structure of lattice dimension 35 Å. The molecular length, determined by molecular simulations, was found to be approximately between 40 and 42 Å, corresponding to a hexagonal lattice dimension of 35 to 37 Å, which is in agreement with experiment and indicates that the columns have the same diameter as the molecular length. Thus the results of the X-ray diffraction studies were in agreement with the model proposed in Fig. 65.

Lyotropic studies on the materials near to the clearing point of the thermotropic phases were found to show that the compounds 47 to 49 exhibit hexagonal phases. As the thermotropic columnar phases were found not to be continuously miscible with water, it was concluded that a structure where the bolaphiles were in their stretched out conformations was not likely. In the presence of water at room temperature, glycolipid 47 showed three SAXS reflections (h = 1, 2, 3) corresponding to the presence of a lamellar Lα phase.
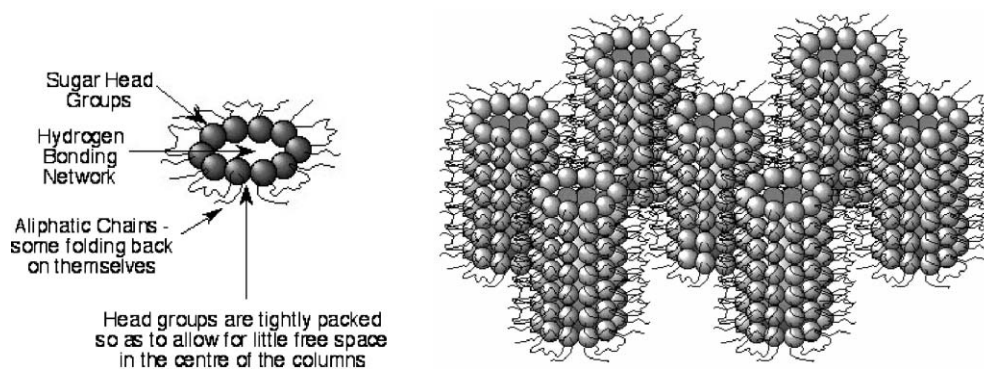

Fig. 65 The proposed columnar structure for compounds such as 47 to 49.
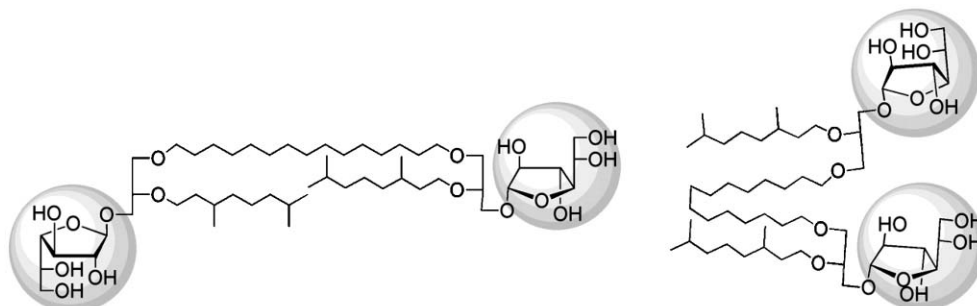

Fig. 66 The linear and hairpin structures proposed for compounds 47 to 49.

However, the material did not take up much water and the lamellar phase coexisted with an excess water, the maximum dimension being 39.8 Å.

Supramolecular aggregates formed by the three materials in aqueous media were observed under electron microscopy. It was found that compounds **47** and **49** formed tubules whereas compound **48** did not. Thus, unlike the self-organisation properties which lead to the formation of liquid crystal phases, the self-assembly leading to the creation of tubules was found to be sensitive to the stereochemistry of the material in question. Interestingly, the tubules that were formed by compounds **47** and **49** appeared to have almost equidistantly separated parallel defect lines running across the long axes of the tubules, see Fig. 67. Periodic defect structures are well-known in thermotropic liquid crystals, and are often manifested *via* a competition between the need for the molecules to form a twisted macrostructure and some structural or space limit on their ability to twist, *e.g.*, Blue Phases, TGB Phases. The competition results in a frustration which is relieved by the creation of defects. In the case of compounds **47** and **49**, the lines running across the tubules were thought to be related to defects produced by a localisation of twist, in a similar way to how twist is localised in the structure of the twist grain boundary phase.[72]

Non-symmetric bolaphiles were also prepared as shown by structures **50** to **52**. All three of these materials are characterised by having a disaccharide and monosaccharide head group. However, for these three materials the comparison was made through changing the linking unit located between the head groups. It is known for example that cyclopentane units are found in the bridging groups of naturally occurring archael lipids, and thus the mimics **50** to **52** were synthesised (as shown in Section 8.10) to examine the effects of bridging units on self-organising and self assembling properties. Interestingly, although all of the materials exhibited thermotropic columnar phases, compounds **50** and **51** also were found to be cubic. Compound **50** prior to heating, *i.e.* in its low temperature mesophase for a substantial amount of time and in the absence of water, gave six reflections in the SAXS spectrum with the spacing ratio $\sqrt{6}/\sqrt{8}/\sqrt{14}/\sqrt{16}/\sqrt{20}/\sqrt{22}$ corresponding to a cubic phase Q230 that has a 90 Å lattice parameter, which is approximately equal to twice the molecular length. A reversible transition took place on heating to the clearing point; SAXS displayed three reflections ($hk = 10, 11, 20$) corresponding to the formation of a hexagonal phase which had a lattice parameter of 44 Å. This distance was found to correspond to the columns in the hexagonal columnar phase having diameters that are approximately equal to the molecular length. As with compound **47**, the cubic phase Q230 of compound **50** consists of two 3D networks of one polarity separated by a continuous medium of opposite polarity with a lattice dimension approximately twice the molecular length, whereas the columnar phase has a hexagonal lattice spacing of approximately the molecular length.

Other asymmetric bolaphiles that were synthesised included the phosphorylated compound **53**.[73] Determination of the thermotropic liquid crystal properties of this material by POM or DSC was not possible because of its strong hygroscopic properties. However, small angle X-ray scattering gave six reflections at $s = 20.0, 35.1$ (strong), $40.3, 53.3, 60.4, 71.1$ 10^{-3} Å^{-1} that were compatible either with a P centred rectangular structure ($hk = 11, 20, 02, 22, 13, 31, 04, 40, 33, 24, 06$ reflections) of lattice dimensions 28.5 by 49.8 Å or with a mixture of two hexagonal phases ($hk = 10, 20, 21$ and $10, 11, 20$ reflections) of lattice dimension 57.4 and 32.9 Å, respectively. Molecular simulations gave an average molecular length from head group to head group of approximately 35 Å, indicating that the strong reflection at 35.1 Å is probably related directly to the molecular length of the material. When the diameters of the columns in a hexagonal phase are approximately equal to the molecular length then the lattice dimension was found to be about 30 Å.

The structure of the mesophase of phosphorylated compound **54**, like **53**, was examined by X-ray diffraction. Two small angle X-ray reflections were observed with a spacing ratio $1/\sqrt{3}$ that corresponded most likely to the first two reflections ($h = 10, 11$) of a hexagonal phase of 34.2 Å lattice dimension. The calculated molecular length was found to be
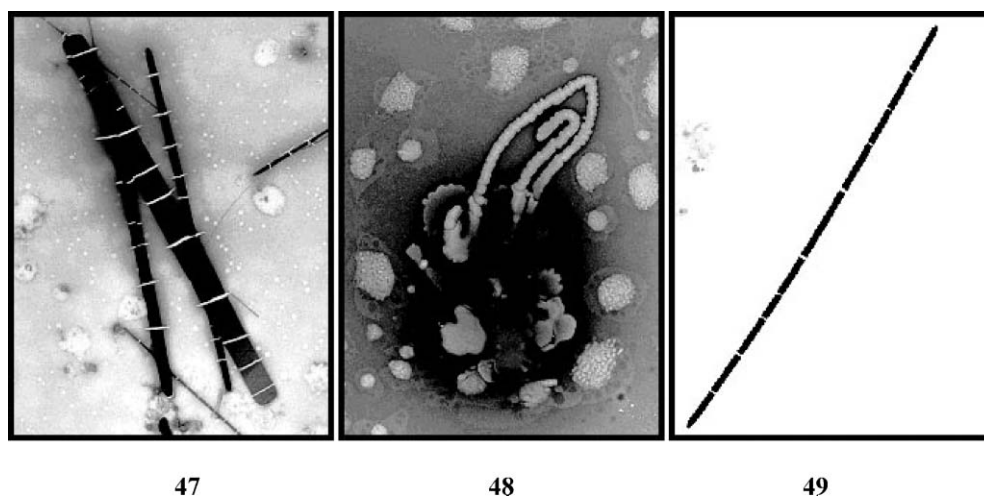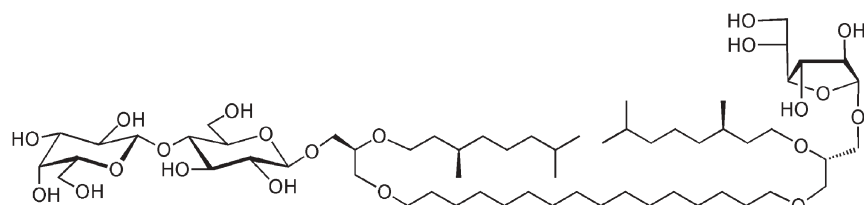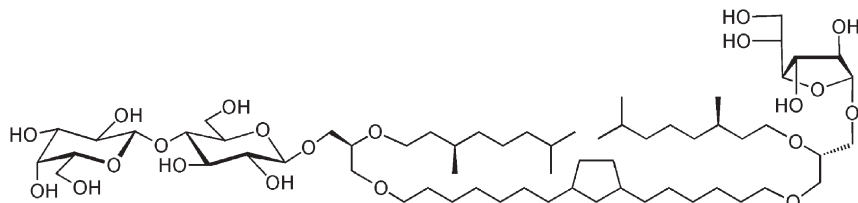

47 **48** **49**

Fig. 67 Electron microscopy micrographs of typical supramolecular aggregates formed by glycolipids **47–49** in aqueous media (negative staining with uranyl acetate).
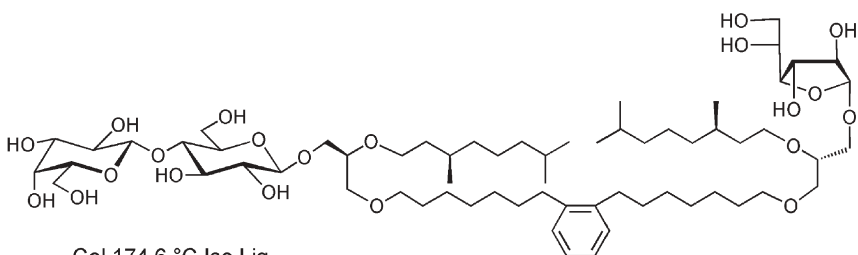
Cub ~70 Col 195.5 °C Iso Liq

50

Cub ~70 Col 181.1 °C Iso Liq

cis:trans = 4:1

51

Col 174.6 °C Iso Liq

52
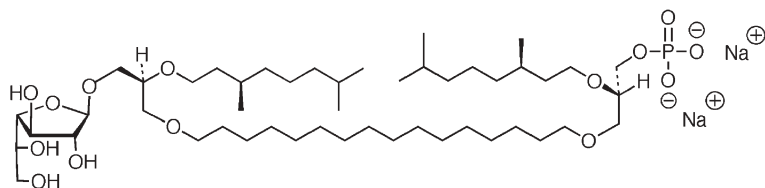
53
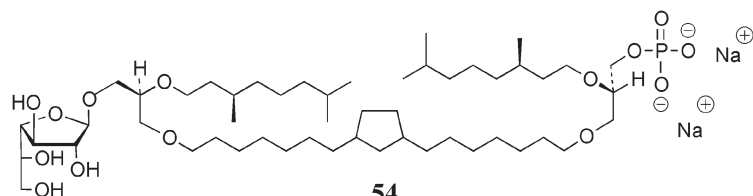
54

between 34 to 36 Å, which give a lattice dimension of between 29.5 and 32 Å. Thus the distances obtained from theoretical modelling and the experimentally determined values are comparable.

As soon as water comes into contact with the columnar phases of **53** and **54**, fluid rod myelin-type structures are observed. This result indicates that the head groups are located towards the exterior surfaces of the columns. Furthermore, the observation of Maltese crosses associated with spherulites was also indicative of the presence of large multi-lamellar vesicles. The X-ray scattering for hydrated glycolipid **53** was rather complex and depended on the amount of water present. Compound **53** tended to exhibit a lamellar phase as the amount of water was increased; for 80%

added water, three reflections (h = 1,2,3) were observed, with a repeat dimension of 102 Å. The X-ray diffraction pattern of hydrated compound **54** consisted of four reflections (h = 1, 2, 3, 4) corresponding to a lamellar Lα phase: with 50% added water, the lattice dimension was 58 Å which is approximately twice the molecular length. In more dilute aqueous media, dispersions of **53** and **54** produced vesicles without sonication, as shown by freeze fracture electron microscopy (Fig. 68); the vesicles were cross-fractured indicating the absence of a fracture plane along the mid-plane of the membrane. This result indicates that the lipid molecules do not have U-shaped conformations, but instead are trans-membrane, thus the membrane is composed of a lipid monolayer. It is interesting to note that

Fig. 68 Freeze Fracture Electron Microscopy (FFEM) of glycolipids **54**. The vesicles were cross-fractured; the lipid molecules spanning the membrane and forming a monolayer prevent the fracture from a propagation along the mid-plane of the membrane. Bar is 290 nm.

(i) $C_nH_{2n+1}Br/KOH$
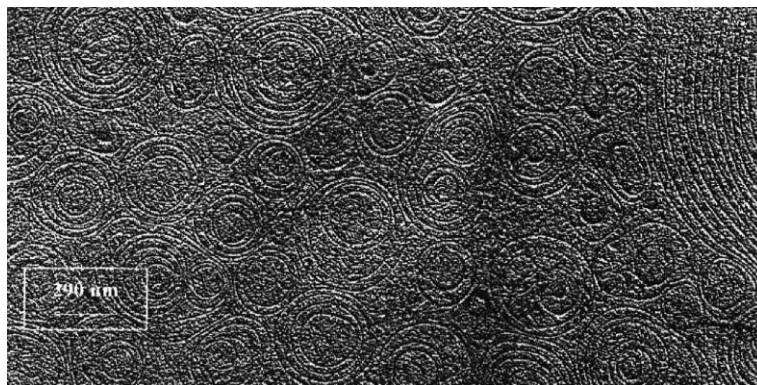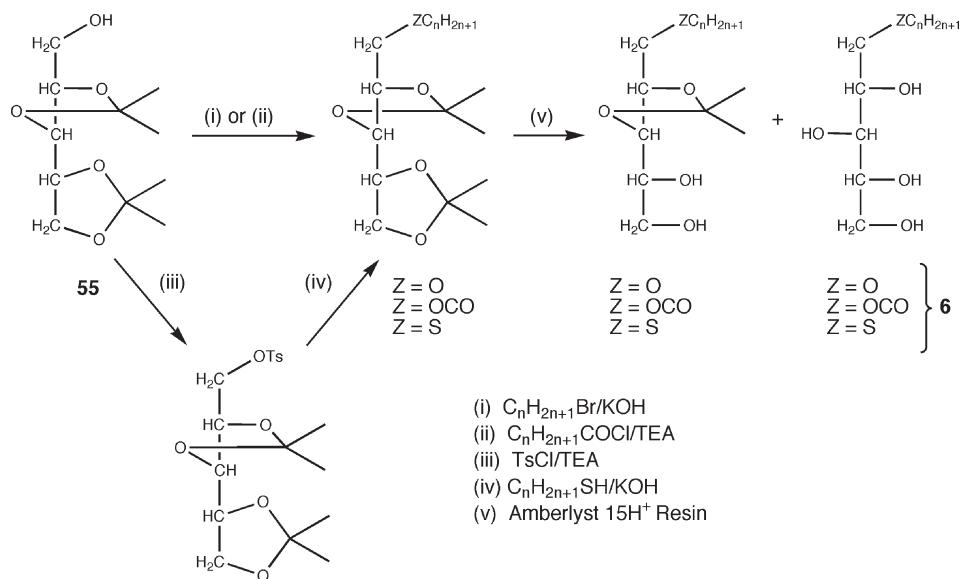(ii) $C_nH_{2n+1}COCl/TEA$
(iii) $TsCl/TEA$
(iv) $C_nH_{2n+1}SH/KOH$
(v) Amberlyst 15H$^+$ Resin

Scheme 1 Synthesis of substituted L-xylitols

the vesicles were still stable at 60 °C as shown by FFEM and by the size distribution obtained from dynamic light scattering measurements.
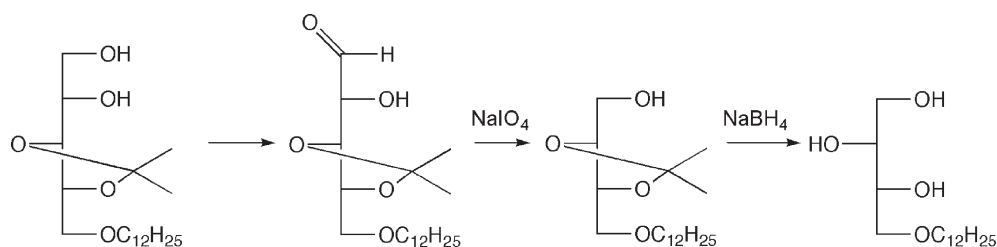
8. Synthetic procedures

8.1 Synthesis of substituted polyols and in particular substituted xylitols

Aliphatic derivatives of xylitol (general structure **6**) were prepared following the general synthetic pathway depicted in Scheme 1. The diacetal substrate, 1,2:3,4-di-O-isopropylidene-D,L-xylitol, **55**, was prepared using the method reported by Regnaut *et al.*[74] The diacetal was subsequently derivatised *via* different routes for the three families of materials. For the ether derivatives the diacetal was directly alkylated with various n-bromoalkanes in the presence of potassium hydroxide (step (i)). The esters were prepared by reaction of the diacetal with various acid chlorides in the presence of triethylamine (TEA) (step (ii)). Thioetherification of the diacetal was achieved by first making the tosylate (step (iii)), and then subjecting this to reaction with suitable thiols in the

presence of potassium hydroxide (step (iv)). The conditions for the deacetalization of the protected intermediates (step (v)) were selected with a view to simultaneously obtaining the desired products and the corresponding monoacetalated compounds. The monoacetalated compounds were found not to be mesomorphic, but nevertheless they provided a new range of surfactants for other applications.

The syntheses of the polyols where the number of CH_2OH groups was increased sequentially, see Fig. 14, are described as follows. The synthesis of 1-O-n-dodecyl-D,L-threitol, **B**, was prepared from the analogous xylitol by an the approach shown in Scheme 2. Selective deprotection of the 1-O-n-dodecyl-2,3:4,5-di-O-isopropylidene-D,L-xylitol followed by oxidative degradation with sodium periodate led to the D,L-threose derivatives; then, sodium borohydride reduction and deacetalation gave the required 1-O-n-dodecyl-D,L-threitol.

1-O-n-Dodecyl-D,L-erythritol, **C**, was prepared from the erythritol monoacetal. Selective tosylation gave the anhydro-derivative from which alkylation at the primary carbon with the dodecyl alcohol and subsequent deacetylation led to the 1-O-n-dodecyl-D,L-erythritol, see Scheme 3.

This journal is © The Royal Society of Chemistry 2007

Chem. Soc. Rev., 2007, **36**, 1971–2032 | 2011

Scheme 2   The synthesis of 1-*O*-*n*-dodecyl-D,L-threitol, **B**.
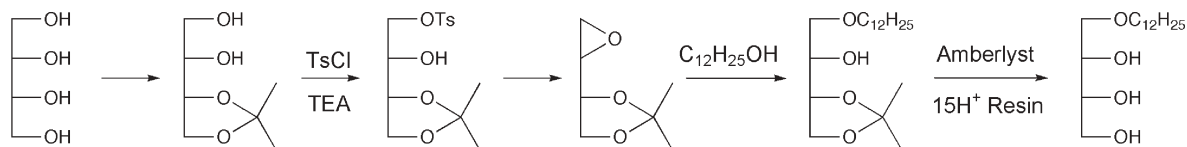
Scheme 3   Synthesis of 1-*O*-n-dodecyl-D,L-erythritol, **C**
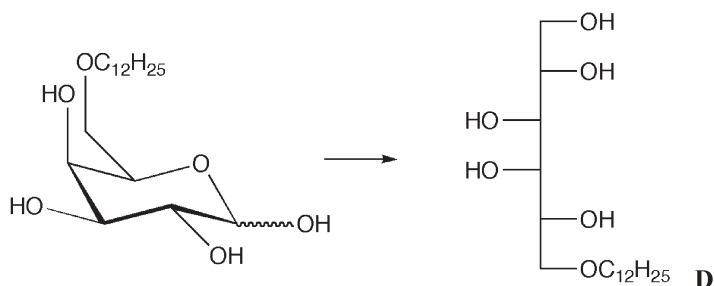
Scheme 4   Synthesis of 6-*O*-n-dodecyl-D-galactitol, **D**.

6-*O*-n-Dodecyl-D-galactitol was obtained according to Scheme 4. The alkylation of diacetonide D-galactopyranose, followed by subsequent deprotection and reduction using sodium borohydride gave the 6-*O*-n-dodecyl-D-galactitol.

Lastly, 6-*O*-n-dodecyl-D-mannitol was obtained according to Scheme 5. The alkylation of monoacetonide D-mannofuranose, subsequent deprotection and sodium borohydride reduction gave the 6-*O*-n-dodecyl-D-mannitol.

The dodecyl xylitols, which involved the study of moving a dodecyl substituent from one position to the next, were synthesised by the following methods. Thus, the *x*-*O*-dodecyl-D-xylitols where the dodecyl substituent is linked to a xylitol moiety at the x position (*x* = 1(5), 2, 3 or 4) by an oxygen atom were synthesized according to Scheme 6. All of the final dodecyl substituted xylitol products were prepared by regio-specific and stereospecific functionalization of D-xylose.

The 5-D-substituted product was prepared *via* derivatization of the anhydro derivative of D-xylose,[75] **56**, using dodecan-1-ol in toluene/dimethyl sulfoxide to give 5-*O*-dodecyl-1,2-*O*-isopropylidene-α-D-xylofuranose, **57**. Treatment of **57** with sulfuric acid (0.3 M) in a mixture of dioxane and water yielded 5-*O*-dodecyl-D-xylofuranose **58**. Compound **58** was subjected to reduction using sodium borohydride and proto-nation with cationic resin H+ to give the final 5-substituted product.

The 2-substituted product was prepared *via* derivatization of the monoacetal of D-xylose,[76] **59**, using dodecyl bromide in toluene/dimethyl sulfoxide and potassium hydroxide as the base to yield methyl 2-*O*-dodecyl-3,5-*O*-isopropylidene-D-xylofuranoside, **60**. Subsequently **60** was deprotected with aqueous acetic acid at 100 °C to give 2-*O*-dodecyl-D-xylopyranose **61**. In a similar way to compound **58**, **61** was
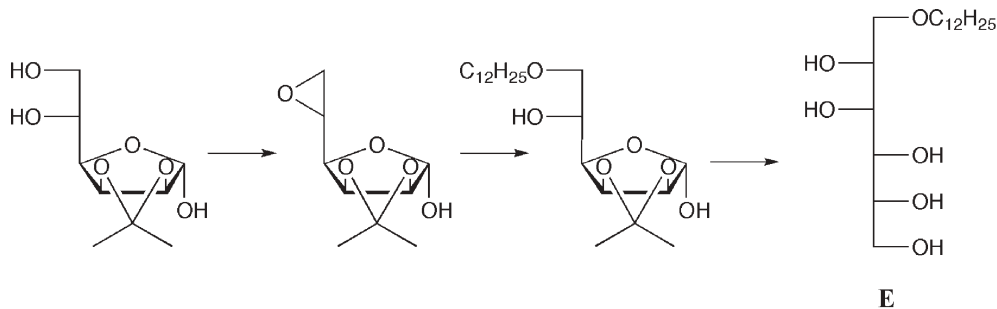
Scheme 5   Synthesis of 6-*O*-*n*-dodecyl-D-mannitol, **E**.
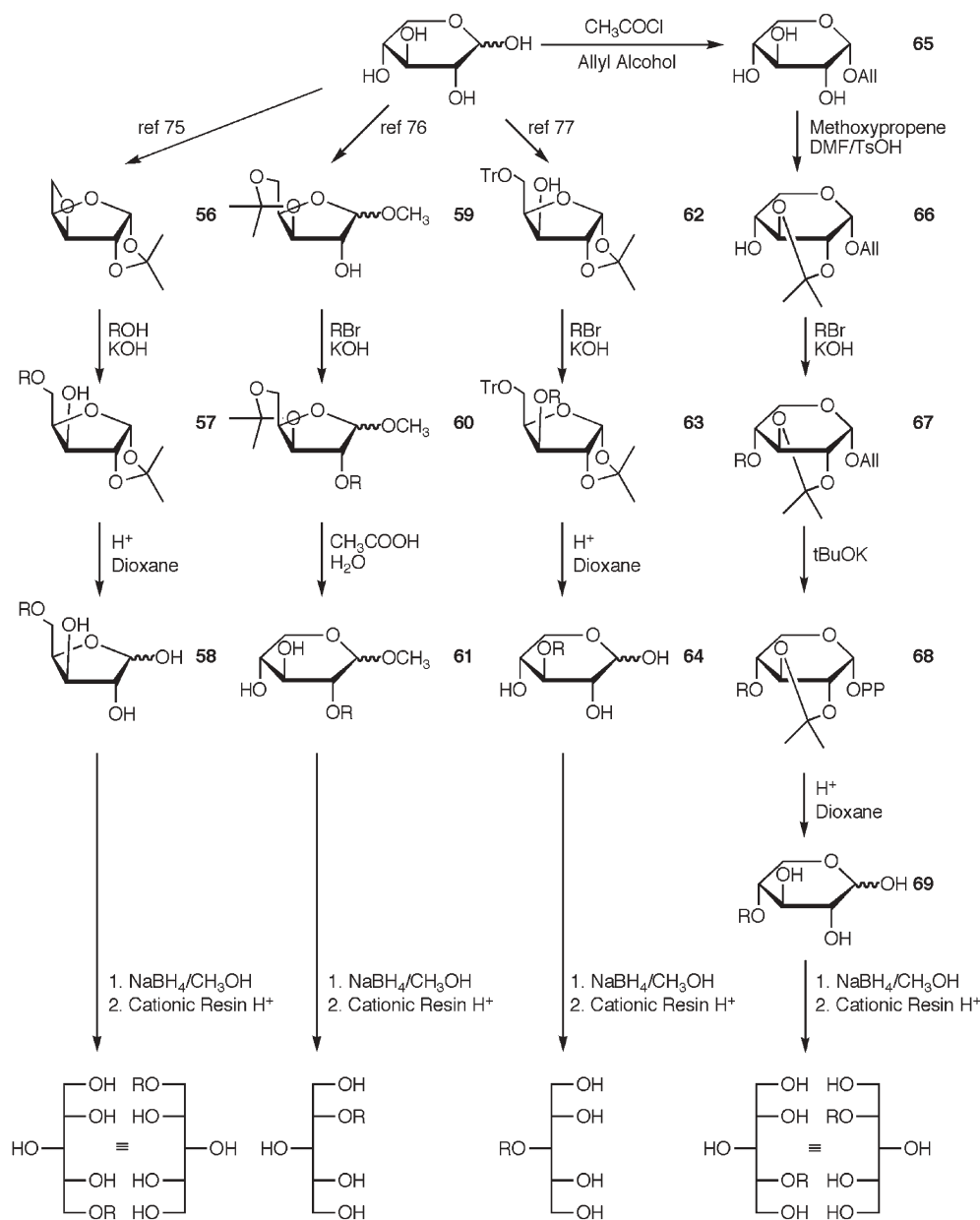
Scheme 6 The synthesis of the *x*-O-dodecyl-D-xylitols

reduced using sodium borohydride and protonated with cationic resin H$^+$ to give 2-O-dodecyl-D-xylitol.

The 3-substituted product was prepared from the trityl monoacetal, **62**, of D-xylose[77] *via* the same synthetic procedure as for the preparation of **60** to give compound **63**, 5-O-trityl-3-O-dodecyl-1,2-O-isopropylidene-α-D-xylofuranose.
Compound **63** was deprotected to give 3-O-dodecyl-D-xylopyranose **64**. In a similar way to compound **58**, **64** was reduced with sodium borohydride and protonated with cationic resin H$^+$ to give 3-O-dodecyl-*meso*-xylitol.

The 4-substituted product was prepared in a six step synthetic procedure starting from D-xylose. D-xylose was firstly treated with acetyl chloride and allyl alcohol to give allyl α-D-xylopyranoside **65**. The product was then protected using methoxypropene and a trace of toluene sulfonic acid in

DMF to give compound **66**. Allyl 2,3-O-isopropylidene-α-D-xylopyranoside, **66**, was derivatised using dodecyl bromide with potassium hydroxide as the base to give the dodecyl product **67**. Treatment of **68** with potassium *tert*-butoxide in toluene/dimethyl sulfoxide gave propenyl 4-O-dodecyl-2,3-O-isopropylidene-α-D-xylopyranoside, **69**, which was subsequently deprotected to yield **69** and reduced with sodium borohydride and protonated with cationic resin H$^+$ to give 4-O-dodecyl-D-xylitol.

8.2 The synthesis of carboxymethyl glucopyranoside derivatives

Recently it was shown that isomaltulose (6-α-D-glucopyranosyl-D-fructofuranose) could be converted conveniently to carboxymethyl tri-O-acetyl-α-D-glucopyranoside (α-CMG) by oxidation.[78] Isomaltulose is also an available disaccharide as it

This journal is © The Royal Society of Chemistry 2007

Chem. Soc. Rev., 2007, **36**, 1971–2032 | 2013
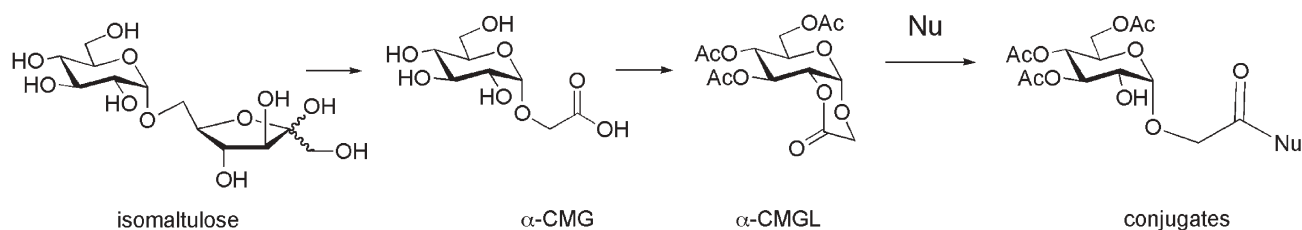
Scheme 7 New conjugates derived from α-CMG and α-CMGL.

is obtained on the industrial scale in one step from sucrose by bioconversion,[79,80] and has therefore been used as a starting material in similar applications to those targeted for the use of sucrose.[81,82] The 2-*O*-lactone of α-CMG (α-CMGL) was shown to react easily with nucleophilic species (alcohols or amines) leading to the formations of neoglucoconjugates (Scheme 7).[38,83–85]

Of the amines used in the ring opening of CMGL, some were selected for preparing new types of α-glucolipids that were investigated in the context of the general study of glycolipid-based liquid crystals. Aliphatic amides, **11**, (C$_6$, C$_8$, C$_{10}$, C$_{12}$, C$_{14}$, C$_{16}$) were obtained in good yields by reaction with α-CMGL in THF and subsequent deacetylation in methanol using catalytic amounts of sodium methanolate. With 3-aminocholesterols α and β obtained in two steps from cholesterol or epicholesterol and the saturated equivalent systems, four new steroidal glucose hybrids were obtained in 80% yields (see structures **12** to **15**).
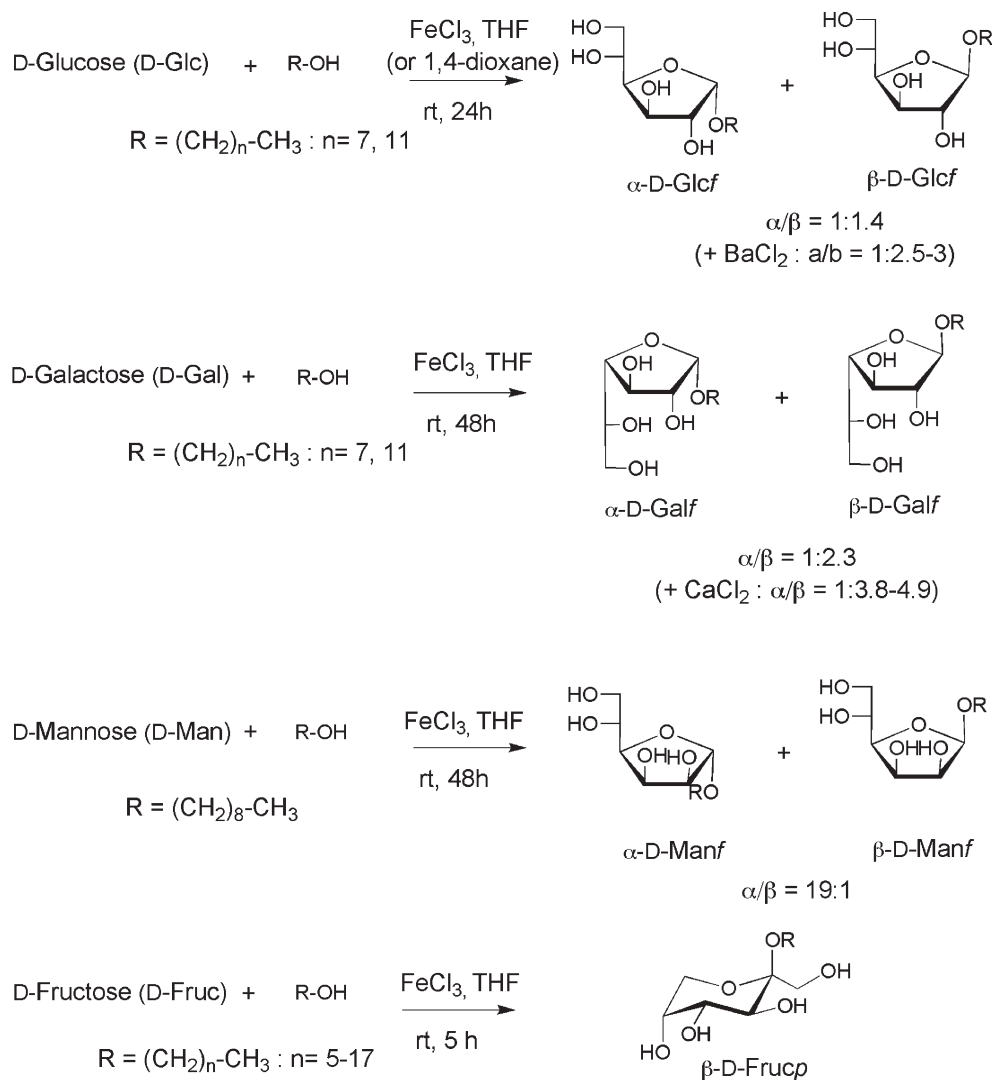
8.3 Synthesis of alkyl D-glycofuranosides and alkyl D-fructopyranosides from *O*-unprotected glycosyl donors

The creation of an *O*-glycosidic bond between a carbohydrate and an aglycon generally requires time consuming protections, activation of the glycosyl donor and deprotections.[86] Within this context, an innovative approach was developed for the production of glycolipids with one tail through a direct synthesis of tautomerically and anomerically pure alkyl D-glycosides from unprotected sugars.[87,88] The Fischer glycosylation of fatty alcohols is the most commonly used method for preparing alkyl D-glycosides but the reaction invariably produces mixtures of α,β-glycopyranosides and corresponding furanosides owing to; (i) tautomeric equilibria, and (ii) *in situ* anomerisations.[86] It was found that, depending on the promoter and on the reaction conditions, either alkyl glycofuranosides or pyranosidic derivatives were obtained in moderate to good yields. The synthesis of tautomerically and anomerically well-defined alkyl *O*-glycosides from unprotected carbohydrates requires; (i) a faster reaction of the alcohol with the sugar than the self-condensation of the monosaccharide, and (ii) a control of the equilibria involving substrates, intermediates and products, including the control of the final α,β stereoselectivity of the products. In order to avoid the self-condensation of monosaccharides, reactions were performed in heterogeneous media, unprotected carbohydrates being slightly soluble in solvents such as tetrahydrofuran (THF), 1,4-dioxane, acetonitrile and dichloromethane. It was found that the glycosylation reaction indeed occurred at room temperature, and was best achieved in tetrahydrofuran or

1,4-dioxane by using iron(III) chloride (FeCl$_3$) as the promoter.[87]

8.3.1 Synthesis of alkyl D-glycofuranosides. The selective formation of the kinetically favoured glycofuranosides was obtained by direct glycosidation of *O*-unprotected aldohexoses (glucose, galactose and mannose) with fatty alcohols (n-octanol or n-dodecanol) in tetrahydrofuran or 1,4-dioxane using ferric chloride as the promoter (Scheme 8).[87] The structures of these compounds were deduced from ^{1}H and ^{13}C NMR data and characterized by elemental analyses and/or high resolution mass spectra. In the case of glucose, the alkyl furanosides were obtained in 70–80% overall yields as mixtures of anomers (typically α/β ∼ 1 : 1.4). Practically no pyranosides were formed in these reactions. After removal of the catalyst, the furanosides were obtained as pure anomers by column chromatography (silica gel) and recrystallisation from ethyl acetate. The NMR data clearly showed the furanosidic form and indicated the stereochemistry of the anomeric centre (*e.g.*, for anomer α: δ^1H = 5.02 ppm, $J_{1,2}$ = 4.2 Hz, δ^{13}C = 103.5 ppm; anomer β: δ^1H = 4.85 ppm, $J_{1,2}$ = 0.6 Hz, δ^{13}C = 109.9 ppm). After experimentation, it was also found that the β/α ratio could be increased through the addition of barium chloride (2 equiv.), thus forming complexes between carbohydrate hydroxyl groups and cationic metal ions (α,β ∼ 1 : 2.5–3). The application of the same synthetic methodology (fatty alcohols, FeCl$_3$, THF) to D-galactose yielded the corresponding alkyl D-galactofuranosides (typically α,β ∼ 1 : 2.3) after 48 h at room temperature. After work-up, pure β-anomers crystallized out of the α,β-mixtures from diethyl ether. The diastereoselectivity was improved in the presence of calcium chloride (1 equiv.) and the α,β ratio reached typically 1 : 3.8–4.9. The assignment of the α and β-galactofuranosidic structures was made by NMR data.[87c] Octyl α-D-mannofuranoside was synthesised through glycosylation of n-octanol with D-mannose. The reaction yielded practically only the α-furanoside (yield 40%; δ_H^1 = 4.89 ppm, $J_{1,2}$ = 3.3 Hz, δ_C^{13} = 110.0 ppm).

8.3.2 Synthesis of the alkyl D-fructopyranosides. Glycosidation of fructose under Fischer conditions generally affords a mixture of the four cyclic forms, *i.e.* anomeric pairs of both pyranoses and furanoses, along with the open-chain ketose form, making tautomerism fixation considerably more difficult.[88,89] It was found that reactions of unprotected D-fructose with primary alcohols in THF and with FeCl$_3$ as a promoter at room temperature for 5 h, exclusively afforded the β-D-fructopyranosides in moderate yields (Scheme 8).[43] The formation of other isomers was not observed, and furthermore

Scheme 8 Synthesis of alkyl D-glycofuranosides and alkyl β-D-fructopyranosides.

neither 5-hydroxymethylfurfural nor difructose dianhydrides were isolated in any significant quantities. The moderate yields (30–35%) can be explained by the high affinity of D-fructose for iron(III) cations.[90] Indeed, the complexation phenomena probably tend to decrease the acidity of the promoter and thus its ability to activate the anomeric centre. In addition, the strong interaction between D-fructose and FeCl$_3$ could also be responsible for the diastereocontrol which results in the stereospecific formation of the β-fructopyranosides. The structures of the compounds can be deduced from the determination of their specific rotations and from NMR spectroscopic data. Measurements of their optical activity afforded values between $-70°$ and $-111°$ which are related to the presence of the β-pyranose form.[91] The data obtained for the specific rotations correlate well with the ^{13}C NMR findings since the C-2 anomeric centre resonates approximately at 101 ppm, *i.e.*, at a lower field than that observed for the alkyl fructofuranosides.[92] Confirmation of the presence of the pyranose form was achieved from the study of *J* coupling values obtained from the ^{1}H NMR spectra. Since the anomeric proton is absent, structural confirmation relied upon the

coupling pattern between H-3 and H-4, and the large $J_{3,4}$ value (10 Hz), which unequivocally indicated a $^2C_5$ conformation.

8.4 Synthesis of sucrose liquid crystals

Sucrose (β-D-fructofuranosyl α-D-glucopyranoside) is by far the most available of all low molecular-weight carbohydrates. Produced from sugar beet or sugar cane (148 million tonnes in 2006), its chemistry has attracted considerable interest because it is cheap, pure, stable, and chemically reactive, and, as with other simple sugars, can be used as an organic raw material replacing those produced from fossil resources.[93–100] Notably, unprotected carbohydrates have been used as the polar part of amphiphilic materials taking advantage of the high polarity due to the numerous hydroxyl groups.[101]

With respect to synthetic glycolipids having potential liquid-crystalline properties,[18,102] a number of sucrose derivatives for which the lipid chain is connected to the sucrose backbone *via* ether and ester linkages have been prepared. With eight hydroxyl groups and two anomeric carbon atoms in the sucrose molecule, the efficiency of its chemistry lies in the
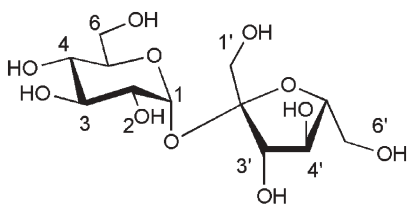
Fig. 69 Sucrose, β-D-fructofuranosyl α-D-glucopyranoside.

ability to understand the relative reactivity of the various functional groups and to control their transformations. Also, since mixtures of products are sometimes obtained, the issue of purification inevitably has to be addressed. In particular for studies investigating structure–properties relationships, high purity is a necessity. The hydroxyl groups of sucrose [3 primary (6,1′,6′) and 5 secondary (2,3,4,3′,4′), see Fig. 69] are all available to react, leading to a maximum of 255 different compounds. Fortunately, the relative rates of reaction of all OH groups depend on the type of transformation and on the reaction conditions.

Two types of selectivity are considered, namely the degree of substitution and the regiochemistry, both of which have important consequences for the properties of ensuing products. Conformational and electronic properties of sucrose, essentially based on intramolecular hydrogen-bonds and the presence of the two anomeric carbons, result in specific reactivity of OH-2, OH-1′, and OH-3′, these two latter hydroxyl groups competing against each other in a strong hydrogen-bond with O-2 (see Fig. 70). The OH-groups prove to be, in some cases, more reactive, for example in the case of the reaction with epoxides leading to hydroxyalkyl ethers. It will also be seen that perturbing this intramolecular hydrogen-bond network by substitution at some of these positions has an influence on the shape of the polar head of the amphiphilic materials and therefore on the type of supramolecular assemblies formed. The other typical behaviour, which favours reaction at the primary positions, will be illustrated in the case of the preparation of esters by chemical or enzymatic methods.[103–106]

8.4.1 Synthesis of sucrose ethers. The ether function is very stable, therefore etherification of unprotected sucrose leads to a kinetic distribution of products, directly reflecting the relative reactivity of the hydroxyl groups. In the case of the reaction with 1,2-epoxydodecane, the reaction mainly follows a typical pathway,[107,108] *i.e.*, the presence in the mixture of two major products with the chain connected at OH-2 and OH-1′ (more than 60% of the monosubstituted products). The
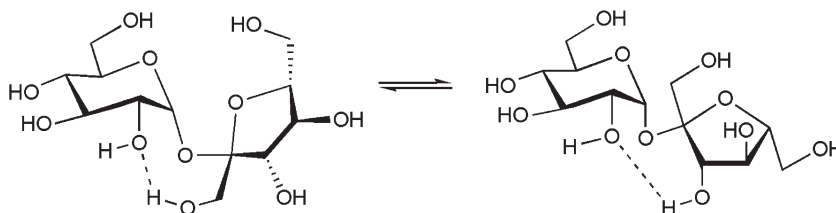
reaction could be performed either in Me$_2$SO in the presence of a base, or in water, with the expectation of slightly lower regioselectivity.[109] In aqueous medium (80% aqueous sucrose solution), the best catalysts are tertiary amines or ammonium resins, which help to overcome the difficulties caused by the heterogeneity of the medium.[110–113] A typical procedure mixes sucrose (in excess) and epoxydodecane in water, or in DMSO, with addition of a base, efficient stirring, and a reaction temperature between 90–110 °C (see Scheme 9).

Yields were determined by HPLC analysis on an analytical C8-grafted column, eluted with MeOH/H$_2$O 82/18, 0.8 mL min^{-1}. All eight possible couples of regioisomers are obtained, see the analytical HPLC (elution with acetonitrile–water 90/10) in Fig. 71. The monosubstituted hydroxydodecyl sucroses obtained from 1,2-epoxydodecane was separated by preparative HPLC using direct-phase semi-preparative NH$_2$-grafted column, with elution by acetonitrile–water 88/12 at a 20 mL min^{-1} flow rate. In addition to the thermotropic behaviour,[53a] the behaviour of these compounds was also evaluated in solution, notably for their foaming properties.[113]

8.4.2 Synthesis of sucrose esters. Sucrose esters of long chain carboxylic acids are of interest in many applications including fat substitutes,[114] bleaching boosters,[115] and emulsifiers in the food and cosmetic industries. For the latter compounds, it is known that their properties depend strongly on their compositions in terms of degree of substitution.

Sucrose ester linkage are relatively unstable, and intramolecular trans-esterifications occur rapidly from the secondary to the primary positions.[116] Therefore, for studies aimed at establishing liquid crystal structure–properties relationships, it is necessary to ensure that the structure of the materials did not change with time, thereby limiting the investigations to esters at the primary positions. The following methods were used and eventually combined; (i) the esterification with acids under Mitsunobu conditions leading to monoesters at position 6 or 6′, and 6,6′-diesters, (ii) the selective esterification at OH-2 followed by controlled migration towards O-6, (iii) protease catalyzed trans-esterification towards monoesters at O-1′, and (iv) lipase-catalyzed transesterification at O-6′.

When esterification is achieved under the Mitsunobu conditions (diethyl azodicarboxylate, Ph$_3$P), mixtures of 6- and 6′-monoesters and 6,6′-diesters are obtained, in proportions depending on the stoichiometry of the reagents (Scheme 10). Typically, a solution of sucrose in anhydrous DMF is added to triphenylphosphine, the carboxylic acid (2.5 equiv.) and DIAD (5.3 mL, 2.7 equiv.). Isolation of the 6-monoester, which is formed faster, is possible.[3,117] After

Fig. 70 Conformations of sucrose in solution.[106]
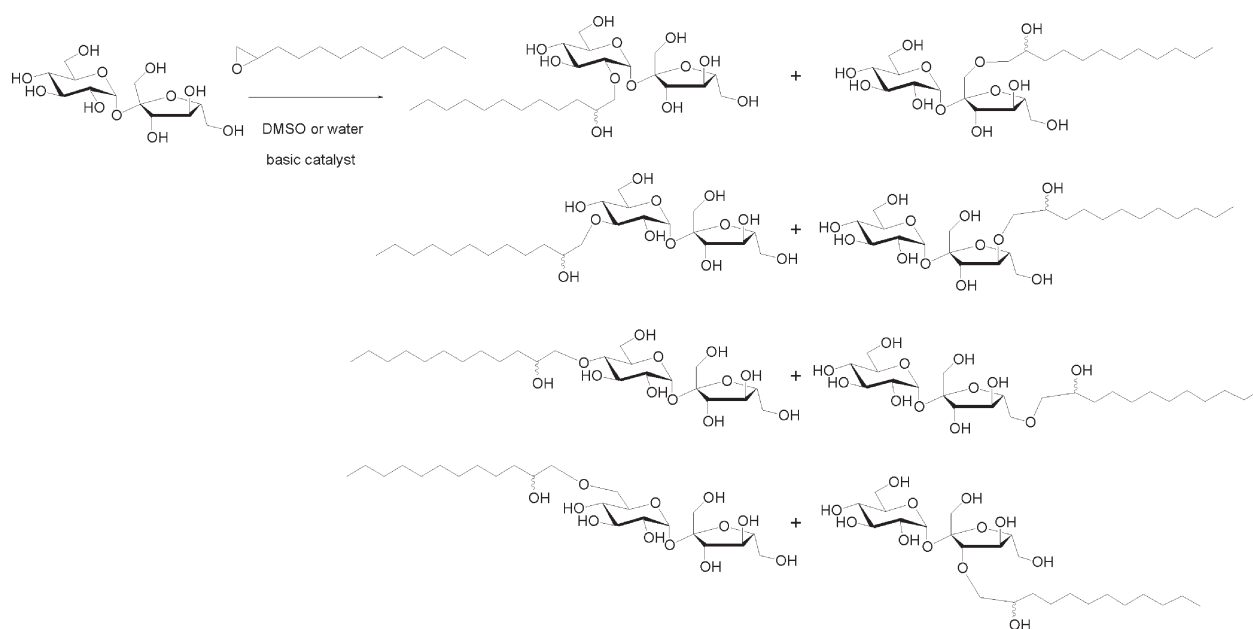
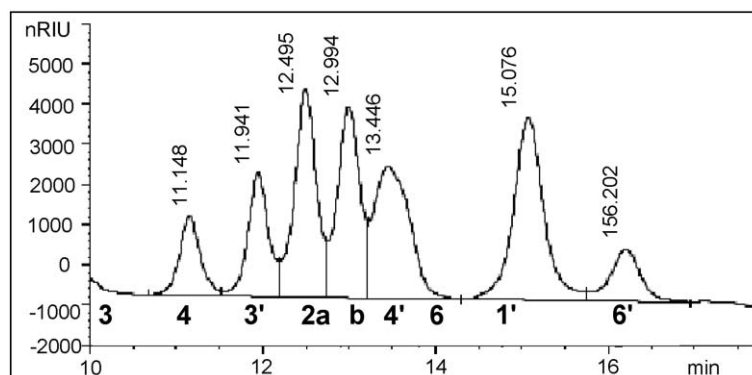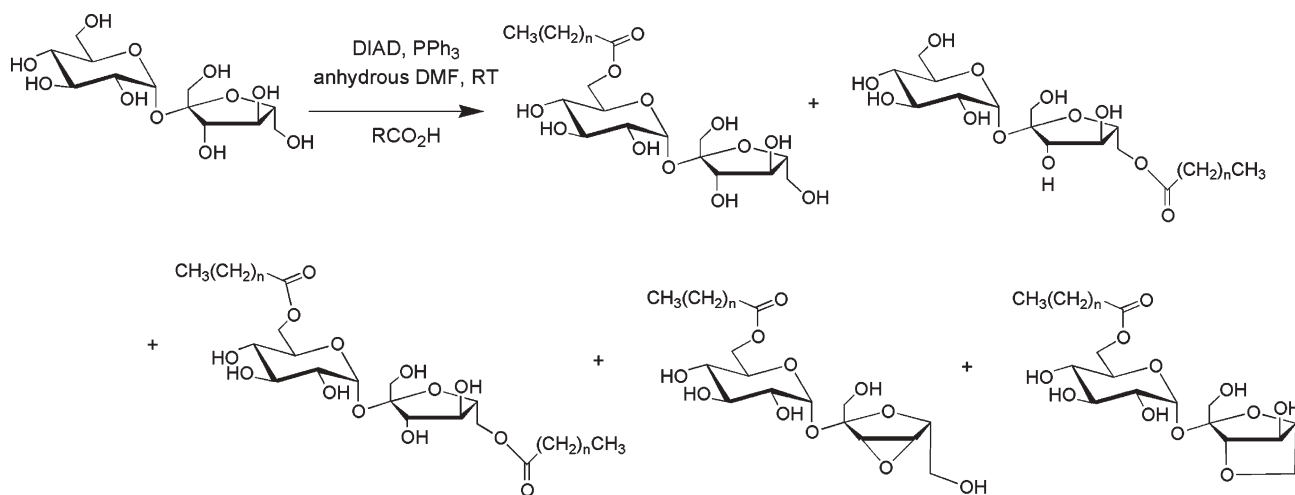**Scheme 9** Hydroxyalkyl ethers of sucrose by reaction with epoxydodecane.

Fig. 71 Separation of all monohydroxydodecyl sucrose ethers by analytical HPLC.

Scheme 10 Preparation of 6- and 6′-mono and 6,6′-diesters of sucrose by the Mitsunobu reaction.
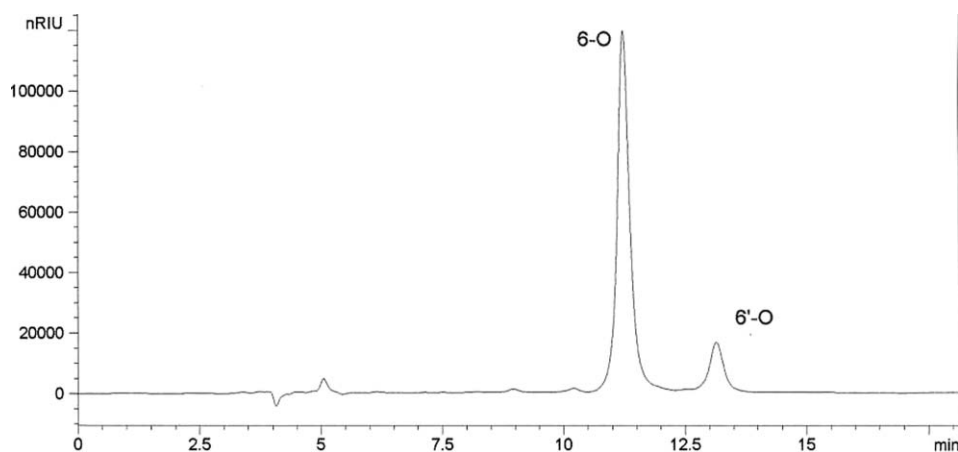
Fig. 72 Analytical HPLC chromatogram of the monoesters obtained by the Mitsunobu reaction.

1–2 days of reaction, and evaporation of DMF, the crude residue is purified by column chromatography and the fractions are then subjected to semi-preparative HPLC to isolate the 6-*O*-acylsucrose, the 6′-*O*-acylsucrose (Fig. 72), and the diester fraction, which has to be separated from the anhydrous derivatives. Indeed, intramolecular etherification competes with the desired intermolecular esterification leading to 6-*O*-acyl- 3′,4′- or 3′,6′-anhydrosucrose as side products, the latter having very close polarity to that of the diester (Fig. 73).[118]

Selective esterification of sucrose takes place at OH-2 when an acylating agent such as *N*-acylthiazolidinethione is used, giving the 2-monoester which can be transformed to the ester at O-6 when DBU is added.[116,119] However, as shown in Fig. 74, though the ester at O-6 is actually the major product, the regioisomeric purity of this material was not good enough to undergo satisfactory preparative purification by HPLC.

To access O-1′ esters, the best alternative to the classical basic catalysis is the use of proteases (see Scheme 11).[120] To make these enzymes work in the esterification sense, the reactions are performed in organic media, in the presence of only a small amount of water that is necessary to preserve their active conformation. Optimized conditions (amount of water, solvent and temperature) compatible with both the solubility of the substrates and the stability and the activity of the enzyme have to be found in each case.[121] Most examples of protease-catalyzed esterifications of sucrose lead to monoesters at position 1′ with high regioselectively (often >90%, see Fig. 75).[120,122] These reactions are performed in DMF, or preferably in Me₂SO, which is much less toxic.[123] The monoesters are then soluble enough in less-polar solvents (acetone or *tert*-butanol) in which some lipases are able to catalyze esterifications. Unlike proteases, which necessitate the activated acyl donors (vinyl or trifluoroethyl esters), lipases catalyze the esterification of simple esters and even carboxylic acids in the presence of a water scavenger. The selectivity of the lipase-catalyzed second esterification is specific for OH-6′, allowing the synthesis of mixed 1′,6′-diesters.[124]

Combinations of enzyme-mediated and purely chemical esterifications (Scheme 12) allowed for the synthesis of the 1,6 and 1′,6′-diesters with various chain lengths, degree of
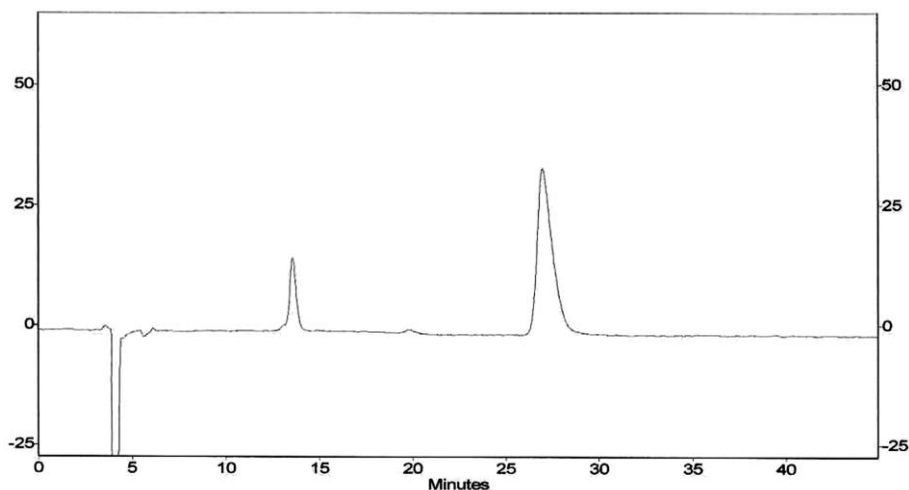
Fig. 73 Analytical HPLC chromatogram of the diester and the 3′,6′-anhydro derivative.
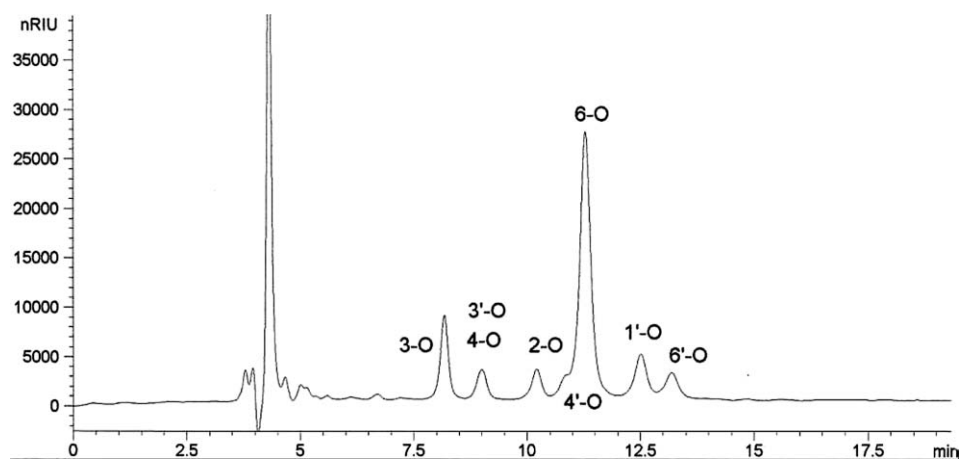
Fig. 74 Mixture of regioisomers obtained by base catalyzed migration of the 2-monoester.
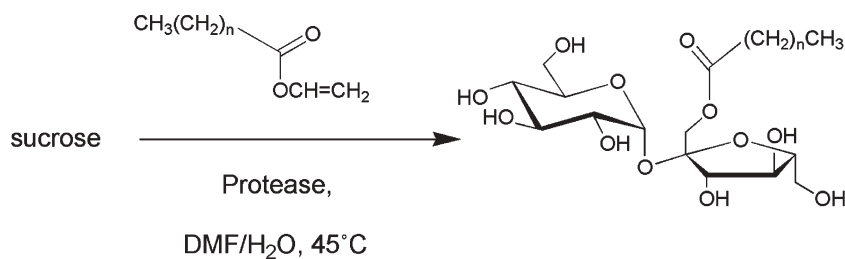
Scheme 11 Protease catalyzed esterification of sucrose at OH-1.

unsaturation, and location on the sugar backbone. The materials were then investigated for their liquid crystal properties,[4,53b,64] and their solution behaviour.[125]

8. 5 Synthesis of the azo derivatives

Phenylazophenyl glycosides have found a large variety of applications, for example as probes of the activity of a polysaccharide α-amylase,[126] as inhibitors of cell growth,[127] as dyes[128] and very recently as gelators.[129] Two routes[54] have been reported in the literature for the synthesis of phenylazophenyl glycosides; either a phenylazophenol derivative was directly glycosylated affording glycosides in moderate yields,[126,130] or a 4-aminophenyl glycoside was diazotized by standard methods and reacted *in situ* with an aromatic

compound.[131] The second synthetic approach was used for the materials described in Section 3.4 as better yields were obtained. The starting materials used were the per-*O*-acetylated 4-aminophenyl β-D-glycopyranosides **70 a–d**[132] (**a**: β-D-*gluco*, **b**: β-D-*galacto*, **c**: β-*lacto*, **d**: β-D-*xylo*, (Scheme 13), which were synthesized in two steps from the corresponding peracetylated glycosyl bromides. The 4-nitrophenyl β-D-glycopyranosides were obtained according to the method of Kleine *et al.* and then reduced by hydrogen transfer. Compound **e**[133] (**e**: α-D-*manno*) was prepared by fusion of 1,2,3,4,6-penta-*O*-acetyl-β-D-mannopyranose and 4-nitrophenol in the presence of zinc chloride,[134] followed by reduction of the 4-nitrophenyl glycoside by hydrogen transfer.
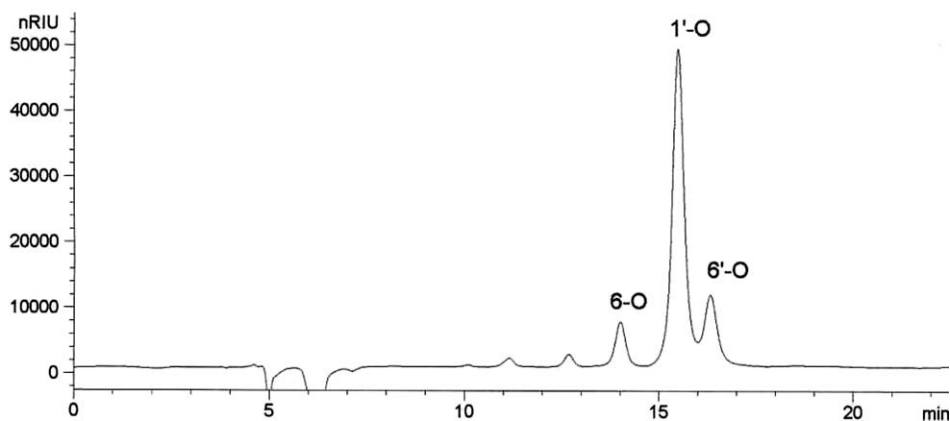
Fig. 75 HPLC chromatogram of the protease-catalyzed monoesterification of sucrose.
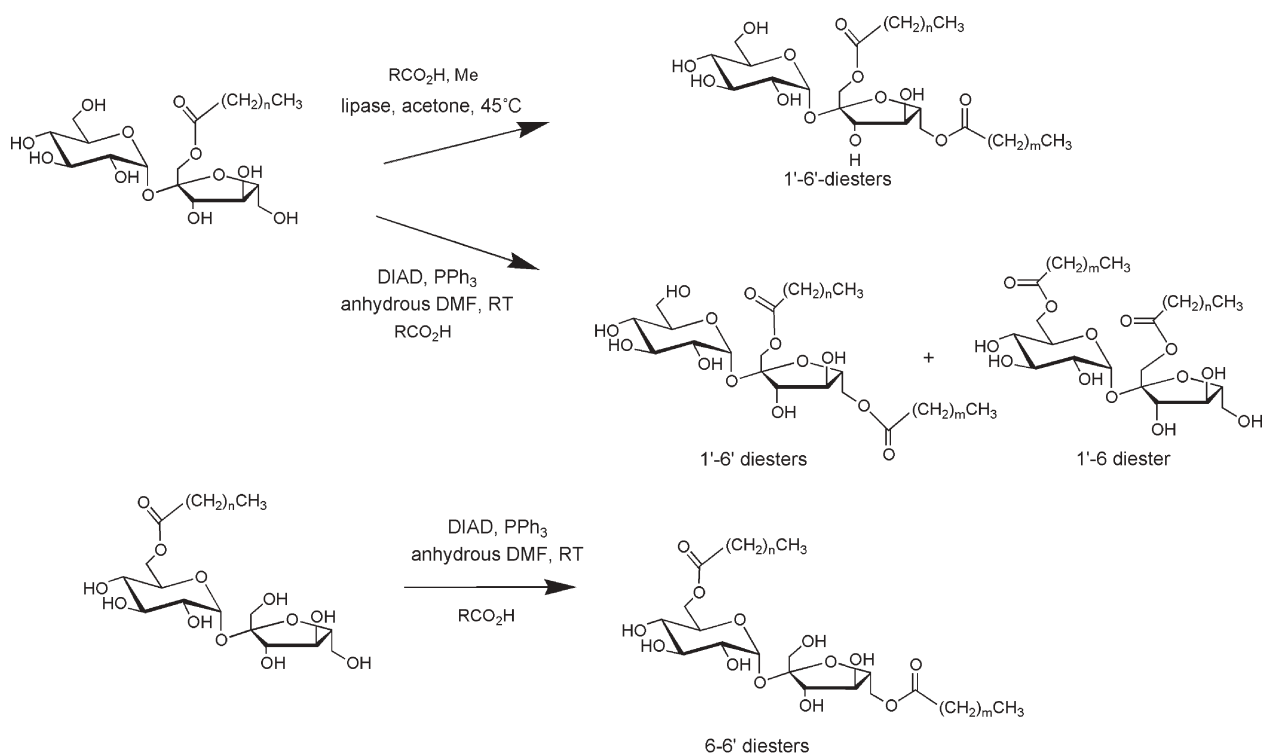
Scheme 12 Mixed-diesters of sucrose prepared by the lipase catalyzed reaction or by the Mitsunobu reaction from 1′- or 6-monoesters, where n and m are integers related to the number of carbon atoms in the methylene chains.
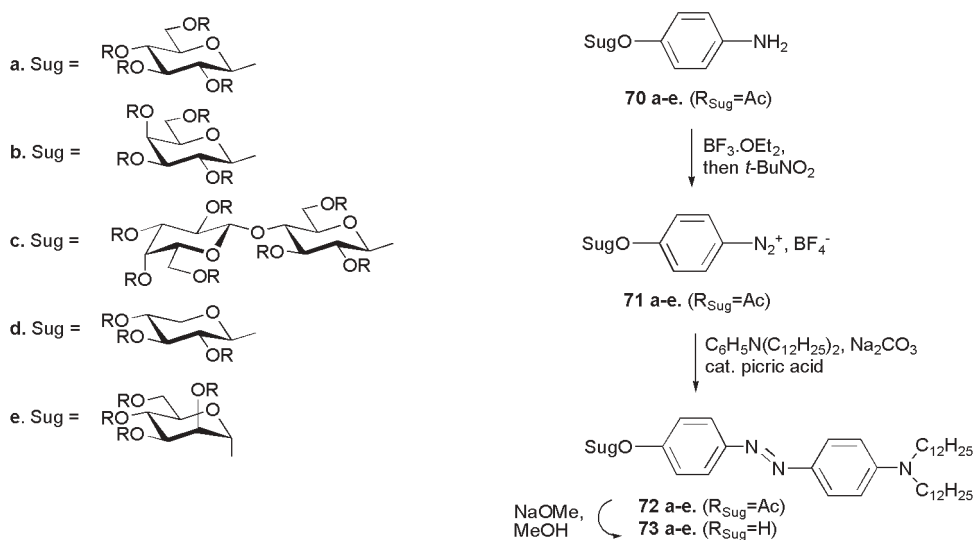
Scheme 13 Reaction pathway to amphiphilic phenylazophenyl glycosides.

Amongst numerous methods described in the literature for the synthesis of aryldiazonium salts of aniline derivatives,[135] the approach using tetrafluoroborates was selected because of their good stability and ease of preparation in anhydrous media from aromatic amines.

The application of the method described by Doyle et al.[136] to the peracetylated 4-aminophenyl glycosides **70a-e** (t-BuONO, BF$_3$.OEt$_2$, −15 °C, CH$_2$Cl$_2$) gave the expected tetrafluoroborates **71a–e** of sufficient purity. The azo coupling reactions were achieved under phase transfer conditions, catalyzed by picrate ions, according to the methodology described by Hashida et al.[137] They suggested that the higher reactivity of the diazonium salts with the picrate counter ion could be ascribed to weaker ion pairing, thereby increasing the electrophilicity of the diazonium ion. The reaction was achieved in a 1,2-dichloroethane and water mixture in the presence of sodium carbonate and a catalytic amount of picric acid. The expected phenylazophenyl derivatives **72a–72e** were obtained in good yields (55–72%) from **71a–71e** and N,N-didodecylaniline.[138] Their structures can be characterised by ^{1}H and ^{13}C NMR spectra and compared with literature data.[139]

The fully deprotected derivatives **73a–73e** were obtained by de-*O*–acetylation under Zemplén conditions in high yields. The materials possessed strong adsorptions in UV: $\lambda_{\max}$(EtOH)/nm 271 ± 1 (ε/dm^3 mol^{-1} cm^{-1} 96000–179000) and 414 ± 2 (14500–24000).

8. 6 Synthesis of ceramide analogues

Syntheses of natural analogues of glycosyl ceramides are time consuming and they need a fine control of stereochemistry on both the lipid and the carbohydrate moieties. Even with the simplest monoglycosyl ceramides which do not require a great number of steps to build the glycan fragment, the syntheses of the sphingosine moiety most often requires 15 to 20 steps. Two main approaches are described in the literature to prepare sphingosine or ceramide analogues as follows; the "chiral pool approach" in which the molecule is built on a chiral backbone, and the "asymmetric induction approach" in which it is built *via* diastereoselective induction onto a chiral synthon. Initially, tartaric acid[140] or carbohydrates were found to be the most often used precursors (*e.g.* D-lyxose,[141,142] D-galactose[143] or D-glucose).[144,145] More recently, cross-metathesis allowed the preparation of a large variety of sphingosine analogues.[142,144,145] In the second approach, diastereoselective reductions or additions are effected on chiral amides, such as Weinreb amide[146–148] or carbonyl derivatives, such as Garner's aldehyde.[149] Other elegant methods were developed to realize such syntheses, which are described in four recent reviews that discuss the preparation of sphingosines, phytosphingosines, ceramides or glycosylceramides.[150]

Due to the complexity and length of preparation of natural sphingolipids, new sphingosine and ceramides analogues are of interest as much as they display organizational properties that can be compared with those of natural glycolipids. Thus, this section describes the synthesis of two families in which the main chain is saturated (phytosphingosine analogue) and does not contain any hydroxyl group. In one family (**I**, Fig. 76), the main chain (C_nH_{2n+1}, $n = 6, 12, 16$) includes an oxygen thereby reintroducing some hydrophilicity; in the other family (**II**) the main chain is a hydrocarbon chain ($C_{14}H_{29}$). In the first family (**I**), the side chain of the sphingosine analogues was maintained with the same stereochemistry as natural ceramides with the amide attached aliphatic chain varied in length (NHCOC$_m$H$_{2m+1}$, $m = 5, 11, 17$), whereas in the second family (**II**) it was kept constant (NHCOC$_{15}$H$_{31}$) but both stereo-isomers at the branching point being examined.

The neoglycolipids **I** were prepared *via* the synthetic pathways shown in Scheme 14.[55]

For this synthetic strategy, 1,2-*O*-isopropylidene-*sn*-glycerol was treated with an excess of n-hexyl, n-dodecyl, or n-hexadecyl bromide under phase-transfer conditions at 80 °C;[151] compounds **74a–c** (Scheme 14) were obtained in yields from 80% to 99%. The isopropylidene acetals were cleaved[152] to afford the corresponding diols. The latter were selectively protected at the primary positions with *tert*-butyldimethylsilyl chloride in the presence of triethylamine and a catalytic amount of 4-(dimethylamino)pyridine in dichloromethane.[153] The secondary position was then activated as a mesylate to afford **75a–c**. The leaving group was then displaced by nucleophilic substitution with sodium azide in dimethylformamide at 100 °C[154] to afford the expected azido compounds. After de-silylation in the usual manner (tetrabutylammonium fluoride in THF),[155] compounds **76a–c** were glycosylated before the introduction of the amido
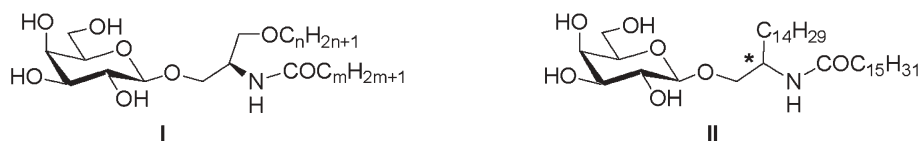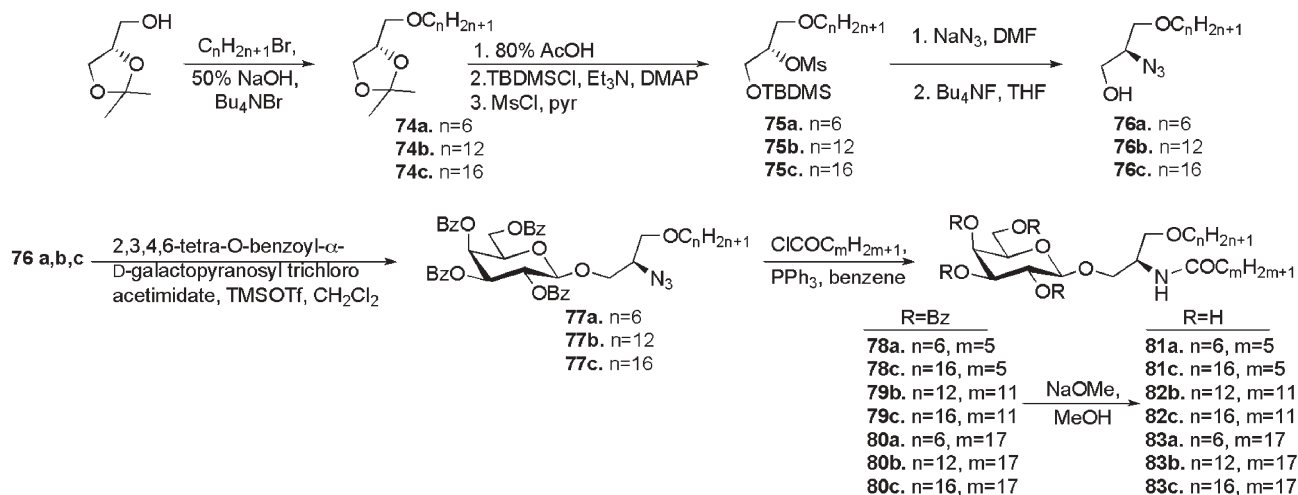
Fig. 76 Targeted families of galactosylceramide analogues

Scheme 14 Reaction pathway to neoglycolipids **I**

This journal is © The Royal Society of Chemistry 2007

Chem. Soc. Rev., 2007, **36**, 1971–2032 | 2021

function at the secondary position of glycerol. Thus, the galactosylation was effected with 2,3,4,6-tetra-O-benzoyl-α-D-galactopyranosyl trichloroacetimidate as the donor and a catalytic amount of trimethylsilyl triflate as the promoter,[156] at 0 °C in dichloromethane to afford glycosides 77a–c. The amido function was then built by a modified Staudinger procedure:[157] condensation of n-hexanoyl, n-dodecanoyl, or n-octadecanoyl chloride with the azido derivatives 77a-c, in the presence of triphenylphosphine, in benzene at room temperature afforded compounds 78a,c, 79b,c, and 80a–c respectively. The protected glycosides were then deprotected by Zemplén conditions, using either methanol or a 1 : 1 mixture of chloroform and methanol,[158] depending on their solubilities to afford the expected compounds 81a,c, 82b,c, and 83a–c.

Neoglycolipids II (89R and 89S) were prepared via the synthetic pathways shown in Scheme 15.[159] The key step of the synthesis is the enantioselective epoxide ring opening, described for shorter alkyl chains by Jacobsen and coworkers.[160,161]

The treatment of 1,2-epoxyhexadecane (84) (R,R)-(−)-N,N′-bis(3,5-di-tert-butylsalicylidene)-1,2-cyclohexanediaminocobalt(III) in water and THF afforded the expected (2S)-hexadecane-1,2-diol (85S) and (2R)-1,2-epoxyhexadecane (84R). The high enantio-selectivity of the reaction (ee > 95%) was confirmed by comparison of the optical rotation of these two products with that of the literature.[162] (2R)-Hexadecane-1,2-diol (85R) and (2S)-1,2-epoxyhexadecane (84S) were similarly obtained from 84 in the presence of (S,S)-(+)-N,N′-bis-(3,5-di-tert-butylsalicylidene)-1,2-cyclohexanediaminocobalt(III) acetate (Scheme 15).

Treatment of diol 84S with triphenylphosphine, diisopropyl-azodicaboxylate (DIAD) and azidotrimethylsilane[163] afforded a 20 : 1 unseparable mixture of (2R)-2-azido-1 trimethylsilyl-oxyhexadecane and (2S)-1-azido-2-trimethylsilyloxyhexade-cane in high yield. De-silylation of the mixture was realized in the presence of an excess of potassium carbonate in dry methanol to afford the 2-azido derivative 86R. The same sequence, applied to diol 84R, afforded 85S.

Glycosylation was carried out with the azidoalcohol acceptors 86R and 86S and 2,3,4,6-tetra-O-benzoyl-α-D-galactopyranosyl trichloroacetimidate[157,164] as the donor (Scheme 15) in the presence of a catalytic amount of

trimethylsilyl trifluoromethanesulfonate at 0 °C to afford fully protected glycosides 87R and 87S. The enantiomeric purities of 87R and 87S were confirmed at this stage ^{13}C by NMR spectroscopy. The transformation of the azido derivatives into N-acyl derivatives was realized via the modification of the Staudinger reaction[165] to afford compounds 88R and 88S. Compounds 88R and 88S were then de-O-benzoylated by the Zemplén procedure to give products 89R and 89S, respectively.

8.7 Synthesis of diether-type glycolipids related to archaeal membrane lipids

The lipids of some methanogenic Archaebacteria as in *Methanospirillum hungatei* species are characterized by high proportions of diether-type components with a 2,3-diphytanyl-sn-glycerol backbone and with glycosyl polar groups at the sn-1 position that include β-D-galactofuranose (β-Galf) moieties.[8,9] The presence of β-Galf is a striking feature since D-galactose, as well as other hexoses, appears only in the pyranose form in mammalian glycolipids and glycoproteins.[9] Within this context, an efficient route to diether analogues possessing; (i) one furanosyl unit as the polar head group, (ii) optically pure (R or S) or racemic glycerol isomers; and (iii) phytanyl, dihydrocitronellyl and/or straight alkyl chains (see Fig. 46) was developed.

The general synthetic pathway to the targeted diethers, described in Section 8.3, involved the preparation of suitable diether-type alcohols from optically pure or racemic glycerol or glycidol followed by their glycosylation with n-pentenyl furanosyl donors derived from D-galactose, D-glucose or D-mannose.[58] The key glycofuranosyl donors were prepared, in one-pot reactions,[166] by ferric chloride promoted glycosyl-ations of 4-penten-1-ol with D-glucose, D-mannose or D-galactose, followed in situ by acetylation (Scheme 16). Glycosidation of D-glucose was carried out in acetonitrile at room temperature in the presence of FeCl₃. As the 4-pentenyl glucosides are water-soluble compounds, acetylation with acetic anhydride was carried out in situ. The ferric chloride promoted glycosidation of D-mannose in acetonitrile was unsuccessful; however, the reaction could be performed in THF at room temperature followed by in situ acetylation. The resulting n-pentenyl mannofuranoside was isolated in 56%
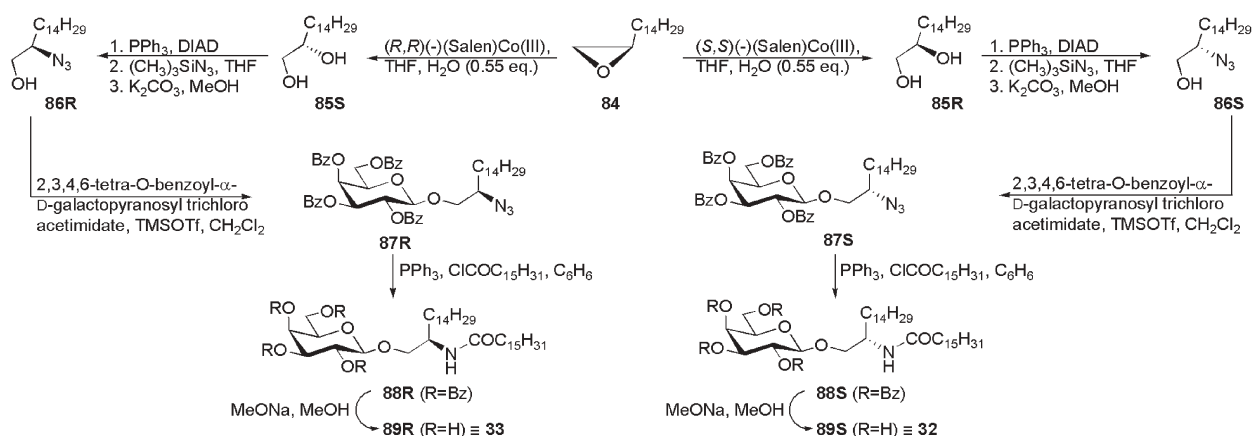
Scheme 15 Reaction pathway to neoglycolipids II.
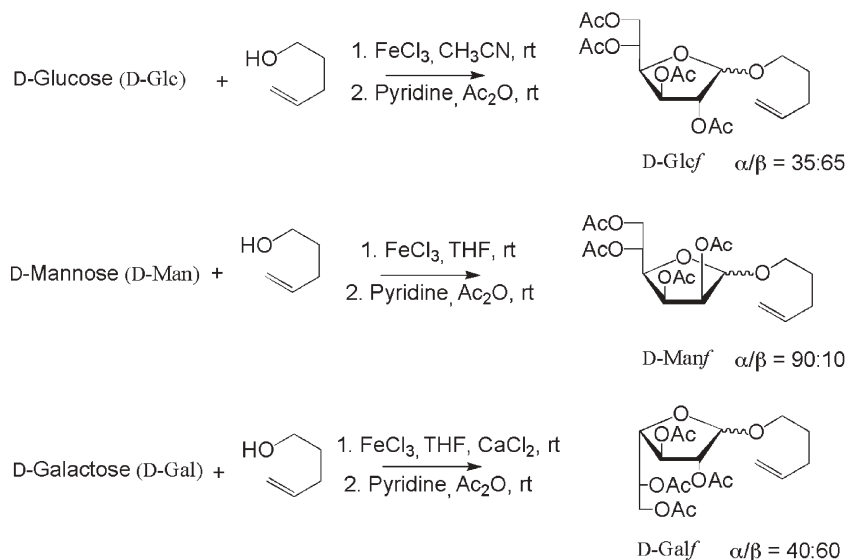
Scheme 16 Preparation of the glycofuranosyl donors.

yield (α,β = 90/10). The major anomer α, was obtained by column chromatography. Glycosylation of 4-penten-1-ol with D-galactose was performed in THF by using ferric chloride as promoter and calcium chloride as the additive in order to prevent the ring expansion from the kinetically favoured galactofuranosidic product to the thermodynamically more stable galactopyranoside. After acetylation, the n-pentenyl D-galactofuranoside was isolated as a mixture of anomers (α,β = 40/60).

Subsequent introduction of the furanosyl units on diethers was achieved by using standard n-pentenyl glycoside (NPG) conditions (NIS, 1.3 equiv., TESOTf, 0.3 equiv. with respect to donors) to afford the resulting glycosides. All reactions resulted in the specific formation of 1,2-*trans* glycofuranosides, probably due to the C-2 ester neighbouring group participation and the anomeric configuration of the donors (Scheme 17).

Conventional deacetylation by sodium methoxide resulted in effective deprotection of the hydroxyl groups to yield the 1,2-*trans* furanosides.

8.8 Synthesis of *N,N'*-bis-(D-mannitolyl)alkylamides

The preparation of a bis-(2,3:5,6-di-*O*-isopropylidene mannitolyl) amine from D-mannose and then on to the synthesis of several novel glycolipids, see structure **37**, was achieved by coupling a diglycitolamine to a long chain acyl or alkyl group. Thereby double headed amphiphiles in which the hydrophilic heads are close together were realised. The scheme for the preparation of the bis-(2,3:5,6-di-*O*-isopropylidene mannitolyl)amine from D-mannose is shown in Scheme 18.

In the first step the α,β-D-mannopyranosylamine was prepared from D-mannose by action of ammonia in methanol,
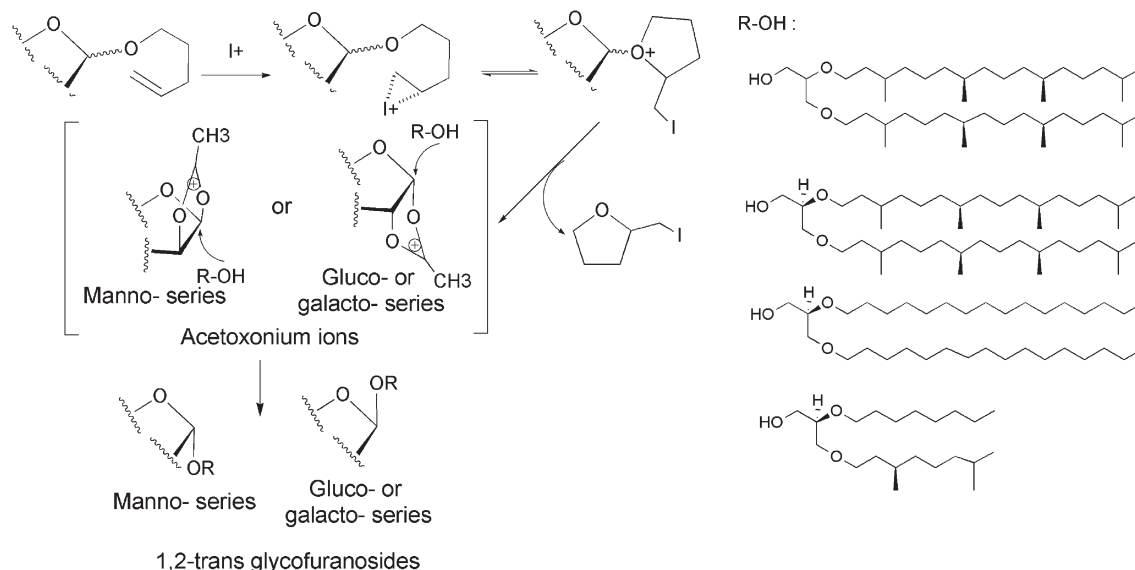
Scheme 17 Mechanistic pathway of the glycosylation reactions.
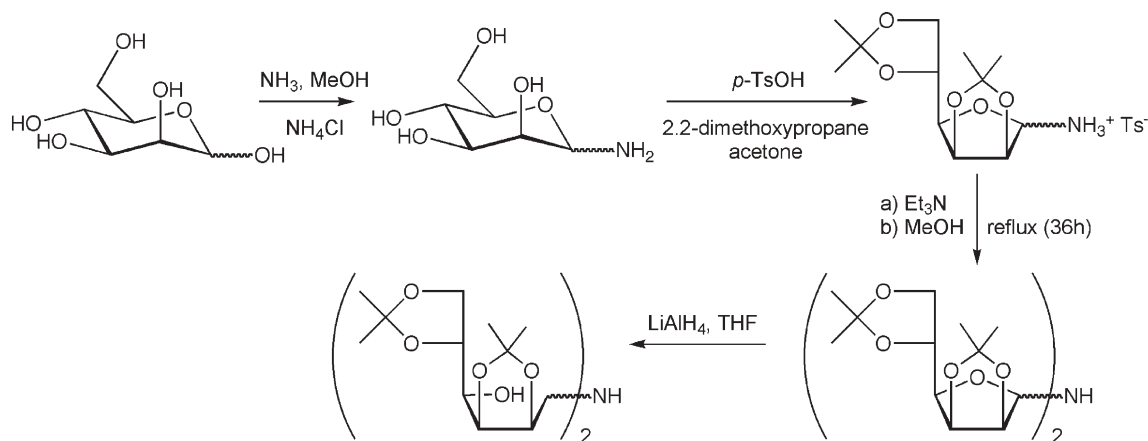
Scheme 18 The synthesis of the bis-(2,3:5,6-di-*O*-isopropylidene mannitolyl) amine

and converted into the *p*-toluene sulfonate salt of the isopropylidene derivative which was obtained in the furanose form. The free amine, which was obtained by treatment with triethylamine, was then dimerized in refluxing methanol[167] with a stream of nitrogen (to remove ammonia) to afford the diglycosylamine bis(2,3:5,6-di-*O*-isopropylidene mannofuranosyl)amine. This material, obtained as a gum, was a mixture of α,α-, α,β- and β,β- isomers. However a white solid product corresponding to the α,α-isomer was obtained by crystallization from methanol or ethanol. The final product was achieved by reduction of the diglycofuranosylamine with lithium aluminium hydride.

The *N*-acylation of the bis-(2,3:5,6-di-*O*-isopropylidene mannofuranosyl)amine was difficult because of steric restrictions. Thus the reaction was achieved in the presence of an acylation catalyst. The direct acylation with an appropriate acid chloride using pyridine as base, ether as solvent and 4-dimethylaminopyridine (DMAP) as a catalyst at room temperature over 30 min gave the desired bis-(2,3:5,6-diisopropylidene mannitolyl)alkamides in good yield. Interestingly, the fully *N*-acylated compound was obtained as the minor product. The removal of the isopropylidene protecting groups was achieved using acidic conditions. The deprotection reaction was carried out at 50 °C in 90% ethanol containing 0.5 M H_2SO_4 for 36 h. At a lower concentration in sulfuric acid (for instance 0.2M) other products corresponding to partial removal of the protecting groups were found.

8.9 Synthesis of sugar derivatives of pentaerythritol

Pentaerythritol has been used in the last ten years as a core component for the syntheses of glycoside clusters. In most cases a spacer has been introduced between the hydroxyl(s) group(s) of the pentaerythritol core and the glycosyl moieties. For example, glycotope biosteres bearing β-D-galactose moieties have been synthesized by the Sonogashira reaction of tetra-*O*-iodobenzyl pentaerythritol and 2-propinyl galactosides,[168] or mannoside clusters were obtained by coupling pentaerythritol tetrabromide with 2-hydroxyethyl mannosides.[169] In the synthesis of some highly hydrophobic Lewis X glycolipids, pentaerythritol was first condensed with triethylene glycol and the hydroxyl groups of the latter were

etherified by phytyl chains and the subsequent product was glycosylated with Lewis X donors.[170] Most often saccharides or oligosaccharides have been coupled to pentaerythritol in a search for multivalency (glycodendrimers) to bind multivalent lectins.[171]

There are only a few examples in the literature of direct glycosylation of partly protected pentaerythritols. One such example involved glycosylation of di-*O*-hexadecyl pentaerythritol with a *N*-acetyl-β-D-glucosaminyl donor.[172] More recently, M. Schmidt *et al.*[173] described the synthesis of mannose clusters having a pentaerythritol core, in which the mannosyl residues were attached directly to the pentaerythritol moiety.

The synthetic pathway to these materials work[66] was achieved through the preparation of the alcohol acceptors as depicted in Scheme 19. The tri-*O*-alkyl pentaerythritols **91a–h** were obtained by direct treatment of pentaerythritol **90** with an excess of alkyl bromide under phase transfer conditions, as described for tri-*O*-heptyl pentaerythritol.[174] Low yields were
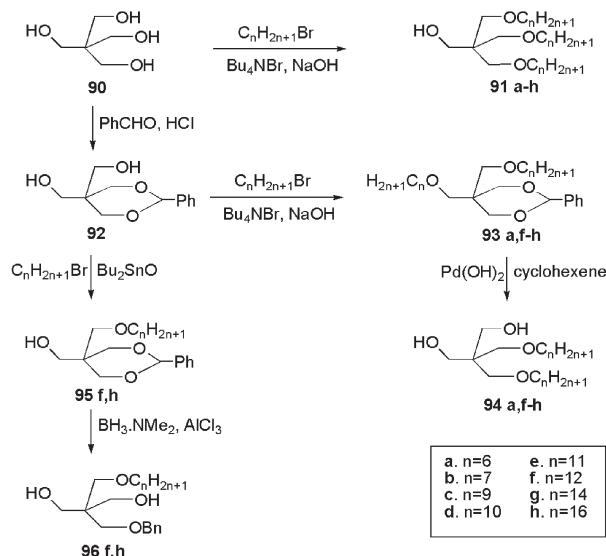
Scheme 19 Reaction pathway to mono-, di- and tri-*O*-alkyl pentaerythritols.

due to the simultaneous formation of mono-, di- and tetra-O-alkyl derivatives. The di-O-alkyl pentaerythritols **94a,f–h**, and O-alkyl-O-benzyl pentaerythritols **96f,h** were obtained from O-benzylidene pentaerythritol **92**.[175] The alkylation under similar conditions as previously described afforded **93a**, **93f–h**, whereas treatment with dibutyltin oxide in methanol, followed by reaction with alkyl bromide in the presence of caesium fluoride afforded **95f,h**. Subsequent cleavage of the benzylidene group by hydrogen transfer afforded compounds **94a,f–h** from **93a,f–h**, whereas reductive cleavage from **95f,h** afforded **96f,h**. The protection of one of the hydroxyl groups of mono-O-alkyl pentaerythritols **96f,h** was necessary because of the lack of reactivity of the trihydroxy compounds in glycosylation reactions.

Galactosylation reactions were performed using 2,3,4,6-tetra-O-benzoyl–α-D-galactopyranosyl trichloroacetimidate (**97**),[176] 2,3,4,6-tetra-O-acetyl-α-D-galactopyranosyl bromide (**98**),[177] or 2,3,4,6-tetra-O-acetyl-α-D-galactopyranosyl trichloroacetimidate[178] as glycosyl donors (Scheme 20).

The per-O-benzoyl D-galactosides **99a,f–h** were obtained respectively from the acceptors **91a**, **91f–h**, donor **97** and trimethylsilyl trifluoromethanesulfonate as the promoter, in yields from 72 to 76%. Alternatively, the per-O-acetyl glycosides **100a–h** were prepared in good yields from the acceptors **91a–h** and donor **98**, using either (I$_2$, DDQ, MeCN)[179] or (Hg(CN)$_2$-HgBr$_2$) as the promoter.

The di-O-alkyl di-O-D-galactoside derivatives **101a,f–h** were synthesized from the imidate **97** and the corresponding diols **94a,f–h** in acceptable yields using TMSOTf as the promoter. For purification and identification purposes, the per-O-acetyl D-galactosides **102a,f–h** were prepared from their benzoyl counterparts **101a,f–h**, by Zemplén de-O-benzoylation and re-O-acetylation.

The trigalactosylation of mono O-alkylpentaerythritol intermediates to compounds **105f,h** was unsuccessful, due to difficulties of separation from the mono and di-O-D-glycosyl by-products. Therefore, **105f,h** were prepared via two glycosylation steps. In the first, the acceptors **96f,h** were glycosylated with the imidate **97**. The di-O-D-galactosyl derivatives
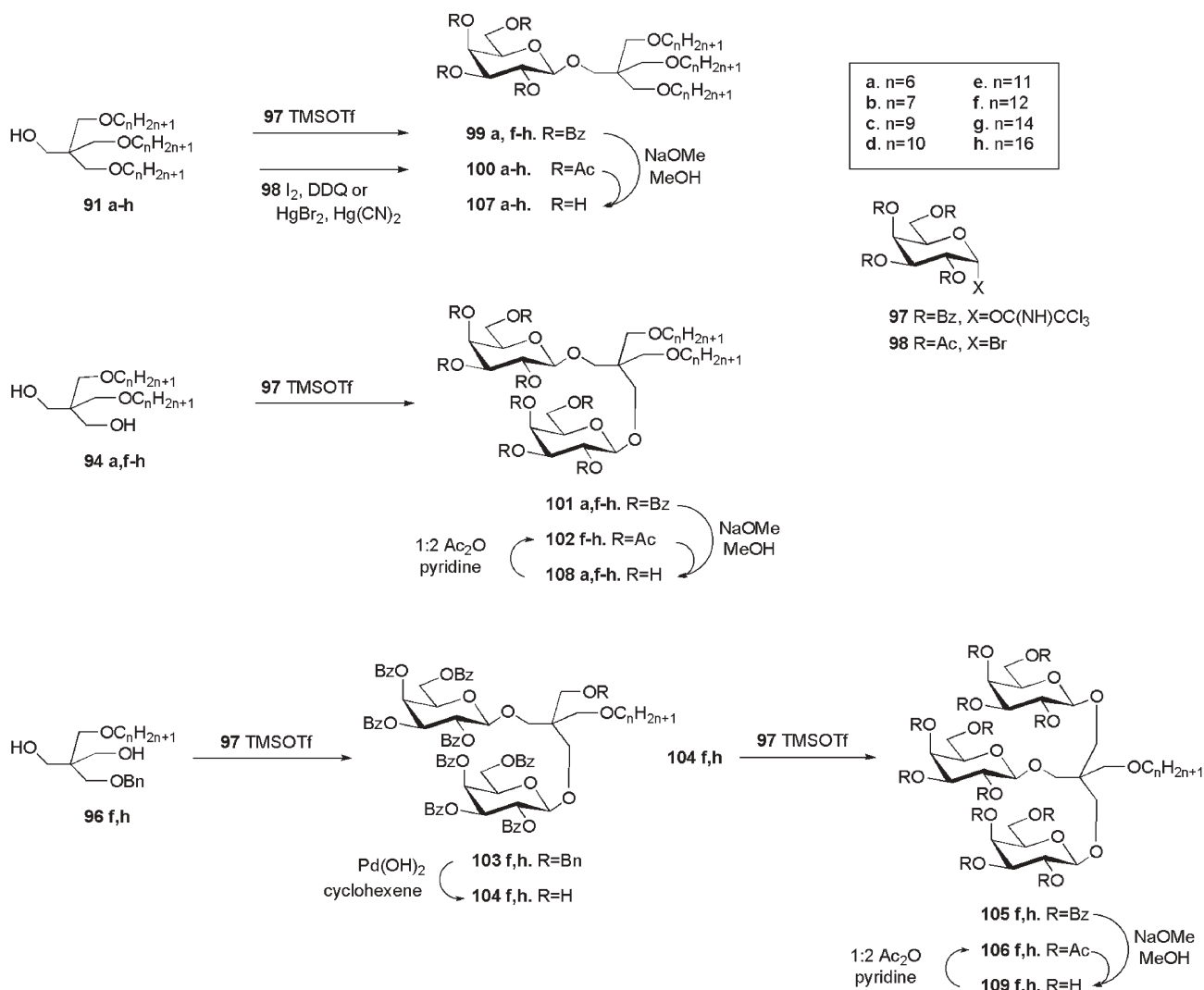
Scheme 20 Reaction pathway to mono-O-alkyl-tri-O-D-galactosyl, di-O-alkyl-di-O-D-galactosyl and tri-O-alkyl-mono-O-D-galactosyl pentaerythritols

103f,h were then transformed by de-*O*-benzylation into acceptors **104f,h** (92%), by hydrogen transfer. The latter were subsequently glycosylated under the same conditions as previously described, affording the *O*-alkyl tris(per-*O*-benzoyl D-galactosyl) pentaerythritols **105f,h**. For purification and identification purposes, de-*O*-benzoylation was achieved under Zemplén conditions (catalytic amount of CH₃ONa in methanol), followed by re-*O*-acylation to obtain the derivatives **106f,h** in good yields.

The fully deprotected derivatives **107a–h**, **108a,f–h** and **109f,h** were prepared in high yield by Zemplén de-*O*-acetylation of the peracetylated derivatives **100a–h**, **102a,f–h** and **106f,h** respectively.

## 8.10 Synthesis of tetraether-type glycolipids related to archaeal membrane lipids

Lipids of methanogenic and thermoacidophilic Archaebacteria are characterized by high proportions of tetraether-type components possessing two different polar headgroups derived from phosphate and/or sugar moieties at opposite ends of a lipidic backbone.[8,9] These unsymmetrical bipolar amphiphiles give rise to monolayered thermostable membranes, which have boosted interest in various biotechnologies.[180] Although some investigations pertaining to the self-assembling properties of some synthetic phosphate-type tetrathers have been undertaken,[9,181] studies on the effects of: (i) the symmetrical or unsymmetrical structure of the lipids, (ii) the presence of anionic phosphate and/or neutral mono- or di-saccharidic moieties and (iii) the structure and composition of the bolaphilic bridging chain are less common. Within this context, optimised syntheses of symmetrical and unsymmetrical hemimacrocyclic bipolar glycolipids (see structures **47** to **54**) have been developed, and are characterized by the presence of: (i) a hexadecamethylene bridging chain or a bridging chain of similar length that also contains a 1,3-disubstituted cyclopentane ring or a 1,2-disubstituted phenyl ring, linked as an ether to two optically pure (*R*), (*S*) or racemic glycerol units at primary positions, (ii) two branched (*R*) or racemic dihydrocitronellyl chains attached to glycerol moieties at secondary positions, and (iii) phosphate and/or glycosidic polar headgroups derived from either lactose or D-galactose (in a furanoid cyclic form, as found in some natural methanogenic lipids).[59,60,71,182] Compounds containing a five-membered ring within the bridging chain were reported to be 4 : 1 diastereomeric mixtures of *cis–trans* isomers of the 1,3-disubstituted cyclopentane ring.

The strategic plan for the synthesis of the bolaphilic glycolipids involved a suitable synthesis of hemimacrocyclic diols and a subsequent introduction of the polar headgroups. Two pathways A and B were developed for the preparation of diols as outlined in Schemes 21 and 22. The key differences in these two strategies result from (i) the structure of the optically pure or racemic starting material, epichlorohydrin or solketal, used as the precursor for the glycerol moiety, and (ii) the coupling of the bridging chain to the glycerol units. In pathway
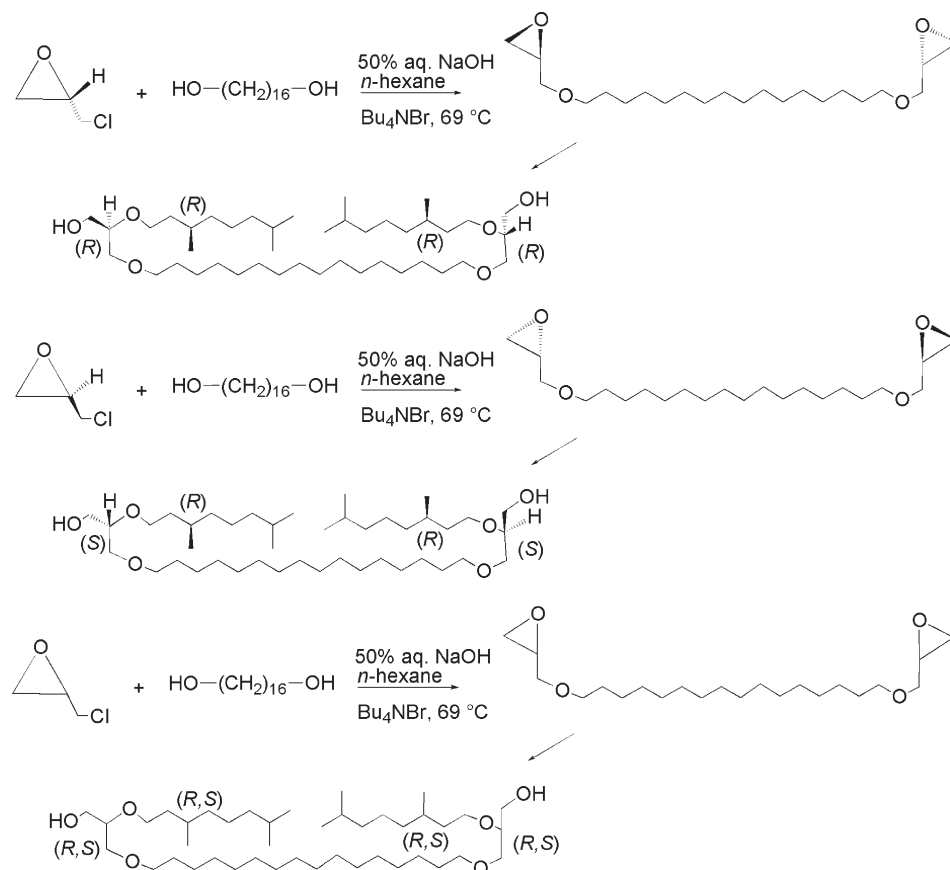
Scheme 21 Synthetic pathway A for the preparation of optically pure or racemic hemimacroclyic diols.
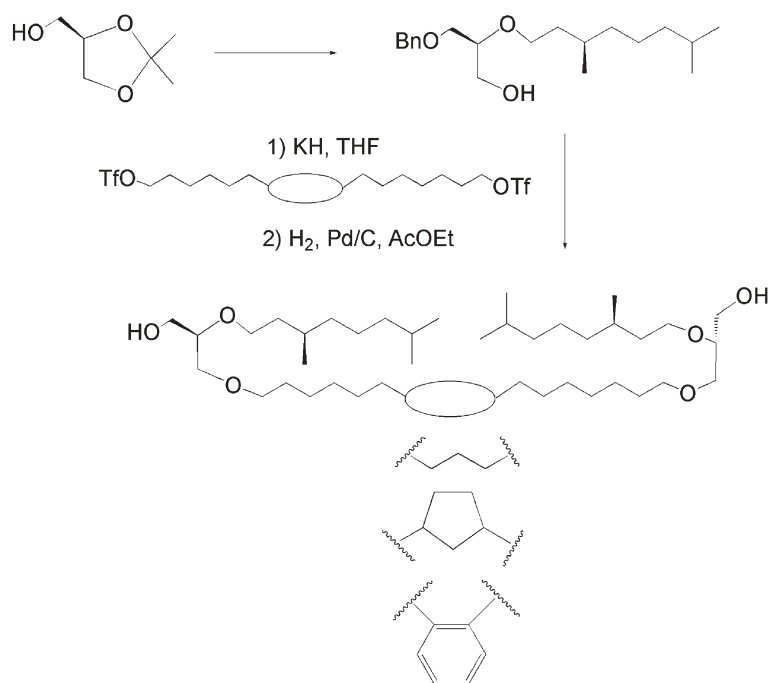
Scheme 22 Synthetic pathway B for the preparation of hemimacrocylic diols containing various aliphatic linkers.

A, the introduction of the bridging chain is performed in the first step of the synthesis through the bisalkylation of the aliphatic diol with optically pure or racemic epichlorohydrins to afford the corresponding diepoxides with complete inversion at the stereogenic centre (Scheme 21).[59,60]

Conversely, for pathway B, the construction of the aliphatic linker between the two glycerols was achieved in the final steps by the use of a glycerol derivative possessing the branched chain at the secondary position. Alkylation of this glyceryl compound was achieved by treatment with an aliphatic ditriflate and potassium hydride at room temperature (Scheme 22).[59,71,182] The latter strategy is more advantageous for the preparation of various hemi-macrocyclic diols insofar as it allows for easier modification of the structure of the bridging

chain. The synthesis of the aliphatic linkers incorporating a cyclopentane ring or a phenyl ring into the middle of the chain was performed *via* a double Wittig reaction between *cis*-1,3-diformylcyclopentane or 1,2-phthalic dicarboxaldehyde and the aliphatic phosphonium salt RO-(CH$_2$)$_6$P$^+$Ph$_3$Br$^-$ (R = H or tetrahydropyranyl).[59,71,182] The Wittig reaction with *cis*-1,3-diformylcyclopentane underwent some partial isomerization to the *trans* isomer, leading to a 4 : 1 mixture of *cis–trans* isomers, respectively.

The synthetic route to the symmetrical diglycosylated lipids was based upon glycosylation reactions of hemi-macrocyclic diols with the n-pentenyl D-galactofuranoside donor under standard n-pentenyl glycoside chemistry (NIS, 1.3 equiv.; ETSiOTf, 0.3 equiv. with respect to the donor) at room
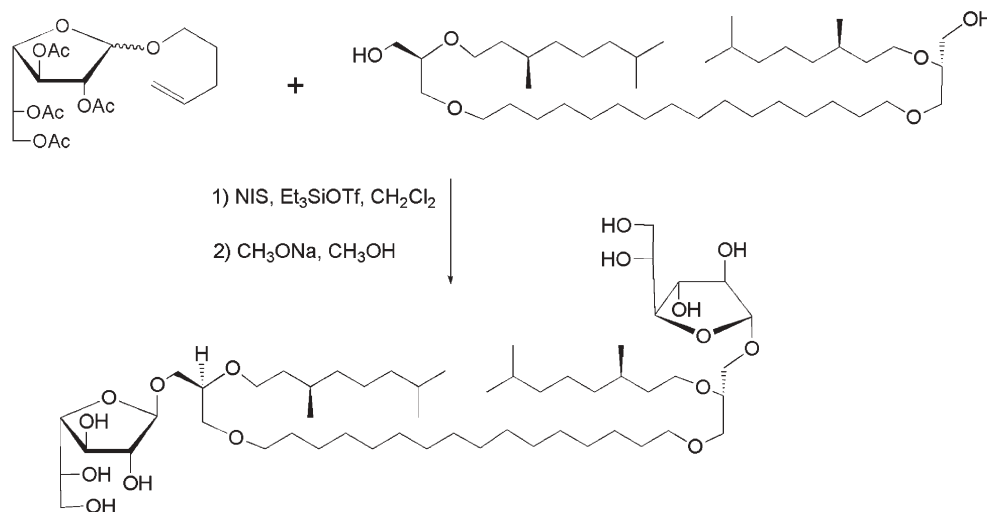
Scheme 23 Synthesis of a symmetrical diglycosylated lipid under n-pentenyl glycoside chemistry.

This journal is © The Royal Society of Chemistry 2007

Chem. Soc. Rev., 2007, **36**, 1971–2032 | 2027
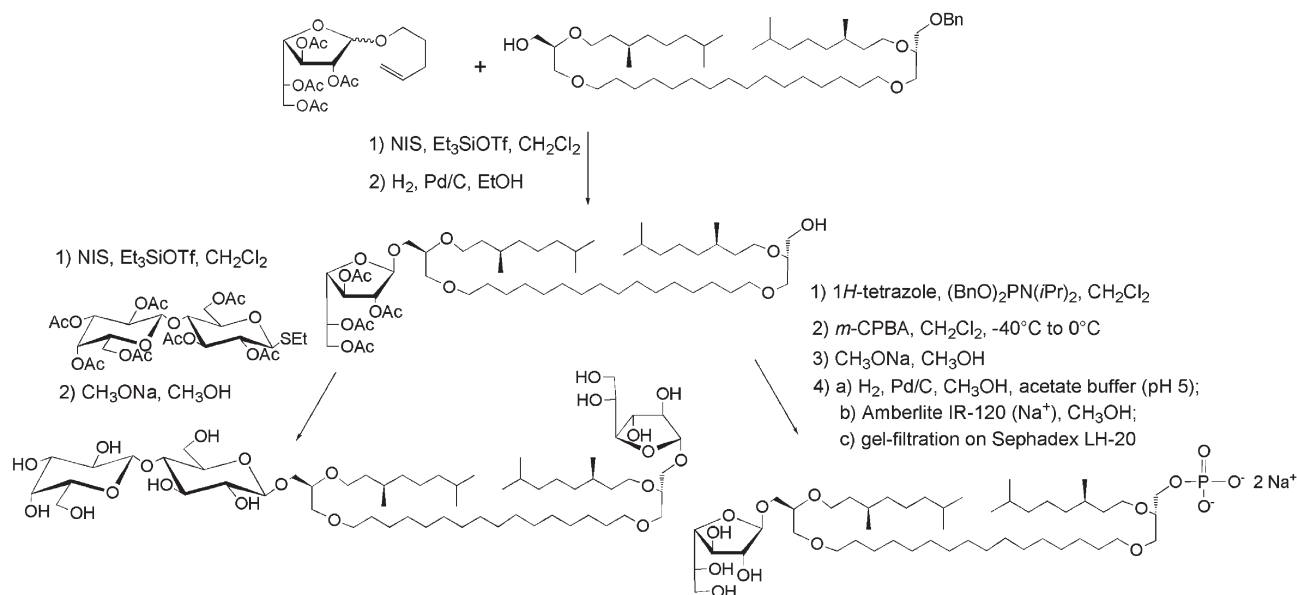
Scheme 24 Synthesis of unsymmetrical neutral and anionic glycolipids possessing a linear hexadecanemethylene bridging chain.

temperature, to provide exclusively the β-linked bis-galacto-furanoside lipids. The high β-selectivity resulted from neighbouring group participation of the C-2 acetyl donor functionality (Scheme 23).[59,60] Deacylation of the symmetrical glycolipids with sodium methoxide in methanol gave the corresponding diglycosylated compounds.

Unsymmetrical glycolipids were obtained through the monobenzylation of the hemi-macrocyclic diols followed by sequential introduction of the β-D-galactofuranosyl and lactosyl or phosphate units respectively.[59,71,182] The introduction of the second disaccharidic head group was performed using lactosyl thioglycoside as a donor (Scheme 24). The preparation of the unsymmetrical anionic phosphate derivatives was carried out through the transformation of the galactosyl hemimacrocyclic alcohols into alkyl dibenzyl phosphates *via* the reaction with *N,N*-diethyl dibenzylphosphoramidite/1*H*-tetrazole followed by *in situ* mild oxidation of the resulting phosphite with 3-chloroperoxybenzoic acid. The transformation of the alkyl dibenzyl phosphates into the phosphate salts was performed by sequential deacetylation of the galactosyl unit, catalytic hydrogenolysis (Pd/C) in a buffered solvent mixture (methanol–acetic acid–sodium acetate, pH 5) avoiding the glycosidic hydrolysis, and treatment with Amberlite IR-120 (Na+ form, water).

Conclusion

This review demonstrates that microsegregation, coupled with curvature, self-assembly and self-organisation, can be used to model not only lyotropic, but also thermotropic mesophase formation in glycolipids. Understanding the details of these processes and the properties of the soft materials that are created is a potentially fundamental issue that underlies biological structure and function. It is through this understanding that novel materials and applications will be generated in the future.

Acknowledgements

References

1 (*a*) W. L. Porter, *Am. Potato J.*, 1972, **49**, 403–437; (*b*) V. Grassert and V. Vill, *Liq. Cryst. Today*, 1994, **4**, 4–5.
2 E. Lederer, *J. Med. Chem.*, 1980, **23**, 819–825.
3 S. Bottle and I. D. Jenkins, *Chem. Commun.*, 1984, 385.
4 V. Molinier, P. H. J. Kouwer, Y. Queneau, J. Fitremann, G. Mackenzie and J. W. Goodby, *Chem. Commun.*, 2003, 2860–2861.
5 J. W. Goodby, *Liq. Cryst.*, 1998, **24**, 25–38.
6 (*a*) G. T. Stewart, *Liq. Cryst.*, 2003, **30**, 541–557; (*b*) G. T. Stewart, *Liq. Cryst.*, 2004, **31**, 443–471; (*c*) G. T. Stewart, in *Liquid Crystals and Plastic Crystals*, ed. G. W. Gray and P. A. Winsor, Ellis Horwood, Chichester, 1974, vol. 1, pp. 308–326; (*d*) S. Hoffmann, High Molecular Weight Liquid Crystals, in the *Handbook of Liquid Crystals*, vol. 3, ed. D. Demus, J. W. Goodby, G. W. Gray, H.-W. Spiess and V. Vill, Wiley-VCH, Weinheim, 1998, pp 393–452; (*e*) G. H. Brown and J. J. Wolken, *Liquid Crystals and Biological Structures*, Academic Press, New York. 1979.
7 D. M. Small, *J. Colloid Interface Sci.*, 1977, **58**, 581–602.

8 (a) T. Langworthy, in *The Bacteria*, vol. 8, ed. C. R. Woese, R. S. Wolfe, Academic Press, New York, 1985, pp. 459–497; (b) M. De Rosa, A. Gambarcorta and A. Gliozzi, *Microbiol. Rev.*, 1986, **50**, 70; (c) G. D. Sprott, *J. Bioenerg. Biomembr.*, 1992, **24**, 555–566.

9 (a) M. Kates, *J. Microbiol. Methods*, 1996, **25**, 113–128; (b) K. Yamauchi and M. Kinoshita, *Prog. Polym. Sci.*, 1993, **18**, 763–804; (c) S. C. Kushwaha, M. Kates, G. D. Sprott and L. C. P. Smith, *Biochim. Biophys. Acta*, 1981, **664**, 156–173; (d) M. Tomoaia-Cotisel, E. Chifu, J. Zsako, A. Mocanu, P. J. Quinn and M. Kates, *Chem. Phys. Lipids*, 1992, **63**, 131–138; (e) M. De Arruda, W. Colli and P. J. Quinn, *Eur. J. Biochem.*, 1989, **182**, 413–421; (f) K. Yamauchi, K. Doi, M. Kinoshita, F. Kii and H. Fukuda, *Biochim. Biophys. Acta*, 1996, **1283**, 163–169.

10 M. Kates, in *The Biochemistry of Archaea (Archaebacteria)*, ed. M. Kates, D. J. Kushner and A. T. Matheson, Elsevier, Amsterdam, 1993; A. Gambacorca, A. Gliozzi and M. De Rosa, *World J. Microbiol. Biotechnol.*, 1995, **11**, 115–131.

11 J. W. Green, *Adv. Carbohydr. Chem.*, 1966, **21**, 95–142.

12 U. Schwarz, *Chem. Commun.*, 2007, B23.

13 F. Reinitzer, *Wien. Sitzber*, 1888, **94**, 719; F. Reinitzer, *Wien. Sitzber*, 1888, **97**, 167; F. Reinitzer, *Monatsh. Chem.*, 1888, **9**, 421.

14 See for example H.-T. Nguyen, C. Destrade and J. Malthete, in *Handbooks of Liquid Crystals*, vol. 2B, ed. D. Demus, J. W. Goodby, G. W. Gray, H.-W. Spiess and V. Vill, Wiley-VCH, Weinheim, 1998, pp. 865—908, and references therein.

15 T. Niori, T. Sekine, J. Watanabe, T. Furukawa and H. Takezoe, *J. Mater. Chem.*, 1996, **6**, 1231–1233.

16 (a) J. W. Goodby, Low Molecular Weight Liquid Crystals I, in the *Handbook of Liquid Crystals*, vol. 2A, ed. D. Demus, J. W. Goodby, G. W. Gray, H.-W. Spiess and V. Vill, Wiley-VCH, Weinheim, 1998, ch 1, pp. 3–21.

17 J. W. Goodby, I. M. Saez, S. J. Cowling, V. Görtz, A. W. Hall, S. Sia, M. Draper, G. Cosquer and E. P. Raynes, *Angew. Chem., Int. Ed.* (accepted).

18 (a) H. Zocher and V. Birnstein, *Z. Phys. Chem.*, 1929, **A142**, 113–125; (b) H. Zocher, in *Liquid Crystals and Plastic Crystals*, ed. G. W. Gray and P. A. Winsor, Ellis Horwood, Chichester, 1974, vol. 1, pp. 64–66; (c) G. A. Jeffrey, *Acc. Chem. Res.*, 1986, **19**, 168–173; (d) C. Tschierske, *Prog. Polym. Sci.*, 1996, **21**, 775–852; (e) J.-G. Riess and J. Greiner, *Carbohydr. Res.*, 2000, **327**, 147–168; (f) R. Miethchen and M. Hein, *Carbohydr. Res.*, 2000, **327**, 169–183; (g) W. von Rybinski and K. Hill, *Angew. Chem., Int. Ed.*, 1998, **37**, 1328–1345; (h) D. Blunk, K. Praefcke and G. Legler, *Liq. Cryst.*, 1994, **17**, 841–846; (i) K. Praefcke, B. Kohne, S. Diele, G. Pelzl and A. Kjaer, *Liq. Cryst.*, 1992, **11**, 1–8; (j) D. Blunk, K. Praefcke and G. Legler, *Liq. Cryst.*, 1995, **18**, 149–150; (k) K. Praefcke, A.-M. Levelut, B. Kohne and A. Eckert, *Liq. Cryst.*, 1989, **6**, 263–270; (l) H. van Doren, E. Smits, J.-M. Pestman, J. Engberts and R. Kellogg, *Chem. Soc. Rev.*, 2000, **29**, 183–199; (m) D. Schwabisch, S. Wille, M. Hein and R. Miethchen, *Liq. Cryst.*, 2004, **31**, 1143–1150; (n) R. Miethchen and M. Hein, *Carbohydr. Res.*, 2000, **327**, 169–183; (o) H. Prade, R. Miethchen and V. Vill, *J. Prakt. Chem./Chem.-Zeit.*, 1995, **337**, 427–440; (p) R. Miethchen, M. Schwarze and J. Holz, *Liq. Cryst.*, 1993, **15**, 185–191; (q) R. Miethchen, J. Holz, H. Prade and A. Liptak, *Tetrahedron*, 1992, **48**, 3061–3068.

19 J. W. Goodby, *Mol. Cryst. Liq. Cryst.*, 1984, **110**, 205–219.

20 G. C. Shearman, O. Ces, R. H. Templer and J. M. Seddon, *J. Phys.: Condens. Matter*, 2006, **18**, 1105–1124.

21 J. W. Goodby, G. H. Mehl, I. M. Saez, R. P. Tuffin, G. Mackenzie, R. Auzély-Velty, T. Benvegnu and D. Plusquellec, *Chem. Commun.*, 1998, 2057–2070.

22 (a) D. C. Carter, J. R. Ruble and G. A. Jeffrey, *Carbohydr. Res.*, 1982, **102**, 59; (b) G. A. Jeffrey and S. Bhattacharjee, *Carbohydr. Res.*, 1983, **115**, 53–58; (c) D. L. Dorset and J. P. Rosenbusch, *Chem. Phys. Lipids*, 1981, **29**, 299–307.

23 (a) H. Prade, R. Miethchen and V. Vill, *J. Prakt. Chem.*, 1995, **337**, 427–440; (b) E. Barrall, B. Grant, M. Oxsen, E. T. Samulski, P. C. Moews, J. R. Knox, R. R. Gaskill and J. L. Haberfeld, *Org. Coat. Plast. Chem.*, 1979, **40**, 67–74; (c) R. Miethchen, J. Holz, H. Prade and A. Lipták, *Tetrahedron*, 1992, **48**, 3061–3068; (d) V. Vill, T. Böcker, J. Thiem and F. Fischer, *Liq. Cryst.*, 1989, **6**, 349–356.

24 J. W. Goodby, *Liq. Cryst.*, 2006, **33**, 1229–1245.

25 J. W. Goodby, M. J. Watson, G. Mackenzie, S. M. Kelly, S. Bachir, P. Bault, P. Godé, G. Goethals, P. Martin, G. Ronco and P. Villa, *Liq. Cryst.*, 1998, **25**, 139–147.

26 (a) G. Friedel, *C. R. Acad. Sci.*, 1923, **67**, 273–474; (b) D. Demus and L. Richter, *Textures of Liquid Crystals*, Verlag Chemie, Weinheim, New York, 1978; (c) G. W. Gray and J. W. Goodby, *Smectic Liquid Crystals, Textures and Structures*, Leonard Hill, Glasgow and London, 1984.

27 J. W. Goodby, J. A. Haley, M. J. Watson, G. Mackenzie, S. M. Kelly, P. Letellier, P. Godé, G. Goethals, G. Ronco, B. Harmouch, P. Martin and P. Villa, *Liq. Cryst.*, 1997, **22**, 497–508.

28 J. W. Goodby, J. A. Haley, M. J. Watson, G. Mackenzie, S. M. Kelly, P. Letellier, O. Douillet, P. Godé, G. Goethals, G. Ronco and P. Villa, *Liq. Cryst.*, 1997, **22**, 367–378.

29 W. V. Dahlhoff, *Z. Naturforsch.*, 1989, **44b**, 1105–1108.

30 J. W. Goodby, J. A. Haley, S. M. Kelly, P. Bault, P. Godé, G. Goethals, G. Ronco and P. Villa, *Proceedings of the 26rd Freiburger Arbeitstagung Flüssigkristalle*, Freiburg, Germany, April 1997, P56 (1–4).

31 P. Bault, P. Godé, G. Goethals, J. W. Goodby, J. A. Haley, S. M. Kelly, G. H. Mehl, G. Ronco and P. Villa, *Liq. Cryst.*, 1998, **24**, 283–293.

32 P. Bault, P. Gode, G. Goethals, J. W. Goodby, J. A. Haley, S. M. Kelly, G. H. Mehl, G. Ronco and P. Villa, *Liq. Cryst.*, 1998, **25**, 31–45.

33 B. Pfannemüller, W. Welte, E. Chin and J. W. Goodby, *Liq. Cryst.*, 1986, **1**, 357–370.

34 S. Bhattacharjee, G. A. Jeffrey and J. W. Goodby, *Mol. Cryst. Liq. Cryst.*, 1985, **131**, 245–255.

35 J. W. Goodby, M. Marcus, E. Chin, P. L. Finn and B. Pfannemüller, *Liq. Cryst.*, 1988, **3**, 1569–1581.

36 J. W. Goodby, J. A. Haley, G. Mackenzie, M. J. Watson, V. Ferrières and D. Plusquellec, *J. Mater. Chem.*, 1995, **5**, 2209–2220.

37 (a) P. Bault, P. Godé, G. Goethals, J. W. Goodby, J. A. Haley, G. H. Mehl, S. M. Kelly, D. Postel, G. Ronco and P. Villa, *Proceedings of the 27rd Freiburger Arbeitstagung Flüssigkristalle*, Freiburg, Germany, March 1998, P47 (1–4); (b) P. Bault, P. Gode, G. Goethals, J. W. Goodby, J. A. Haley, S. M. Kelly, G. H. Mehl and P. Villa, *Liq. Cryst.*, 1999, **26**, 985–997.

38 S. Chambert, A. Doutheau, Y. Queneau, S. J. Cowling, J. W. Goodby and G. Mackenzie, *J. Carbohydr. Chem.*, 2007, **26**, 27–39.

39 C. T. Imrie and G. R. Luckhurst, Low Molecular Weight Liquid Crystals II, in the *Handbook of Liquid Crystals*, vol. 2B, ed. D. Demus, J. W. Goodby, G. W. Gray, H.-W. Spiess and V. Vill, Wiley-VCH, Weinheim, 1998, pp. 801–834.

40 B. Lindberg, *Adv. Carbohydr. Chem. Biochem.*, 1990, **48**, 279–318.

41 M. A. Clarke, A. V. Bailey, E. J. Roberts and W. S. Tsang, *Carbohydrates as Organic Raw Materials*, VCH, ed F. W. Lichtenthaler, 1991, pp 169 and references therein.

42 D. Plusquellec, G. Chevalier, R. Talibart and H. Wróblewsky, *Anal. Biochem.*, 1989, **179**, 145–153 and references therein.

43 V. Ferrières, T. Benvegnu, M. Lefeuvre, D. Plusquellec, G. Mackenzie, M. J. Watson, J. A. Haley, J. W. Goodby, R. Pindak and M. K. Durbin, *J. Chem. Soc., Perkin Trans. 2*, 1999, 951–959.

44 Y. Bouligand, *J. Phys. (Paris)*, 1980, **41**, 1297–1306; Y. Bouligand, *J. Phys. (Paris)*, 1980, **41**, 1307–1315.

45 H. Zheng, C. K. Lai and T. M. Swager, *Chem. Mater.*, 1995, **7**, 2067–2077.

46 L. F. Tietze, K. Böge and V. Vill, *Chem. Ber.*, 1994, **127**, 1065–1068.

47 H. W. Raaijmakers, B. Zwanenburg and G.J.F. Chittenden, *Recl. Trav. Chim. Pays-Bas,*, 1994, **113**, 79.

48 W. V. Dahlhoff, *Synthesis*, 1987, 366–368.

49 (a) T. Böcker and J. Thiem, *Tenside Surfactants Deterg.*, 1989, **26**, 318–324; (b) M. P. de Nijs, L. Maat and A. P. G. Kieboom, *Recl. Trav. Chim. Pays-Bas*, 1990, **109**, 429–433; (c) K. Matsumara, K. Imai, S. Yoshikawa and T. Uchibori, *J. Am. Oil Chem. Soc.*, 1990, **67**, 996–1001; (d) K. Shinoda, T. Yamaguchi and R. Hori, *Bull. Chem. Soc. Jpn.*, 1961, **34**, 237–241.

This journal is © The Royal Society of Chemistry 2007

Chem. Soc. Rev., 2007, **36**, 1971–2032 | 2029

50 A. Lubineau, H. Bienaymé, Y. Queneau and M. C. Schermann, *New J. Chem.*, 1994, **18**, 279–285.

51 Y. D. Ma, A. Takada, M. Sugiura, A. Fukuda, T. Miyamoto and J. Watanabe, *Bull. Chem. Jpn.*, 1994, **67**, 346–351.

52 S. Fischer, H. Fischer, S. Diele, G. Pelzl, K. Jankowski, R. R. Schmidt and V. Vill, *Liq. Cryst.*, 1994, **17**, 855–861.

53 (*a*) Y. Queneau, J. Gagnaire, J. J. West, G. Mackenzie and J. W. Goodby, *J. Mater. Chem.*, 2001, **11**, 2839–2844; (*b*) V. Molinier, P. J. H. Kouwer, J. Fitremann, A. Bouchu, G. Mackenzie, Y. Queneau and J. W. Goodby, *Chem.–Eur. J.*, 2006, **12**, 3547–3557.

54 N. Laurent, D. Lafont, F. Dumoulin, P. Boullanger, G. Mackenzie, P. H. J. Kouwer and J. W. Goodby, *J. Am. Chem. Soc.*, 2003, **125**, 15499–15506.

55 F. Dumoulin, D. Lafont, P. Boullanger, G. Mackenzie, G. Mehl and J. W. Goodby, *J. Am. Chem. Soc.*, 2002, **124**, 13737–13748.

56 (*a*) D. A. Mannock and R. N. McElhaney, *Biochem. Cell Biol.*, 1991, **69**, 863–867; (*b*) D. A. Mannock, R. N. A. H. Lewis and R. N. McElhaney, *Chem. Phys. Lipids*, 1987, **43**, 113–127; (*c*) D. A. Mannock, R. N. A. H. Lewis and R. N. McElhaney, *Chem. Phys. Lipids*, 1990, **55**, 309–321; (*d*) L. Six, K.-P. Rueß and M. Liefländer, *Tetrahedron Lett.*, 1983, **24**, 1229–1232; (*e*) H. Kuttenreich, H.-J. Hinz, M. Inczedy-Marcsek, R. Koinova, B. Tenchov and P. Laggner, *Chem. Phys. Lipids*, 1988, **47**, 245–260.

57 (*a*) E. L. Chang, *Biochim. Biophys. Res. Commun.*, 1994, **202**, 673–679; (*b*) K. Yamauchi, K. Doi, Y. Yoshida and M. Kinoshita, *Biochim. Biophys. Acta*, 1993, **1146**, 178–182; (*c*) K. Yamauchi, K. Togawa and M. Kinoshita, *Bull. Chem. Soc. Jpn.*, 1993, **66**, 2097–2100; (*d*) K. Tomioka, F. Kii, H. Fukuda and S. Katoh, *J. Immunol. Methods*, 1994, **176**, 1–7.

58 R. Auzély-Velty, T. Benvegnu, G. Mackenzie, J. A. Haley, J. W. Goodby and D. Plusquellec, *Carbohydr. Res.*, 1998, **314**, 65–77.

59 G. Lecollinet, R. Auzély-Velty, M. Danel, T. Benvegnu, G. Mackenzie, J. W. Goodby and D. Plusquellec, *J. Org. Chem.*, 1999, **64**, 3139–3150.

60 R. Auzély-Velty, T. Benvegnu, D. Plusquellec, G. Mackenzie, J. A. Haley and J. W. Goodby, *Angew. Chem., Int. Ed.*, 1998, **37**, 2511–2515.

61 V. Vill and R. Hashim, *Curr. Opin. Colloid Interface Sci.*, 2002, **7**, 395.

62 D. F. Ewing, J. W. Goodby, S. Guenais, P. Letellier, G. Mackenzie, I. Piastrelli and D. Plusquellec, *J. Chem. Soc., Perkin Trans. 1*, 1997, 3459–3463.

63 J. J. West, G. Bonsergent, G. Mackenzie, D. F. Ewing, J. W. Goodby, T. Benvegnu, D. Plusquellec, S. Bachir, P. Bault, O. Douillet, P. Godé, G. Goethals, P. Martin and P. Villa, *Mol. Cryst. Liq. Cryst.*, 2001, **363**, 23–44.

64 V. Molinier, P. H. J. Kouwer, J. Fitremann, A. Bouchu, G. Mackenzie, Y. Queneau and J. W. Goodby, *Chem.–Eur. J.*, 2007, **13**, 1763–1775.

65 (*a*) F. Hardouin, A.-M. Levelut, J. J. Benatter and G. Sigaud, *Solid State Commun.*, 1980, **33**, 337–340; (*b*) F. Hardouin, G. Sigaud, N. H. Tinh and M. F. Achard, *J. Phys. (Paris) Lett.*, 1981, **42**, 63–66.

66 (*a*) F. Dumoulin, D. Lafont, T.-L. Huynh, P. Boullanger, G. Mackenzie and J. W. Goodby, *Chem.–Eur. J.*, 2007, **13**, 5585–5600; (*b*) K. Praefcke, P. Psaras and A. Eckert, *Liq. Cryst.*, 1993, **13**, 551–559.

67 C. Tschierske, *J. Mater. Chem.*, 2001, **11**, 2647–2671.

68 F. Hentrich, S. Diele and C. Tschierske, *Liq. Cryst.*, 1994, **17**, 827–840.

69 J. W. Goodby, unpublished results.

70 G. Ferrante, I. Ekiel and G. D. Sprott, *Biochim. Biophys. Acta*, 1987, **921**, 281–291.

71 G. Lecollinet, A. Gulik, G. Mackenzie, J. W. Goodby, T. Benvegnu and D. Plusquellec, *Chem.–Eur. J.*, 2002, **8**, 585–593.

72 (*a*) J. W. Goodby, M. A. Waugh, S. M. Stein, E. Chin, R. Pindak and J. S. Patel, *Nature*, 1989, **337**, 449–452; (*b*) J. W. Goodby, M. A. Waugh, S. M. Stein, E. Chin, R. Pindak and J. S. Patel, *J. Am. Chem. Soc.*, 1989, **111**, 8119–8125.

73 G. Lecollinet, R. Auzély-Velty, T. Benvegnu, G. Mackenzie, J. W. Goodby and D. Plusquellec, *Chem. Commun.*, 1998, 1571–1572.

74 I. Regnaut, G. Ronco and P. Villa, *FR Pat.*, No. 89 15995, Générale Sucrière, 1989.

75 P. Martin, J. Y. Conan, B. Harmouch, D. Postel, G. Ronco, C. Rouch and P. Villa, *Chem. Lett.*, 1994, **1**, 141–144.

76 B. Baker, R. Schaub and J. Williams, *J. Am. Chem. Soc.*, 1962, **77**, 7–12.

77 W. Sowa, *Can. J. Chem.*, 1968, **46**, 1586–1589.

78 S. Trombotto, A. Bouchu, G. Descotes and Y. Queneau, *Tetrahedron Lett.*, 2000, **41**, 8273–8277.

79 R. Weidenhagen and S. Lorenz, *Angew. Chem.*, 1957, **69**, 641.

80 H. Schiweck, M. Munir, K. M. Rapp, B. Schneider and M. Vogel, in *Carbohydrates as Organic Raw Materials*, ed. F. W. Lichtenthaler, VCH, Weinheim, 1991, Vol. 1, pp. 57–94.

81 F. W. Lichtenthaler and S. Peters, *C. R. Chim.*, 2004, **7**, 65–90.

82 F. W. Lichtenthaler, *Acc. Chem. Res.*, 2002, **35**, 728–737.

83 S. Trombotto, M. Danel, J. Fitremann, A. Bouchu and Y. Queneau, *J. Org. Chem.*, 2003, **68**, 6672–6678.

84 A. Le Chevalier, R. Pierre, R. Kanso, S. Chambert, A. Doutheau and Y. Queneau, *Tetrahedron Lett.*, 2006, **47**, 2431–2434.

85 V. Sol, A. Charmot, P. Krausz, S. Trombotto and Y. Queneau, *J. Carbohydr. Chem.*, 2006, **25**, 345–360.

86 (*a*) R. R. Schmidt, *Angew. Chem., Int. Ed. Engl.*, 1986, **25**, 212–235; (*b*) J. Banoub, P. Boullanger and D. Lafont, *Chem. Rev.*, 1992, **92**, 1167–1195; (*c*) G. J. Boons, *Tetrahedron*, 1996, **52**, 1095–1121; (*d*) H. Pellissier, *Tetrahedron*, 2005, **61**, 2947–2993.

87 (*a*) J. N. Bertho, V. Ferrières and D. Plusquellec, *J. Chem. Soc., Chem. Commun.*, 1995, 1391–1393; (*b*) V. Ferrières, J. N. Bertho and D. Plusquellec, *Tetrahedron Lett.*, 1995, **36**, 2749–2752; (*c*) V. Ferrières, J. N. Bertho and D. Plusquellec, *Carbohydr. Res.*, 1998, **311**, 25–35.

88 A. M. van der Heijden, T. C. Lee, F. van Rantwijk and H. van Bekkum, *Carbohydr. Res.*, 2002, **337**, 1993–1998.

89 (*a*) A. T. J. W. de Goede, M. P. J. van Deurzen, I. G. van der Leij, A. M. van der Heijden, J. M. A. Baas, F. van Rantwijk and H. van Bekkum, *J. Carbohydr. Chem.*, 1996, **15**, 331–349; (*b*) A. M. van der Heijden, F. van Rantwijk and H. van Bekkum, *J. Carbohydr. Chem.*, 1999, **18**, 131–147; (*c*) H. Regeling, B. Zwanenburg and G. J. F. Chittenden, *Carbohydr. Res.*, 1998, **314**, 267–272.

90 K. Kruger and L. Nagy, *Biocoordination Chemistry*, Simon and Schuster, 1990, pp. 236.

91 B. Schneider, F. W. Lichtenthaler, G. Steinke and H. Schiweck, *Liebigs Ann. Chem.*, 1985, 2443–2452.

92 Y. Haraguchi, A. Yagi, A. Koda, N. Inagashi, K. Noda and I. Nishioka, *J. Med. Chem.*, 1982, **25**, 1495–1499.

93 *Carbohydrates as Organic Raw Materials*, ed. F. W. Lichtenthaler, VCH, Weinheim, **vol. 1**, 1991.

94 *Carbohydrates as Organic Raw Materials*, ed. G. Descotes, VCH, Weinheim, **vol. 2**, 1993.

95 *Carbohydrates as Organic Raw Materials*, ed. H. van Bekkum, H. H. Röper and A. G. J. Voragen, VCH Weinheim, **vol. 3**, 1996.

96 *Carbohydrates as Organic Raw Materials*, ed. W. Praznik and H. Huber, WUV-Univ, Vienna, **vol. 4**, 1998.

97 R. Khan, *Adv. Carbohydr. Chem. Biochem.*, 1976, **33**, 235–294.

98 R. Khan, *Pure Appl. Chem.*, 1984, **56**, 883–844.

99 M. A. Godshall, *Int. Sugar J.*, 2001, **103**, 378–384.

100 Y. Queneau, S. Jarosz, B. Lewandowski and J. Fitremann, *Adv. Carbohydr. Chem. Biochem.* 2007, vol. 61, in press.

101 K. Hill and O. Rhode, *Fett/Lipids*, 1999, **101**, S25–33.

102 D. Blunk, K. Praefcke and V. Vill, in *Handbook of Liquid Crystals*, vol. 3, High Molecular Weight Liquid Crystals, ed., D. Demus, J. W. Goodby, G. W. Gray, H.-W. Spiess and V. Vill, Wiley-VCH, Weinheim, 1998, pp 305–340.

103 D. C. McCain and J. L. Markley, *Carbohydr. Res.*, 1986, **152**, 73–80.

104 J. C. Christofides and D. B. Davies, *J. Chem. Soc., Chem. Commun.*, 1985, 1533–1534.

105 S. Pérez, in *Sucrose: properties and applications*, ed. M. Mathlouthi and P. Reiser, Blackie, Glasgow, 1995, pp. 11–32.

106 F. W. Lichtenthaler, S. Immel and U. Kreis, in *Carbohydrates as Organic Raw Materials*, ed. F. W. Lichtenthaler, VCH, Weinheim, **vol. 1**, 1991, pp 1–32.

107 E. Reinefeld and K. D. Heincke, *Chem. Ber.*, 1971, **104**, 265–269.

108 F. W. Lichtenthaler, S. Immel and P. Pokinskyj, *Liebigs Ann. Chem.*, 1995, 1938–1947.

109 J. Gagnaire, G. Toraman, G. Descotes, A. Bouchu and Y. Queneau, *Tetrahedron Lett.*, 1999, **40**, 2757–2760.

110 E. Gérard, H. Götz, S. Pellegrini, Y. Castanet and A. Mortreux, *Appl. Catal., A*, 1998, **170**, 297–306.

111 J. Gagnaire, A. Cornet, A. Bouchu, G. Descotes and Y. Queneau, *Colloids Surf., A*, 2000, **172**, 125–138.

112 R. Pierre, I. Adam, J. Fitremann, F. Jerome, A. Bouchu, G. Courtois, J. Barrault and Y. Queneau, *C. R. Chim.*, 2004, **7**, 151–160.

113 N. Villandier, I. Adam, F. Jérôme, J. Barrault, R. Pierre, A. Bouchu, J. Fitremann and Y. Queneau, *J. Mol. Catal. A: Chem.*, 2006, **259**, 67–77.

114 C. C. Akoh, *Food Sci. Technol. (N. Y.)*, 2002, **117**, 695–727.

115 I. Janicot, A. Bouchu, G. Descotes and E. Wong, *Tenside Surfactants Deterg.*, 1996, **33**, 290–296.

116 V. Molinier, K. Wiesniewski, A. Bouchu, J. Fitremann and Y. Queneau, *J. Carbohydr. Chem.*, 2003, **22**, 657–669.

117 S. Abouhilale, J. Greiner and J.G. Riess, *Carbohydr. Res.*, 1991, **212**, 55–64.

118 V. Molinier, J. Fitremann, A. Bouchu and Y. Queneau, *Tetrahedron: Asymmetry*, 2004, **15**, 1753–1762.

119 (*a*) K. Baczco, C. Nugier-Chauvin, J. Banoub, P. Thilbault and D. Plusquellec, *Carbohydr. Res.*, 1995, **269**, 79–88; (*b*) C. Chauvin, K. Baczko and D. Plusquellec, *J. Org. Chem.*, 1993, **58**, 2291–2295.

120 (*a*) A. M. Klibanov, *Chem.-Tech. (Heidelberg)*, 1986, 354–359; (*b*) S. Riva, J. Chopineau, A. P. G. Kieboom and A. M. Klibanov, *J. Am. Chem. Soc.*, 1988, **110**, 584–589; (*c*) J. S. Dordick, *Biotechnol. Prog.*, 1992, **8**, 259–267.

121 (*a*) S. Riva, in *Carbohydrate Polyesters as Fat Substitutes*, ed. C. C. Akoh and B. G. Swanson, M. Dekker Inc., New York, 1994, pp. 37–64; (*b*) M. Woudenberg-van Oosterom, F. van Rantwijk and R. A. Sheldon, *Biotechnol. Bioeng.*, 1996, **49**, 328–333.

122 (*a*) G. Carrea, S. Riva, F. Secundo and B. Danieli, *J. Chem. Soc., Perkin Trans. 1*, 1989, 1057–1061; (*b*) F. J. Plou, M. A. Cruces, M. Bernabe, M. Martin-Lomas, J. L. Parra and A. Ballesteros, *Ann. N. Y. Acad. Sci.*, 1995, **750**, 332–337.

123 (*a*) F. J. Plou, M. A. Cruces, M. Ferrer, G. Fuentes, E. Pastor, M. Bernabé, M. Christensen, F. Comelles, J. L. Parra and A. Ballesteros, *J. Biotechnol.*, 2002, **96**, 55–66; (*b*) N. R. Pedersen, P. J. Halling, L. H. Pedersen, R. Wimmer, R. Matthiesen and O. R. Veltman, *FEBS Lett.*, 2002, **519**, 181–184; (*c*) P. Potier, A. Bouchu, G. Descotes and Y. Queneau, *Tetrahedron Lett.*, 2000, **41**, 3597–3600; (*d*) P. Potier, A. Bouchu, J. Gagnaire and Y. Queneau, *Tetrahedron: Asymmetry*, 2001, **12**, 2409–2419.

124 (*a*) P. Potier, A. Bouchu, G. Descotes and Y. Queneau, *Synthesis*, 2001, 458–462; (*b*) M. Ferrer, M. A. Cruces, M. Bernabé, A. Ballesteros and F. J. Plou, *Biotechnol. Bioeng.*, 1999, **65**, 10–16.

125 V. Molinier, B. Fenet, J. Fitremann, A. Bouchu and Y. Queneau, *J. Colloid Interface Sci.*, 2005, **286**, 360–368.

126 C. Osada, *Eur. Pat. Appl.*, EP 298,516 (Cl. C07/H15/203) 11 Jan 1989, JP Appl. 87/170499, 08 Jul 1987; 20 pp., *Chem. Abstr.*, 1989, **111**, 58265.

127 M. D. Serpe and E. A. Nothnagel, *Planta*, 1994, **193**, 542–550.

128 M. J. L. Arias, E. Girardi, J. A. Navarro, P. Savarino, J. Valldeperas and G. Viscardi, *Dyes Pigm.*, 2000, **46**, 37–42.

129 M. Amaike, H. Kobayashi and S. Shinkai, *Chem. Lett*, 2001, 620–621.

130 (*a*) C. D. Hurd and W. A. Bonner, *J. Org. Chem.*, 1946, **11**, 50–54; (*b*) C. D. Hurd and R. P. Zelinski, *J. Am. Chem. Soc.*, 1947, **69**, 243–246; (*c*) S. Hiroshi, *Jpn. Pat.*, 02 83 391, 1990, (*Chem. Abstr.*, 1990113, 132695s).

131 (*a*) I. Ganjian and D.V. Basile, *Anal. Biochem.*, 1997, **264**, 252–255; (*b*) E. Barni, C. Barolo, P. Quagliotto, J. Valldeperas and G. Viscardi, *Dyes Pigm.*, 2000, **46**, 29–36; (*c*) M. Amaike, H. Kobayashi, K. Sakurai and S. Shinkai, *Supramol. Chem.*, 2002, **14**, 245–253.

132 (*a*) S. Ram and R. E. Ehrenkaufer, *Tetrahedron Lett.*, 1984, **25**, 3415–3418; (*b*) H. P. Kleine, D. Weinberg, R. J. Kaufmann and R. S. Sidhu, *Carbohydr. Res.*, 1982, **142**, 333–337; (*c*) R. Roy, F. D. Tropper, T. Morisson and J. Boratynski, *J. Chem. Soc., Chem. Commun.*, 1991, 536–538; (*d*) C. K. De Bruyne and F. van Wijnendaele, *Carbohydr. Res.*, 1967, **4**, 101–103.

133 D. Page, D. Zanini and R. Roy, *Bioorg. Med. Chem.*, 1996, **4**, 1949–1961.

134 J. Conchie and A. Levy, *Methods Carbohydr. Chem.*, 1962, **2**, 345–347.

135 (*a*) K. Schank, in *The Chemistry of Functional Groups: The Chemistry of Diazonium and Diazo Groups*, ed. S. Pataï, John Wiley & Sons, New York, **vol. 2**, 1978, pp. 645–658; (*b*) C. Colas and M. Goeldner, *Eur. J. Org. Chem.*, 1999, 1357–1366.

136 M. P. Doyle and W. J. Bryker, *J. Org. Chem.*, 1979, **44**, 1572–1574.

137 Y. Hashida, K. Kubota and S. Sekiguchi, *Bull. Chem. Soc. Jpn.*, 1988, **61**, 905–909.

138 K. Liang, K.-Y. Law and D.-G. Whitten, *J. Phys. Chem. B*, 1997, **101**, 540–546.

139 (*a*) P. Savarino, G. Viscardi, E. Barni, R. Carpignano and L. A. Fedorov, *Dyes Pigm.*, 1990, **13**, 71–80; (*b*) L. A. Fedorov, P. Savarino, V. I. Dostovalova, G. Viscardi, R. Carpignano and E. Barni, *Magn. Reson. Chem.*, 1991, **29**, 747–748; (*c*) S. Simova, R. Radeglia and E. Ganghänel, *J. Prakt. Chem.*, 1982, 777–786.

140 (*a*) X. Lu and R. Bittmann, *Tetrahedron Lett.*, 2005, **46**, 1873–1878; (*b*) X. Lu, G. Arthur and R. Bittman, *Org. Lett.*, 2005, **7**, 1645–1648.

141 G.-T. Fan, Y.-S. Pan, K.-C. Lu, Y.-P. Cheng, W.-C. Lin, S. Lin, C.-H. Lin, C.-H. Wong, J.-M. Fang and C.-C. Lin, *Tetrahedron*, 2005, **61**, 1855–1862.

142 C.-W. Chang, Y.-N. Chen, A.-K. Adak, K.-H Lin, D.-L. M. Tzou and C.-C. Lin, *Tetrahedron*, 2007, **63**, 4310–4318.

143 A. Lee, K. J. Farrand, N. Dickgreber, C. M. Hayman, S. Jürs, I. F. Hermans and G. F. Painter, *Carbohydr. Res.*, 2006, **341**, 2785–2798.

144 V. D. Chaudhari, K. S. A. Kumar and D. D. Dhavale, *Org. Lett.*, 2005, **7**, 5805–5807.

145 A. N. Rai and A. Basu, *J. Org. Chem.*, 2005, **70**, 8228–8230.

146 R. M. Ndonye, D. P. Izmirian, M. F. Dunn, K. O. A. Yu, S. A. Porcelli, A. A. Khurana, M. Kronenberg, S. K. Richardson and A. R. Howell, *J. Org. Chem.*, 2005, **70**, 10260–10270.

147 T. Yamamoto, H. Hasegawa, T. Hakogi and S. Katsumura, *Org. Lett*, 2006, **8**, 5569–5572.

148 V. T. Pham, J. E. Joo, Y.-S. Tian, C.-Y. Oh and W.-H. Ham, *Arch. Pharmacal Res.*, 2007, **30**, 22–27.

149 (*a*) G. Righi, S. Ciambrone, C. D'Achille, A. A. Leonelli and C. Bonini, *Tetrahedron*, 2006, **62**, 11821–11826; (*b*) C. Peters, A. Billich, M. Ghobrial, K. Högenauer, T. Ullrich and P. Nussbaumer, *J. Org. Chem.*, 2007, **72**, 1842–1845; (*c*) T. Murakami and K. Furusawa, *Tetrahedron*, 2002, **58**, 9257–9263.

150 (*a*) Y. D. Vankar and R. R. Schmidt, *Chem. Soc. Rev.*, 2000, **29**, 201–216; (*b*) A. R. Howell and A. J. Ndakala, *Curr. Org. Chem.*, 2002, **6**, 365–391; (*c*) J. Liao, J. Tao, G. Lin and D. Liu, *Tetrahedron*, 2005, **61**, 4715–4733; (*d*) P. B. Savage, L. Teyton and A. Bendelac, *Chem. Soc. Rev.*, 2006, **35**, 771–779.

151 R. Nouguier, M. Mchich, P. Maldonado and H. Grangette, *Bull. Soc. Chim. Fr.*, 1985, **4**, 602–607.

152 M. L. Lewbart and J. J. Schneider, *J. Org. Chem.*, 1969, **34**, 3505–3512.

153 S. K. Chaudary and O. Hernandez, *Tetrahedron Lett.*, 1979, 99–102.

154 G. E. Keck and E. J. Enholm, *J. Org. Chem.*, 1985, **50**, 146–147.

155 E. J. Corey and A. Venkateswarlu, *J. Am. Chem. Soc.*, 1972, **94**, 6190–6191.

156 S. Rio, J.-M. Beau and J.-C. Jacquinet, *Carbohydr. Res.*, 1991, **219**, 70–91.

157 P. Boullanger, V. Maunier and D. Lafont, *Carbohydr. Res.*, 2000, **324**, 97–106.

158 B. Reinhard and H. Faillard, *Liebigs Ann. Chem.*, 1994, 193–203.

159 D. Lafont, M.-N. Bouchu, A. Girard-Egrot and P. Boullanger, *Carbohydr. Res*, 2001, **336**, 181–194.

160 M. Tokunaga, J. F. Larrow, F. Kakiuchi and E. N. Jacobsen, *Science*, 1997, **277**, 936–938.

161 E. N. Jacobsen, *Acc. Chem. Res.*, 2000, **33**, 421–431 and references therein.

162 (*a*) D. Hernanz, F. Camps, A. Guerrero and A. Delgado, *Tetrahedron: Asymmetry*, 1995, **6**, 2291–2298; (*b*) P. S. Savle, M. J. Lamoreaux, J. F. Berry and R. D. Gandour, *Tetrahedron: Asymmetry*, 1998, **9**, 1843–1846.

This journal is © The Royal Society of Chemistry 2007

Chem. Soc. Rev., 2007, **36**, 1971–2032 | 2031

163 (*a*) A. Pautard-Cooper and S. A. Evans, Jr., *Tetrahedron*, 1991, **47**, 1603–1610; (*b*) I. Mathieu-Pelta and S. A. Evans, Jr., *J. Org. Chem.*, 1992, **57**, 3409–3413.

164 I. A. Ivanova, A. J. Ross, M. A. J. Ferguson and A. V. Nikolaev, *J. Chem. Soc., Perkin Trans. 1*, 1999, 1743–1754.

165 V. Maunier, P. Boullanger and D. Lafont, *J. Carbohydr. Chem.*, 1997, **16**, 231–235.

166 R. Velty, T. Benvegnu, M. Gelin, E. Privat and D. Plusquellec, *Carbohydr. Res.*, 1997, **299**, 7–14.

167 (*a*) K. Linek and J. Alfoldi, *Carbohydr. Res.*, 1987, **164**, 195–205; (*b*) K. Linek, J. Alfoldi and J. Defaye, *Carbohydr. Res.*, 1993, **247**, 329–335.

168 B. Liu and R. Roy, *Tetrahedron*, 2001, **57**, 6909–6913.

169 T. K. Lindhorst, M. Dubber, U. Krallmann-Wenzel and S. Ehlers, *Eur. J. Org. Chem.*, 2000, 2027–2034.

170 J. Esnault, J.-M. Mallet, Y. Zhang, P. Sinaÿ, T. Le Bouar, F. Pincet and E. Perez, *Eur. J. Org. Chem.*, 2001, 253–260.

171 (*a*) F. Perez-Balderas, F. Hernandez-Mateo and F. Santoyo-Gonzalez, *Tetrahedron*, 2005, **61**, 9338–9348; (*b*) H. Al-Mughaid and T. B. Grindley, *J. Org. Chem.*, 2006, **71**, 1390–1398.

172 S. Chierici, P. Boullanger, L. Marron-Brignone, R. M. Morelis and P. R. Coulet, *Chem. Phys. Lipids*, 1997, **87**, 91–101.

173 M. Schmidt, B. Dobner and P. Nuhn, *Eur. J. Org. Chem.*, 2002, 669–674.

174 R. M. Nouguier and M. Mchich, *J. Org. Chem.*, 1987, **52**, 2995–2997.

175 C. H. Issidories and R. Gulen, *Org. Synth.*, 1958, **38**, 65–67.

176 (*a*) D. Lafont, B. Gross, R. Kleinegesse, F. Dumoulin and P. Boullanger, *Carbohydr. Res.*, 2001, **331**, 107–117; (*b*) S. Rio, J.-M. Beau and J.-C. Jacquinet, *Carbohydr. Res.*, 1993, **244**, 295–313.

177 K. P. R. Kartha and H. J. Jennings, *J. Carbohydr. Chem.*, 1990, **9**, 777–781.

178 R. R. Schmidt and M. Stumpp, *Liebig Ann. Chem.*, 1983, 1249–1256.

179 K. P. R. Kartha, M. Aloui and R. A. Fields, *Tetrahedron Lett.*, 1996, **37**, 8807–8810.

180 (*a*) G. C. Choquet, G. B. Patel and G. D. Sprott, *Can. J. Microbiol.*, 1996, **42**, 183–186; (*b*) G. D. Sprott, D. L. Tolson and G. B. Patel, *FEMS Microbiol. Lett.*, 1997, **154**, 17–22; (*c*) G. B. Patel, B. J. Agnew, L. Deschatelets, L. P. Flemming and G. D. Sprott, *Int. J. Pharm.*, 2000, **194**, 39–49.

181 (*a*) J. M. Kim and D. H. Thompson, *Langmuir*, 1992, **8**, 637–644; (*b*) T. Eguchi, K. Arakawa, K. Kakinuma, G. Rapp, S. Ghosh, Y. Nakatani and G. Ourisson, *Chem.–Eur. J.*, 2000, **6**, 3351–3358; (*c*) L. A. Cuccia, F. Morin, A. Beck, N. Hébert, G. Just and R. B. Lennox, *Chem.–Eur. J.*, 2000, **6**, 4379–4384.

182 M. Brard, W. Richter, T. Benvegnu and D. Plusquellec, *J. Am. Chem. Soc.*, 2004, **126**, 10003–10012.